2008

Empirical Relationships Betweenload Test Data And Predicted Compression Capacity Of Augered Cast-in-place Piles In Predominantly

Donald McCarthy
University of Central Florida

EMPIRICAL RELATIONSHIPS BETWEEN LOAD TEST DATA AND PREDICTED COMPRESSION CAPACITY OF AUGERED CAST-IN-PLACE PILES IN PREDOMINANTLY COHESIONLESS SOILS

by

DONALD JEFFERY MCCARTHY JR.
B.S. University of South Alabama, 2005

A thesis submitted in partial fulfillment of the requirements
for the degree of Master of Science
in the Department of Civil and Environmental Engineering
in the College of Engineering and Computer Science
at the University of Central Florida.
Orlando, Florida

Summer Term
2008

ABSTRACT

Augered Cast-In-Place (ACIP) Piles are used in areas were the loading from a superstructure exceeds the soil bearing capacity for usage of a shallow foundation. In Northwest Florida and along the Gulf Coast, ACIP piles are often utilized as foundation alternatives for multi-story condominium projects. Data from 25 compression load tests at 13 different project sites in Florida and Alabama were analyzed to determine their individual relationships between anticipated and determined compression load capacity. The anticipated capacity of the ACIP pile is routinely overestimated due to uncertainties involved with the process of estimating the compressive capacity and procedures of placing the piles; therefore, larger diameter and deeper piles are often used to offset this lack of understanding. The findings established in this study will provide a better empirical relationship between predicted behaviors and actual behaviors of ACIP piles in cohesionless soils. These conclusions will provide the engineer with a better understanding of ACIP pile behaviors and provide a more feasible approach to more accurately determine the pile-soil interaction in mostly cohesionless soils.

ACKNOWLEDGMENTS

I would like to thank many people who have either guided me or provided inspiration to me throughout this journey. Thank you to Dr. Kuo, who generously allowed me to perform this research study via long distance and provided valuable input along the way. I would like to thank Dr. Diane Bagwell for her many hours of help throughout the thesis process. I would like to thank my fiancée Tara Bagwell for allowing me to pursue my dream and for her sacrifices during this process. I could not have done this without the help of my good friend Mike Hudson, thank you for your support. Finally, I would like to thank my mother and father who provide me inspiration every day to keep pushing forward and to never give up.

I dedicate this research project to my mom and dad.

TABLE OF CONTENTS

LIST OF FIGURES

LIST OF TABLES

LIST OF ACRONYMS/ABBREVIATIONS

ACIP	Augered-Cast-In-Place
ASTM	American Society for Testing and Materials
DFI	Deep Foundations Institute
Eq.	Equation
FHWA	Federal Highway Administration
ft	foot
GSP	Generalized Soil Profile
ICC	International Code Council
IBC	International Building Code
in.	inch
kN	kilo-Newton
lb(s)	pound(s)
m	meter
min.	minimum
mm	millimeter
NAVFAC	Navy Facilities Manual
OCR	Overconsolidation Ratio
SM	Silty Sand

SP	Poorly Graded Sand
SPSS	Statistical Package for the Social Sciences (Software)
SPT	Standard Penetration Test
SW	Well Graded Sand
USACE	United States Army Corps of Engineers
USCS	Unified Soil Classification System
μm	micrometer
vs.	versus

CHAPTER 1 - INTRODUCTION

1.1 Background

Deep foundations are commonly used in areas prone to having sub-surface conditions that consist of loose sands and/ or soft clayey soils and are inadequate to support the heavy bearing super-structure with poor subsurface conditions, thus conventional shallow foundation design is not adequate to carry the large loading implied by the super-structure, therefore, a deep foundation is required. Deep foundation includes pile foundations, drilled shafts, and caisson foundations.

Deep foundations cost more and require more time to install; therefore, owners typically want to avoid the use of deep foundations if possible. Pile foundations are commonly used to transfer large loads from a superstructure to denser cohesionless soil layers. Piles normally fall into two main categories based on method of installation: displacement piles and non-displacement piles (also known as replacement piles) according to Craig (1999). These types of foundations resist the superstructures load by the skin friction of the pile with resistance to the in-situ soils surrounding the pile and/ or the base of the pile (tip bearing capacity).

Displacement piles are typically cast off-site and transported to the construction site. These piles are most commonly driven or jacked into the ground which displaces an equivalent soil volume by lateral or vertical displacement of the soil during installation (Craig, 1999). The most common types of piles used in construction practices are concrete, grout, steel, and timber.

Before pile foundations are determined to be necessary, a thorough investigation of subsurface soils at the project site must be conducted. After the subsurface investigation, the engineer will estimate the soil properties and use empirical relationships to determine the size and depth of the pile needed to resist the imposed loads with some factor of safety. According to Bowles (1996) "A cast-in-place pile is formed by drilling a hole in the ground and filling it with concrete. The hold may be drilled (as in caissons), or formed by driving a shell or casing into the ground." Piles are capable of resisting imposed compression, tension, and lateral loads with a certain amount of deflection. This research project focuses on the ultimate capacity of non-displacement piles, Augered Cast-In-Place (ACIP) piles which are uncased and cast in cohesionless soils, and their reactions to static compressive loading.

1.2 Statement of the Problem

The problem discussed in this research study is the relationship between actual load test data and current empirical methods of determining the ultimate compression capacity of ACIP pile in a mostly granular soil (cohesionless) stratum. The research question to be reviewed in this study is:

1. Will there be a deviation between anticipated empirical capacity equations and interpreted physical load test data?
2. If there is a difference between anticipated empirical capacity equations and interpreted physical load test data, determine the significance of the variation between the two methods.

3. If there is a difference between anticipated empirical capacity equations and interpreted physical load test data, determine which methods provide the best fit relationship when compared to one another?
4. If there is a best fit relationship between interpreted physical load test data and anticipated empirical capacity equations, can an empirical method of predicting anticipated compressive capacity be determined to provide a better fit between methods?

1.3 Research Objectives

The objectives of this research are categorized into two parts. First, the review of current methods utilized to asses the static pile design process. The areas of improvement will be identified and may result with the design of more economical and safer projects in the future. Second, the current soil models used to represent soil interaction with the pile shaft and pile base are presented for review and analysis. The objective is to examine the non-linear soil behavior and increased resistance by various pile base soil reaction methods. This study may validate the results of the physical field load tests recorded on many projects.

There are multiple factors of uncertainty when analyzing the application of ACIP piles. Current theories to estimate the compressive capacity of piles require the ultimate capacity to be divided by a factor of safety of 2 (IBC, 2003) to produce an allowable (working) capacity. This factor of safety is due to the uncertainty in the theories of pile-soil reactions, the uncertainty of sub-surface conditions, and the variation in construction practices.

This study might allow the engineer to predict with more certainty the ultimate capacity of ACIP piles in cohesionless soils. This empirical method might allow the engineer to design with more certainty and efficiency, thus lowering the cost of construction for the owner.

1.4 Significance of the Study

This study has important implications because the capacities of ACIP piles in cohesionless soils are not fully understood, hence, the large factors of safety applied to the ultimate capacity. Engineers typically use more conventional methods of analyzing ACIP piles with more basic bored-hole (drilled shaft) techniques, which do not account for the increased stress created by the pressurization of grout into the excavated casting. A better understanding of this relationship may be concluded as a result of this study. This conclusion may provide a more realistic approach to determine an empirical relationship between cohesionless soils and the ACIP piles resistance to imposed loading. This study examined the compressive behaviors of single ACIP piles for the transfer of imposed loads. The application of studying pile group foundation or combined pile with additional transfer of load from the pile cap into the soil and between the piles was not examined.

Specifically, the study attempted to examine the (a) ultimate capacity of ACIP piles based on current analytical and empirical methods, (b) allowable deflection criteria within the load test interpretation limits, and (c) the installation and testing procedures of ACIP piles.

1.5 Limitations

A limitation is some part of the study that the researcher is aware of which might have a negative affect on the generalizability or results of the study but one in which the researcher has little or no control (Gay, 2001). There are two identifiable limitations in this study:

1. *Biases of the researcher*. According to Evertson and Green (1986), bias refers to the way one perceives events in such a way that some facts might be overlooked, distorted, or falsified. The manner in which one interprets things is based on his or her value system (Patton, 2002). The researcher is a civil engineer with 5 years experience in dealing with soil and its related properties.
2. *Limited population*. According to Creswell (1994), delimitation is something that narrows the scope of the study. The study was delimited to 25 ACIP pile load tests in Florida and Alabama.
3. *Correlation research design.* The limitations of correlation research appear when predictions can be made for two variables. However, inferences about the cause of the relationship cannot be made, which is the greatest limitation of the correlational design.

CHAPTER 2 – REVIEW OF LITERATURE

2.1 Introduction

According to Kulhawy and Chen (2005) there has been a renewed interest in ACIP piles and how early studies focused on ACIP pile placement and the quality assurance issues (e.g., Neate 1988, Flemming 1994, Esrig et al. 1994). Some later studies examined the compressive capacity of ACIP piles (e.g., Van Impe 1988, Neely 1991, McVay et al. 1994, O'Neil et al. 2002, Zelada and Stephenson 2000). A comprehensive review of the literature was conducted in the area of Augered Cast-In-Place (ACIP) piles. Based on this literature review, the researcher focused on the following categories which became the major headings of the literature review presented in this paper: (a) soil properties, (b) skin friction resistance, (c) Meyerhof point bearing capacity, (d) Vesic point bearing capacity, (e) Janbu point bearing capacity, (f) Chin-Kondner's interpretation of physical load test data, (g) Army Corps of Engineers interpretation of physical load test data, and (h) Tangent Method of interpretation of physical load test data. A search of the literature was conducted by screening documents for current, primary, diverse, and relevant sources which included peer reviewed journals, books, government documents, and theses. The key words used in this search were (a) Auger-Cast-In-Place pile, (b) pile in sand, (c) deep foundation, (d) skin friction, (e) bearing capacity, (f) Meyerhof, (g) Chin-Kondner load test, (h) Vesic bearing capacity, (i) Janbu bearing capacity, (j) Army Crops of Engineers, (k) Florida Department of Transportation foundation, (l) Department of Environmental Protection, (m) American Petroleum Institute, (n) Federal Highway Administration, and (c) American Society for Testing and Materials.

2.2 Cohesionless Soil Properties

Different soil conditions are classified by groups and sub-groups. These soil classification methods provide a common language to concisely express the general characteristics of soils, which are infinitely varied, without detailed descriptions (Das, 2005). For this study, cohesionless soils were encountered at each project site, which are defined as a sand or gravel by the Unified Soil Classification System (USCS).

The American Society for Testing and Materials (ASTM) provides ASTM D2487 which provides a standard for classification of soils as referenced by the unified soil classification system. ASTM D2487 defines cohesionless soils into two sub-categories:

1. *Coarse* - passes 3-in. (75-mm) sieve and retained on 3⁄4-inch (19-mm) sieve
2. *Fine*—passes 3⁄4-in. (19-mm) sieve and retained on No. 4 (4.75-mm) sieve.

Fine soils as defined by ASTM D2487 are classified as sand and are defined by the following:

1. Sand - as particles of rock that will pass a No. 4 (4.75-mm) sieve and be retained on a No. 200 (75-µm) U.S. standard sieve with the following subdivisions:
    a. *Coarse* - passes No. 4 (4.75-mm) sieve and retained on No.10 (2.00-mm) sieve
    b. *Medium* - passes No. 10 (2.00-mm) sieve and retained on No. 40 (425-µm) sieve
    c. *Fine* - passes No. 40 (425-µm) sieve and retained on No. 200 (75-µm) sieve

2.2.1 Standard Penetration Testing (SPT) Correlations for Properties of Soils

The data provided by the geotechnical reports for each site included SPT (Standard Penetration Test) results and some laboratory data. This SPT data was used to analyze the in-situ properties of the soil. The needed soil parameters to determine the effective stress on the shaft of the pile include, the relative density (D_r), effective stress friction angle (ϕ'), and the horizontal soil stress coefficient (K_o). From these relationships, the bearing capacity properties of the soils could be predicted.

The soil conditions encountered during this investigation consisted of sand as classified by the USCS (SP or SW) which is defined as poorly-graded and well-graded respectively, slightly-silty sand (SP-SM), and silty sand (SM). The values of γ used in this study ranged from 102 to 126 lb/ft^3 for poorly graded sand (SP) and from 102 to 130 lb/ft^3 for slightly silty to silty sand (SP-SM). In order to determine the relative density of the sandy soil profiles, the angle of internal friction (ϕ') was determined based on Meyerhof's (1976) study. This method of determining the angle of internal friction was determined by correlating the SPT value obtained during the soil exploration and using (Bowles, 1996) table for empirical values. Once the values for relative density were determined, Figure 1 was consulted to determine the minimum and maximum dry unit weight values. The unit weight (γ) of soil was provided by the U.S. Department of the Interior Bureau of Reclamation (1998) based on the relative density (D_r) of the soil profile and is shown graphically in Figure-1. For soils with USCS designation of SP, line 56C-212 was utilized and for soils with USCS designation of SP-SM or SM, line 22R-180 in

Figure-1. The relative unit weight values were used when calculating the ultimate skin friction and point bearing capacity of the ACIP piles.

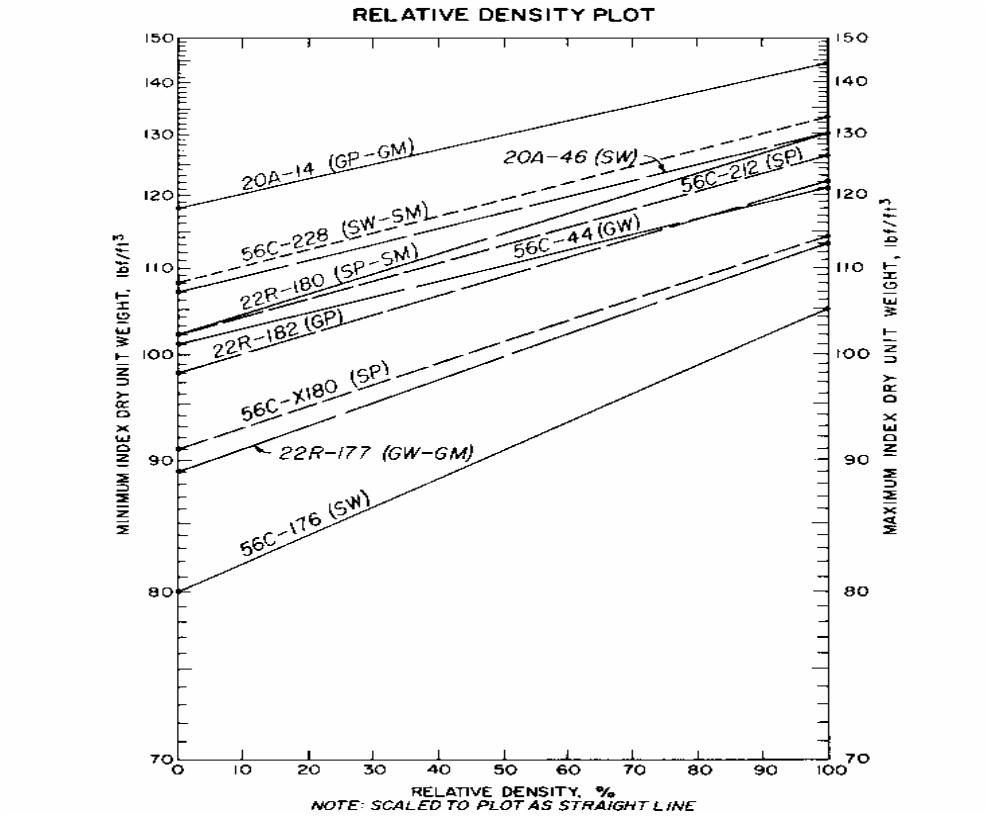

Figure 1-Density Plot vs. Unit Weight (U.S. / B.R., 1998)

2.3 Deep Foundations

According to information provided by (Turner & Kulhawy, 1994) many problems exist when analyzing deep foundations and theories relative to there compressive capacity. Turner &

Kulhawy said that Vesic (1964) identified four factors that will affect the behavior of deep foundations in sand:

1. Curvature of the Mohr-Coulomb failure envelope.
2. Relative independence of shaft diameter on butt displacement at failure.
3. Arching.
4. Relative compressibility.

Soil arching (Turner & Kulhawy, 1994) refers to a stress redistribution with depth resulting in a limiting value of side resistance at some critical depth. The piles in this study were not loaded to failure, therefore, Vesic's study of variables with deep foundations in sand were not applied to this study.

2.4 Augered Cast-In-Place Pile Foundations

Augered cast piles are formed by drilling a continuous flight auger into the ground until reaching the required depth, then by pumping sand-cement grout or concrete down the hollow stem as the auger is steadily withdrawn. The sides of the holes are supported at all times by the soil-filled auger, eliminating the need for temporary casing or bentonite slurry (Neely, 1989). Van den Elzen (1979) suggested that the soil is radially displaced by the auger as it advances to the boring termination depth. This process causes the density of the soil around the pile to increase.

"The development of the augered, cast-in-place (auger-cast) piling technique evolved in the late 1940's from the process of pressure grouting open holes and holes backfilled with coarse aggregates (Neate, 1988)."

2.4.1 Installation of ACIP Pile Foundation

The equipment used to install the ACIP piles usually consists of a crawler-mounted crane with box leads and a continuous flight, hollow-stem auger driven by an auger drive head (gearbox) and a power unit having a specified rated torque and horsepower. The geotechnical engineer of record for the project provides criteria for the installation of ACIP piles. When installing the ACIP pile, a representative for the geotechnical engineer or owner must be present to observe and document the installation process. Some common parameters used for the majority of samples tested in this study include the following:

1. The test pile should be of a specified diameter and a specified length to achieve anticipated compressive capacities.
2. Test pile installation procedures should be carefully monitored and documented by a qualified geotechnical engineer or geologist.
3. A minimum volume of grout must be pumped into the base of the excavated hole before extraction of auger. Typically around 5 linear feet of grout must be placed in

the excavated hole in order to maintain positive (head) pressure prior to initiating withdrawal of the auger.

4. A target grout factor (actual grout volume divided by theoretical grout volume) of 1.15 to 1.5 (depending on soil conditions) or greater should be achieved during the installation of the test pile(s).
5. A grout return depth or pressure head (head of grout above the injection point) of at least 5 to 10 feet should be achieved at the completion of grouting.
6. An incremental grout factor equal to at least 115 percent of the theoretical pile volume should be achieved in each 5-foot pile segment.
7. Piles which subside immediately following grouting should be topped up using appropriate methods to prevent soil inclusions into the tops of the piles.
8. All reinforcing steel should be inserted into the piles manually and without mechanical assistance.
9. At least 100% of the pile theoretical volume should be pumped into the pile following the observance of grout return at the ground surface.

In this study all piles were installed to a specified tip elevation, rather than a refusal criterion. The refusal criterion is usually defined by the auger reaching a significantly solid stratum of soil and/ or rock and thus the auger can not be extended to a further depth (Crowther, 1988). All piles appeared to have maintained a constant positive pressure head while grouting. Also, all piles achieved a minimum of 115% grout factor volume, i.e., total grout volume divided

by theoretical pile volume. These criteria help control the installation practices of the contractor and are determined by the geotechnical engineer based on soil conditions and ground water levels.

2.5 Static Load Testing of Auger-Cast-In-Place Pile Foundations

Often engineering analysis of soils is not sufficient to predict ultimate capacity of pile foundations. As a result, static pile load tests provide a way to measure the capacity of a pile so that the engineer can use this information to adjust the predicted ultimate capacity of pile foundations. "A load test is a method used in the examination of the amount of weight that can be carried by a structural unit. Load tests can be performed on individual units, groups of units, or the entire foundations (Crowther, 1988)." The pile load test program should be considered as part of the design and construction process, and not performed in response to an immediate construction problem (Fleming, 1985). Pile tests may be performed before or during the construction process. Typically, if a problem occurs with installation of the pile, a pile test may be performed to determine the capacity of the pile.

For the samples used in this study, single piles were statically loaded to a pre-determined load and the deflection was measured. Deflection is defined as the distance in which the pile butt or top moves under an applied load (Das, 2007). In some instances the engineer requested that multiple tests be performed at one site. Multiple tests on a single site could be performed for the following reasons: (a) the foundation encompasses a large area and/ or soil conditions vary, (b)

the depth of pile is still uncertain so multiple tests will be performed at varying depths, and (c) the piles will support loads in tension, compression, and/ or lateral resistance. In this study, all test piles were tested for compression capacity at the beginning of the project to help aide the engineer in determining the allowable bearing capacity of each pile for its associated project.

The data obtained in this research project consisted of load testing using the method provided by ASTM D1143 (1994). This method can be performed using a slow maintained load test or the quick maintained load test. According to ASTM D1143 the quick and slow maintained method should be tested with the following criteria:

1. Quick Maintained Load - Apply the load in increments of 10 to 15 % of the proposed design load with a constant time interval between increments of 2 ½ min or as otherwise specified. Add load increments until continuous jacking is required to maintain the test load or until the specified capacity of the loading apparatus is reached, whichever occurs first, at which time stop the jacking. After a 5 minute interval or as otherwise specified, remove the full load from the pile.
2. Slow Maintained Load - Unless failure occurs first, load the pile to 200 % of the anticipated pile design load for tests on individual piles or to 150 % of the group design load for tests on pile groups, applying the load in increments of 25 % of the individual pile or group design load. Maintain each load increment until the rate of settlement is not greater than 0.01 in. (0.25 mm)/h but not longer than 2 hours. Provided that the test pile or pile group has not failed, remove the total test load anytime after 12 hours if the butt settlement over a one-hour period is not

greater than 0.01 in. (0.25 mm); otherwise allow the total load to remain on the pile or pile group for 24 hours. After the required holding time, remove the test load in decrements of 25 % of the total test load with 1 hours between decrements. If pile failure occurs continue jacking the pile until the settlement equals 15% of the pile diameter or diagonal dimension.

Han (1999) suggests that the static pile load test is the most effective test for piles since it demonstrates the actual loads which will be superimposed on the pile. This data provided from the static load test provides definitive information in regards to compressive capacity and deflection of the pile. Since most theories are based from the results of static load tests and its relationship with pile interaction with soils, it is commonly used in practice today. After installing the test pile(s), multiple reaction piles must be installed to provide resistance while the hydraulic jack applies a load to the compression pile (as shown in Figure-2). Figure-2 depicts the use of four reaction piles and one test pile (in center). The reaction piles are placed in a tension mode as the test pile is compressively loaded. Also, these reaction piles may serve as the tension test piles and/ or lateral test piles.

Figure 2- View of static load test on Pensacola Beach in Florida.

This entire static load test process of installing test and reaction piles requires more time and finances and therefore is less economical than other tests. However, as mentioned previously, the static pile test is most understood and most commonly specified by geotechnical engineers when testing ACIP piles.

2.6 Interpretation of Static Load Test Results

The interpretation of load test data should be performed by qualified engineers (IBC, 2003). According to Kulhawy and Chen (2005), and as stated by (Hirany and Kulhawy, et. al. 1988,

1989) the "interpreted failure load" has been defined qualitatively as "the load beyond which a small increase in load produces a significant increase in displacement." The load test should have pre-defined parameters of testing. Some examples of criteria for acceptance for the static load test were defined by Crowther (1988) and include:

1. A maximum total (gross) settlement under a specified load.
2. A maximum specified test load, regardless of settlement.
3. A maximum settlement under the design load and an excess capacity of some specified additional load.
4. A maximum plastic deformation (net settlement) after the test load is removed.

The load-displacement curves for non-displacement foundations can be described as three distinct regions (Kulhawy &Chen, 2005) as provided by (e.g., Hirany and Kulhawy, 2002), (a) initial essentially linear, (b) nonlinear transition, and (c) final essentially linear. A study provided by the International Code Council (International Building Code, 2005) describes the results of 10 bored piles and 14 driven pile reported by Duzceer and Saglamer (2002). This study reported that the Davisson Method for analyzing load test data has the ability to consistently provide conservative relationships to predicted load capacities of piles. The ratio of the results to the average of all results evaluated provided and average value of 0.945 with a covariance of 0.092. The Chin Kondner method was also analyzed in this study and resulted with an average of 1.511 with a covariance of 0.326. This provided information indicates that the Chin Kondner method overestimates the ultimate capacities of piles and therefore, may not be used as an acceptable

method of evaluating pile capacity from physical load test data in the upcoming edition of the International Building Code (IBC).

In this study all test piles were incrementally loaded to a predefined compressive capacity and then unloaded to measure the amount of rebound of the pile. The compressive rebound is defined as the deflection of the pile upwards after removing the load from the top of the pile. In most instances, the piles were then re-loaded for a 2nd time and then unloaded. The results from this process were used to determine the overall net deflection. In these instances both the 2nd loading of net deflection and the ultimate capacity of the test pile were analyzed to interpret the load test data for each ACIP pile

.

2.6.1 Davisson's Method

When investigating the capacity of an ACIP pile, the elastic compression becomes an important part of the overall deflection of the pile. This deflection must be accounted for when determining ultimate capacity of a pile from analyzing the pile load test. According to the Naval Facilities Engineering Command (1986) and their research on foundations, the elastic compression of pile (δ_E) when considered as a free column can be determined as:

$$\delta_E = \frac{QL_p}{AE} \qquad [2.1]$$

Q = test load, lbs

L_p = pile length, in. (for end bearing piles)

A = cross-sectional area of pile material, in^2

E = Young's Modulus for pile material, $lb/in^2 = 5700\sqrt{f'_c}$ [2.2]

f'_c = compressive strength of pile material

The failure load (S_f) according to Davisson's work is defined as the load which produces a displacement of the pile head equal to:

$$S_f = \delta_E + \left(0.15 + \frac{D}{120}\right) \quad [2.3]$$

D = pile diameter, in

In order to interpret the pile load test data and determine the failure load using Davisson's method, the following methodology should be applied (NAVFAC, 1986).

1. Calculate the elastic compression of pile when considered as a free column.
2. Determine the scales of plot such that the slope of pile elastic compression line is approximately 20º.
3. Plot pile head total displacement vs. applied load.
4. Failure load is defined as the load which produces a displacement of pile head equal to (S_f)
5. Plot failure criterion as described in (4), represented as a straight line, parallel to the line of pile elastic compression. The intersection of failure criterion with observed load deflection curve defines the failure load.

6. Where observed load displacement curve does not intersect failure criterion, the maximum test load should be taken as the failure load.
7. Apply a factor of safety of at least 2.0 to failure load to determine the allowable load.

The Davisson method was originally recommended for use with the quick maintain load test method. One advantage of using Davisson's method to interpret load test data is the failure load (S_f) can be plotted before the test based on Davisson's equation and the elastic compression theory determined by assuming the pile acts as a free head column. This allows the engineer to determine what loading should be applied in order for the load-displacement curve to cross the failure load line as shown in Figure 2. This loading diagram was provided using data from sample number 13 and test pile number one.

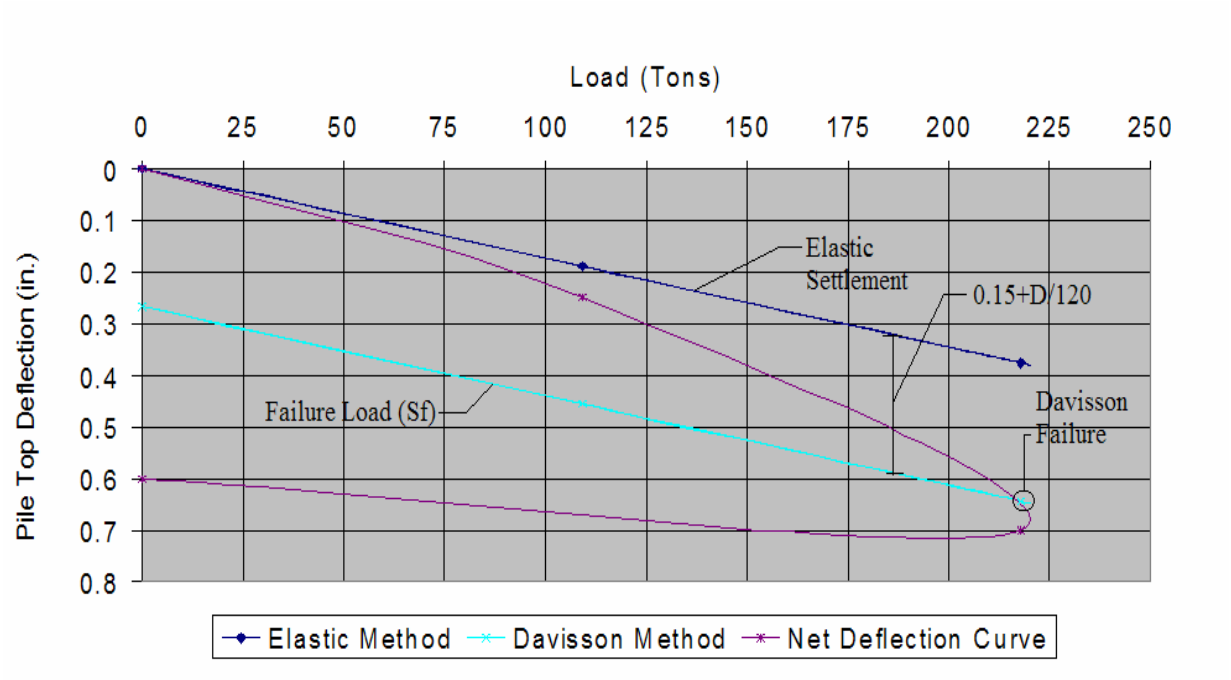

Figure 3-Davisson Load Deflection Curve

From a study published by the FHWA and provided by Tolosko (1999), after studying 63 bored (non-displacement) piles and there reactions under load tests, he found out that the ratio of Davisson's Method and designated static analysis ranged from 0.9 to 1.1.

2.6.2 Chin-Kondner's Method

According to Roscoe (1984), Chin and Vail (1973) proposed a method of separating the skin friction and end bearing resistant components of the pile and from the results of conventional pile load tests using the "stability plot" method proposed by Chin (1970). Chin's method assumed a relationship existed between the applied load (P) and the settlement (Δ) is hyperbolic. The relationship follows that a plot of (Δ /P) versus (Δ) (as known as the stability plot) provides a linear relationship. Chin-Kondner defined this relationship as:

$$\frac{\Delta}{P} = m * \Delta + C \qquad [2.4]$$

m = slope of straight portion of the stability plot

C = the y-intercept of the straight portion of the stability plot

Δ = the amount of pile movement (settlement or deflection)

P = the applied load to the top of the pile.

Roscoe (1984) provided information from Chin and Vail (1973) who defined the ultimate load as the inverse slope of the stability plot which is equal to m^{-1}. This method of load test interpretation relies on the testing of the pile to be performed in equal time increments. Figure 3 illustrates the Chin and Vail graphical representation for interpreting load test data and predicting the ultimate capacity of a pile.

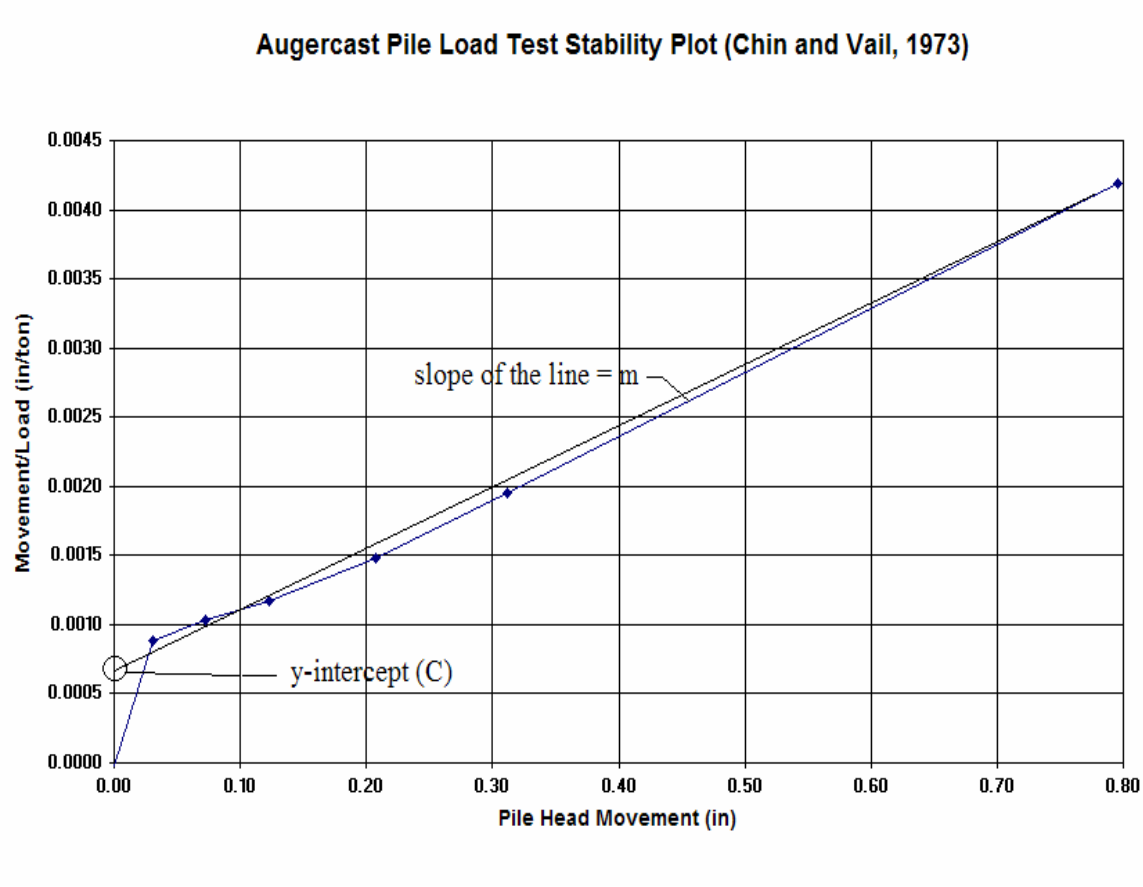

Figure 4-Chin-Kondner Plot

ASTM methods allow the test pile to be loaded with a variation in time increments; thus at times this method provides unrealistic ultimate pile compressive capacities. This method of analysis provided that "the end bearing on the pile resistance is negligible at small settlements and that the stability plot for the initial stages of the test is a measure of shaft friction only." (Roscoe, 1984)

2.6.3 Army Corps of Engineer's Method

The United States Army Corps of Engineers (1991) suggest that the ultimate pile capacity occurs when the load-deflection curve reaches a net deflection of ¼ inch. This implies that the load applied where the net deflection equals to ¼ inch is the ultimate load. This load is then divided by a factor of safety of two or three to determine the allowable capacity of the pile. This method will be utilized to interpret the load test results of each sample in this study. Figure 4 presents the load-deflection graph clarity provides the ultimate capacity as defined by the USACE engineer's method of interpretation of load test data.

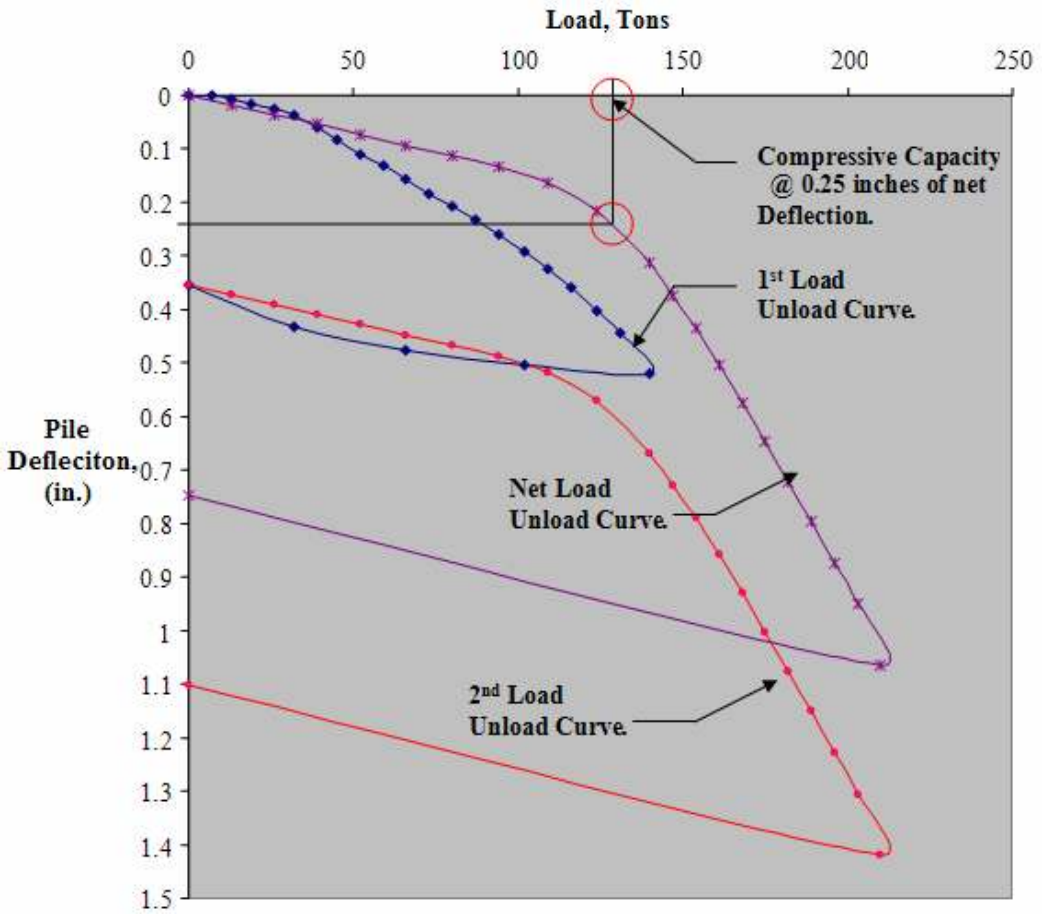

Figure 5-Load Deflection Plot w/ USACE Method

The net deflection curve was also inspected to determine the ultimate capacity given at 5% of the pile diameter (Ng, 2004). This method allows engineers to approximate the ultimate capacity from interpretation of load test data quickly.

2.6.4 Tangent Method

Butler and Hoy (Butler & Hoy, 1977) presented a method of interpretation of load capacity of drilled shafts and was also presented by Charles in 2004. Charles (2004) provided that Butler and Hoy defined the method of load failure as the "the maximum slope of the load-movement cure or the load at which the slope of the load-displacement curve is greater than 0.05 in/Ton. The Tangent method implies that the following techniques should be applied to utilize this method accurately (USACE, 1992).

1. Draw a tangent line to the curve at the graph's origin
2. Draw another tangent line to the curve with the slope equivalent to the slope of 1 inch per 40 kips (40,000 lbs) of load.

Ultimate bearing capacity is the load at the intersection of the tangent lines. Figure 5 represents the Tangent approach to determine the ultimate pile capacity from pile load test. The data for Figure 5 was provided by sample number 13 and test pile number one.

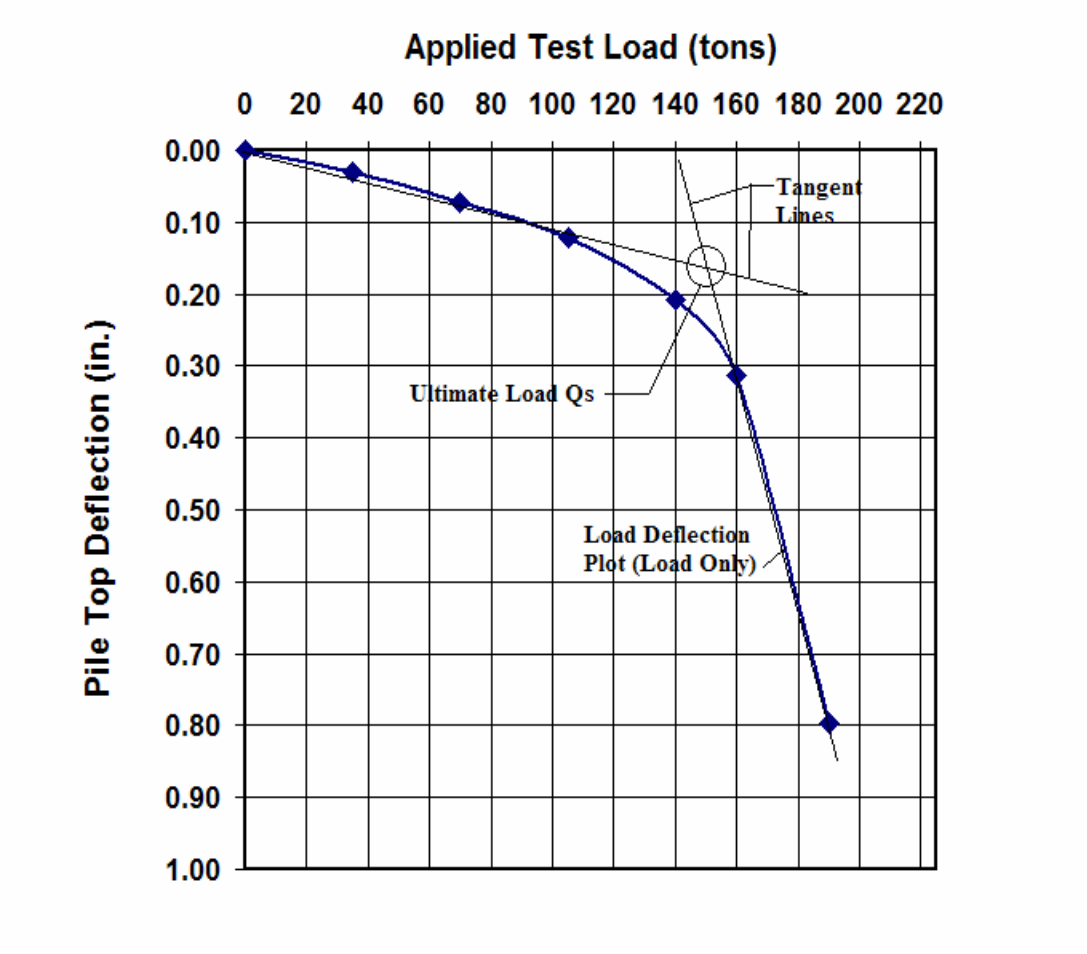

Figure 6-Load Deflection Plot w/ Tangent Method

Kulhawy and Chen (2005) reported on the axial capacity of 58 ACIP piles in cohesionless soils and determined that the load-displacement behavior based on empirical methods versus results of using the slope tangent method. It was found that interpreted Tangent failure load was approximately equal to 1.22, which according to Kulhawy and Chen (2005) is consistent for drilled shaft foundations in axial compression. This method when compared to

Chin Kondner's method provides a better approximation for the behavior of ACIP piles under compressive loading.

2.7 Soil Interaction with Auger-Cast-In-Place Foundation

Vesic (1963) performed model tests on piles and determined that for long piles the friction provided by the soil interaction with the pile reaches a constant value at a critical depth of approximately 15 pile diameters. A critical depth range is provided by the Naval Facilities Engineering Command (NAVFAC, 1986) and ranges from 10 to 40 pile diameters. For this study, the critical depth is determined by Vesic's recommended depth of 15 pile diameters.

When analyzing the point bearing capacity, the factor (N_q) from which end bearing is calculated depends upon the relative density of the soil beneath the pile toe. If loosening occurs during construction the end bearing component may be substantially reduced. Shaft friction is usually calculated by assuming the angle of friction, δ, between pile and soil to be the angle of friction of the soil, ϕ', (Touma and Reese, 1974).

2.7.1 Analysis of Compression Capacity

The equations utilized for estimating the compressive capacity for ACIP piles revolved around the basic theory that the ultimate load-carrying capacity Q_u of a pile (Das, 2007) is given by the following equation:

$$Q_u = Q_p + Q_s \qquad [2.5]$$

Q_p = load-carrying capacity of the pile point

Q_s = frictional resistance (skin friction) derived from the soil-pile interface

This basic static's equations was presented by Das (2007) and shown as follows:

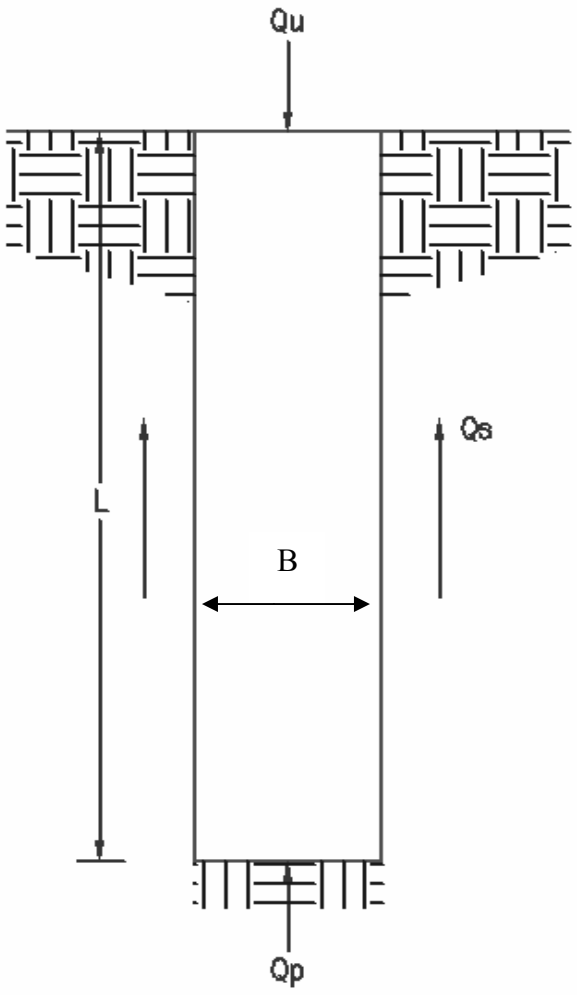

Figure 7-ACIP Pile Free Body Diagram

Kulhawy and Chen (2005) reported that for small values of L/B (length of pile divided by the diameter of pile) the side frictional resistance of the pile provides minimal resistance and therefore, pile-tip bearing capacity is the dominating source of compressive resistance. It was also reported that as the value of the critical depth increases, the side resistance begins to dominate and at some depth the pile then behaves as a friction pile and does not rely strongly on the end (point) bearing capacities.

2.7.2 Frictional Resistance Capacity

Das (2007) provided information in regards to the variation of frictional resistance (f) and how the unit skin friction increases with depth more or less linearly to a depth of (L') and then remains constant thereafter. According to Das, "The magnitude of the critical depth (L') may be 15 to 20 pile diameters. A conservative estimate would be $L' \approx 15D$." In this study, the critical depth value ranged from 17.5 to 22.5 feet based on $L' \approx 15D$. This frictional resistance is demonstrated by Das (2007) and shown in Figure-7.

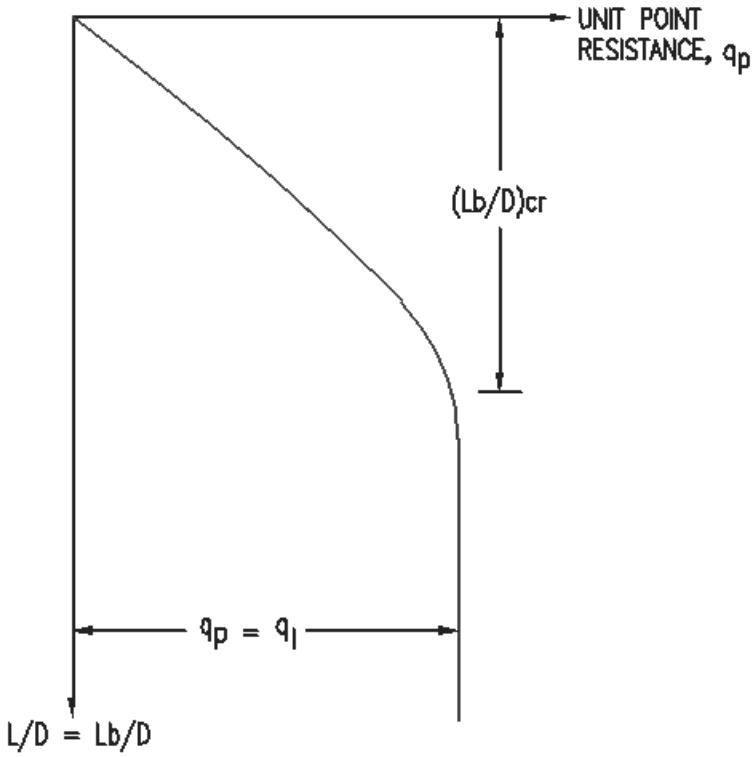

Figure 8-Critical Depth Figure (Das, 2007)

Based on the information provided previously, the frictional resistance of a pile in cohesionless soils can be determined by the following equation:

$$f = (K)(\sigma_o')\tan\delta' \qquad [2.6]$$ for a depth (z) = 0 to L'

or $f = f_{z=L'}$ [2.9] for the depth (z) = L' to L

K = effective earth pressure coefficient

σ_o' = effective vertical stress at the depth under consideration

δ' = soil-pile friction angle

Das (2007) presented data for the magnitude of *K* and how it varies with depth. These recommendations include K_o (at-rest pressure coefficient) for various pile types. For bored or jetted piles, Das (2007) recommends:

$$K \approx K_o = 1 - \sin\phi' \qquad [2.7]$$

The values for δ' appear to be in the range from $0.5\phi'$ to $0.8\phi'$ according to various investigations and as reported by (Das, 2007). According to Das (2007) and work presented by Coyle and Castello (1981), proposed that skin friction can be determined by:

$$Q_s = f_{av} pL = (K\overline{\sigma}_o' \tan\delta')pL \qquad [2.8]$$

$\overline{\sigma}_o'$ = average effective overburden pressure

δ' = soil-pile friction angle (Coyle and Castello, 1981) = $0.8\phi'$ [2.9]

f_{av} = average unit frictional resistance

This method is commonly used for driven piles, but can be modified and used with low-displacement pile equations to relate with bored pile.

The development of skin friction of ACIP piles is usually less than when compared to driven piles. Since tests were performed in cohesionless soils, drained loading could be assumed for all analyses. The methods used to analyze the compressive capacity of all ACIP test piles in

this study where (a) skin friction resistance, (b) Meyerhof's point bearing capacity, (c) Janbu's point bearing capacity, and (d) Vesic's point bearing capacity.

The point bearing resistance capacity of a pile provides additional capacity against compressive load in conjunction with the skin friction resistance of the pile. The point bearing capacity was analyzed for all samples separately and combined with skin friction results to predict variations in analyzing the ultimate compressive capacities and the results are included in Appendix-A.

The ultimate pile bearing capacity according to Terzaghi's equation for circular footings can be determined by the following equation (Das, 2007).

$$q_u = q_p = c' N_c + qN_q^* + \gamma D N_\gamma^* \qquad [2.10]$$

N_c, N_q^*, N_γ^* are all bearing capacity factors that include shape and depth factors

Since this study only includes cohesionless soils (c'=0) and the width of a pile *D* is relatively small as compared to the overall length of pile, Eq. 2.10 can be reduced too:

$$q_u = q' N_q^* \qquad [2.11]$$

The variable q' replaces the tern *q* for the sense of effective vertical stress. Figure 8 shows the reactions when compressive forces are applied to a pile by Das (2007) for the ultimate pile load, Q_u.

$$Q_u = Q_p + Q_s \qquad [2.12]$$

Q_p = pile bearing capacity provided by pile tip

Q_s = pile bearing capacity provided by skin friction resistance of the pile surface

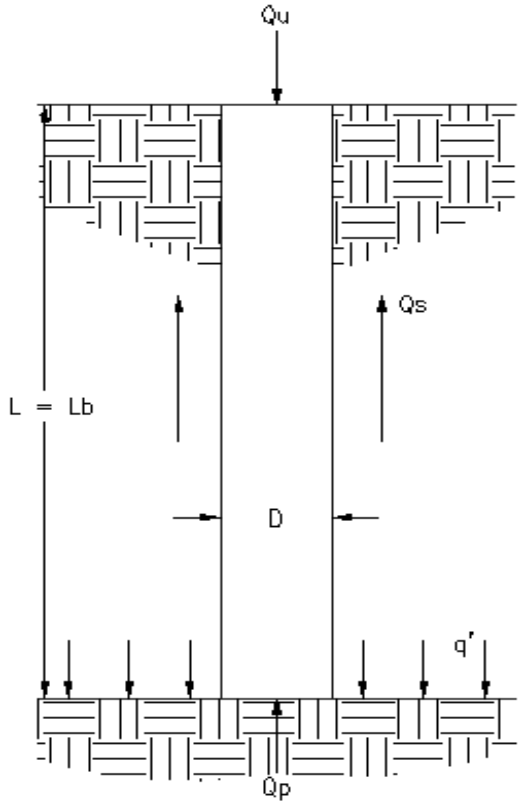

Figure 9-Effective Vertical Stress Free Body Diagram

2.7.3 Meyerhof's Point Bearing Capacity

Meyerhof (1976) developed methods for determining the point bearing capacity, q_p, for piles in sand using the following equation:

$$Q_p = A_p q_p = A_p q' N_q^* \qquad [2.13]$$

$A_p =$ area of the pile tip

$q_p =$ unit point resistance

$q' =$ effective vertical stress at the level of the pile tip

$N_q^* =$ bearing capacity factor

However, Q_p should not exceed the following equation:

$$Q_p \leq A_p q_l \quad [2.14]$$

$$q_l = 0.5 p_a N_q^* \tan\phi' \quad [2.15]$$

$p_a =$ atmospheric pressure (=100kN/m^2 or 2000 lb/ft^2)

$\phi' =$ effective soil friction angle of the bearing stratum

These values for N_q^* according to Meyerhof (1976) range from approximately 53 for $\phi' = 30°$ to approximately 310 for $\phi' = 40°$. Meyerhof also suggested that the ultimate point resistance q_l in a homogeneous granular soil may be obtained from standard penetration test results as:

$$q_l = 0.4 p_a N_{60} \frac{L}{D} \leq 4 p_a N_{60} \quad [2.16]$$

$N_{60} =$ the average value of the standard penetration number near the pile point (about 10D above and 4D below the pile point), where D is the pile diameter.

$L =$ length of Pile

2.7.4 Vesic's Point Bearing Capacity

Vesic et al. (1963) noted that the shaft friction is mobilized at small settlement (6 to 10mm) and that end bearing is not fully mobilized until much greater settlements of up to 30 percent of the pile diameter have occurred. According to Das (2007) and his comment on Vesic's theory for estimating Q_p based on the effective stress parameters the following equation was produced:

$$Q_p = A_p Q_p = A_p (c' N_c^* + \overline{\sigma}_o' N_\sigma^*) \quad [2.17]$$

c' = cohesion of soil = 0, for cohesionless soils

$\overline{\sigma}_o'$ = mean effective normal ground stress at the level of the pile point

N_c^*, N_σ^*, N_q = bearing capacity factors

$$\overline{\sigma}_o' = \left(\frac{1+2K_o}{3}\right) q' \quad [2.18]$$

K_o = earth pressure coefficient at rest

$$K_o = 1 - \sin\phi' \quad [2.19]$$

$$N_\sigma^* = \frac{3N_q^*}{(1+2K_o)} \quad [2.20]$$

$$N_c^* = \left(N_q^* - 1\right)\cot\phi' \quad [2.21]$$

2.7.5 Janbu's Point Bearing Capacity

Another method commonly used to calculate the point bearing capacity of a pile is defined by Janbu (1976) and provided by (Das, 2007). Janbu defines the ultimate point bearing capacity of a pile as follows:

$$Q_p = A_p(c' N_c^* + q' N_q^*) \quad [2.22]$$

$$N_q^* = (\tan\phi' + \sqrt{1+\tan^2\phi'})^2 (e^{2\eta'\tan\phi'}) \quad [2.23]$$

$$N_c^* = (N_q^* - 1)\cot\phi' \quad [2.24]$$

However, since *c'* is equal to zero for cohesionless soils, N_c^* may be neglected. The angle η' is defined by Das (2007) in tabular form where they can be related to the internal soil friction angle. This angle shows a relationship between the pile bearing point and the soil failure plane. This relationship shows that for η' equal to 75º (for cohesionless soils) N_c^* values range from 21.82 to 30.14 and Nq^* values range from 13.60 to 18.40 for ϕ' equal to 30º respectively. For denser cohesionless soils, η' equal to 90º can be anticipated. For this η' value, N_c^* values range from 48.11 to 75.31 and Nq^* values range from 75.31 to 64.20 for ϕ' equal to 40º respectively.

2.8 Summary

The ultimate capacity of ACIP piles could be the result of a variety of factors. The definition of failure was well stated by Leonard (1982) when failure was defined as "an unacceptable difference between expected and observed performance." This implies that if the total settlement exceeds the value which is allowed, this does not automatically suggest a failure in the foundation. The results of 66 load tests in cohesionless soils were performed by Neely (1991) and from these tests, the following conclusions were presented:

1. There is no indication of any significant difference between the shaft resistance of sand-cement grout piles and concrete piles.
2. Empirical methods for designing bored piles in sand consistently underestimated the ultimate bearing capacity of the ACIP piles.
3. The study showed that the parameters that provide the best design correlations, on the basis of standard penetration N-values, are the overall length of the pile and the SPT blow count at pile tip elevation.
4. The pile capacity may be substantially underestimated from bearing capacity calculations, if the pile has been undergrouted, i.e., the total grout volume is less than or a small percentage greater than the theoretical volume.

The piles in this study all provided grout factors greater than 1.15 and therefore undergrouting was not a concern. The SPT values were used to predict the in-situ soil properties so the bearing capacity at the pile tip elevation and the skin friction capacity could be

determined. The ultimate capacity was determined empirically and the load test data were interpreted using various methods to determine the actual ultimate capacity of the pile. In practice, the engineer divides the ultimate capacity of the pile by a factor of safety (usually 2 to 3) and therefore, has some room for error.

Due to the insufficient load test instrumentation of the ACIP piles in this study, the side frictional resistance and the point bearing capacity cannot be evaluated separately with the various methods of interpreting load test data. Therefore, the measured side frictional resistance and point bearing capacity cannot be compared to the predicted capacities separately with much confidence. This imprecise relation and multiple factors of uncertainty makes deep foundation engineering as much of an art as it is a science.

In this chapter, a literature review was performed to provide the reader with relevant information about (a) ACIP piles, (b) ACIP pile static load testing, (c) interpretation of static load test data, (d) analytical theories to determine pile capacity based on in-situ soil properties, and (e) properties derived from SPT testing and their possible relationship with each other.

CHAPTER 3 - METHODOLOGY

3.1 Introduction

This chapter discusses the methodology and analysis used in the static design of ACIP piles. Based on the results of the literature review found in Chapter Two, the application of more reliable empirical relationships may be applied to the design of ACIP piles in cohesionless soils. Data obtained from 25 load tests were analyzed and several methods of interpretation of load test data were studied to determine if a more precise empirical relationship exists between anticipated load and actual load resistance of the pile in the given soil conditions.

The methods studied were categorized as theory of soil interaction with pile and interpretation of load test data. The theory of soil interaction was performed by calculating the skin resistance of the shaft of the pile and several point bearing capacity equations. Based on the literature review the following methods were used to determine point bearing capacity: Meyerhof, Vesic, and Janbu. Multiple methods were used to determine which overall method, i.e., skin friction and/ or point bearing capacity would produce the closest relationship to ultimate capacity versus the actual load test data interpretation. The methodology used in this study includes data collection, compilation of data, comparison of the results, and analysis and evaluation of methods.

3.2 Data Collection

The data collected in this study were compiled from geotechnical investigations and ACIP pile load test reports from 13 sites along the Florida and Alabama coast. Data were acquired from MACTEC Engineering, Inc and Schmidt Dell & Associates. The majority of the ACIP pile load tests were performed on piles supporting condominium structures along the Gulf of Mexico. The ACIP piles varied in size from 14 to 16 inches in diameter and 18.5 to 80 feet in length below ground surface.

3.3 Compilation of Data

The geotechnical reports reviewed for each site provided information regarding soil classification, soil resistance to Standard Penetration Testing (SPT), ground water levels, and some laboratory results. The standard penetration test with a split spoon was used to collect soil samples and this information provided data that the engineer can use to estimate soil properties. The standard split-spoon consists of a steel tube that is split longitudinally into halves to remove the soil sample after driving. A borehole is created and then the split spoon is driven into the soil at the bottom of the borehole by means of a hammer blow. The hammer blows occur at the top of the drilling rod. The hammer has a weight of 140 lbs and drops a distance of 30 inches for each blow (Das, 2002). The total number of hammer blows which occur over the final 12 inches of split-spoon movement provide a field standard penetration number (N_f). N_f must be corrected for the overburden soil pressure. This corrected N_f value along with experience with soil conditions

in the areas of the load tests was used to determine in-situ soil properties. The water table at time of soil sampling was provided in each geotechnical report. Some reports also provided the 24 hour groundwater reading, which is the ground water level measured 24-hours after the soil was sampled. This ground water level is more accurate than the initial reading and was used as the depth to groundwater for analyzing the data for each load test.

The data obtained from the geotechnical reports were compiled for each load test. The sub-surface conditions were analyzed and compiled into singular generalized soil profiles (GSP) for the location of each load test. These soil profiles identify ground water table elevations, SPT values, and soil type. The data were then compiled into singular soil profiles to better understand the sub-surface conditions encountered by each ACIP test pile and to accurately compare the same soil profile for each empirical method used.

For each site, a load test was performed in general conformance to the method provided by American Society for Testing and Materials (ASTM) Designation D 1143-81 (Reapproved 1994) for each ACIP pile and the data were presented in a separate report for each site. The data were analyzed for each load test, and in most cases the data from each test were presented in a tabular format which provided measurements of the deflection (inches) of the top of the pile at a specified measured load (tons). The deflection, is the measurement of the pile butt movement in response to a given load, readings were averaged at each incremental load and a plot was created to graphically demonstrate the response. These graphs provided valuable information in regards to the behavior of the pile, most importantly, the piles reaction to unloading of compressive force

(known as the rebounding effect). The load test data along with the plots is presented in the Appendix D.

3.4 Comparison of Results

After compiling the data, the results were compared to determine if a relationship exists between the empirical relationships of anticipating the compressive load capacity of the pile and the load test interpretation methods. This empirical data were compared to the interpretation of the physical load test data. Most load test data analyzed did not provide extensive laboratory testing of the soils; therefore, the relationships drawn by SPT resistance are predicted using known relationships as described in Chapter Two. In each soil profile, the properties of the in-situ soils were given values of density, unit weight, and friction angle based from the SPT values provided in the geotechnical report.

For purposes of this study, the deflection of the test pile was not determined empirically. Therefore, the load test data results were directly compared statistically to the ultimate capacity determined by multiple theoretical methods without consideration for the anticipated deflection of the ACIP pile.

3.5 Analysis Data

Understanding the reasons why both the empirical methods and the interpretation of load test data provide a wide range of ultimate compressive capacities is a difficult task. Many factors

applied to the empirical equations, especially for point bearing capacity, i.e., Vesic, Meyerhof, and Janbu's methods vary by an order of magnitude in some cases. This has many researchers believing that this variation in bearing capacity factors is the reason why the range in ultimate pile capacity is so great. The intent of this research is to investigate the possible relationships that exists between the compressive load test results in cohesionless soils and (a) skin friction, (b) skin friction and Meyerhof's method of determining point bearing capacity, (c) skin friction and Vesic's method of determining point bearing capacity, and (d) skin friction and Janbu's method of determining point bearing capacity types.

3.6 Evaluation of Data

The chi-square test is used to test if a sample of data came from a population with a specific distribution (Snedecor and Cochran, 1989). Chi-Square was used to predict a relationship between each of the interpretation of the load test methods and each of the anticipated empirical relationship methods. The data in this study met the nine assumptions associated with this type of analysis: (a) random selection of data, (b) a sufficiently large sample size, (c) adequate cell sizes, (d) independent observations, (e) similar distributions, (f) known distribution, (g) non-directional hypotheses , (h) finite values, and (i) normal distribution of deviations (**http://www2.chass.ncsu.edu/garson/pA765/chisq.htm**, retrieved 2/5/08). For the Chi-Square goodness-of-fit computation the hypothesis is defined by the following two

statements (**http://www.itl.nist.gov/div898/handbook/eda/section3/eda35f.htm**, retrieved 2/8/08):

H_0: The data follow a specified distribution.

H: The data do not follow a specified distribution.

H_0 is defined as the null hypothesis, which states that during any analysis of physical load test data when compared to that of anticipated load test data, the result will show that a relationship exists. If a relationship does not exist, then the specific distribution will be analyzed as H. Chi-squared was used to prove that H_0 followed a specific distribution and if a Chi-squared value was determined to be equal to or less than 0.05, then the null hypothesis could be satisfied. The research hypotheses are shown in Appendix H, and were used to examine the relationship between load test data and predicted behaviors of ACIP pile in a predominantly granular soil profile.

The data are divided into *k* bins and the test statistic is defined as:

$$\chi^2 = \sum_{i=1}^{k} (Q_i - E_i)^2 / E_i \qquad [3.1]$$

Q_i = observed frequency for bin i

E_i = the expected frequency for bin i, where:

$E_i = N(F(Y_u) - F(Y_l))$

F = the cumulative distribution function for the distribution being tested

Y_u = the upper limit for class i

Y_l = the lower limit for class i

N = the sample size

Furthermore, eta squared was performed (as defined by H) to determine the best relationship between the interpretation of the load test methods and the anticipated empirical relationship methods since H_0 was not satisfied. Eta squared is the percent of variance in the dependent variable explained linearly by the independent variable (Kirk, 1982) (**http://www2.chass.ncsu.edu/garson/pa765/eta.htm**, retrieved 2/6/08). Eta squared can be defined by the following equation:

$$\eta^2 = \frac{SS_{effect}}{SS_{total}} \qquad [3.2]$$ where:

SS_{effect} = effective variance

SS_{total} = total variance

The results of the eta squared test produced predicted relationships between the methods of determining compressive capacity of ACIP piles and the load test interpretation of compressive capacities using the eta squared technique. The association between values produced using the eta squared technique can be found using Table 3.1 (Tabachnick and Fidell, 1989).

Table 1 Eta Relationship Table

Eta Relationships Between Nominal and Interval Variables	
Eta Value	***Association Between Variables***
0 to 0.09	No Association
0.1 to 0.29	Small Association
0.3 to 0.49	Moderately Small Association
0.5 to 0.69	Moderate Association
0.7 to 0.89	Moderately Large Association
0.9 to 0.99	Large Association
1.0	Perfect Association

For the data which had an eta value of 0.737 it can be described as "There is a moderately large association between the method of interpretation of load test data provided by the Army Corps of Engineers and the anticipated capacity of the ACIP pile using the combined Meyerhof's point bearing capacity equation and skin friction equation," as shown in Chapter 2.

3.7 Research Design

The design used in this study is a correlational design. The goal of correlational research is to identify predictive relationships. When two variables are related, predictions can be made

for the variables. However, inferences about the cause of the relationship cannot be made, which is the greatest limitation of the correlational design.

3.8 Summary

The chi-squared and eta-squared methods were chosen based on the type of data which were to be analyzed. Since the load test data is nominal, chi-squared provided a way to generalize the strength of relationship and determine the probability value between the interpretation of load test results and anticipated load capacity of each ACIP test pile. Probability values equal to or less than 0.05 can be generalized as part of the population. The eta-squared values show that as the probability value approaches 1.0, the data can be generalized into better fit and therefore, a relationship can be drawn from which shows statistically which interpretation of load test data method is best fit with which method of predicting compressive capacity of ACIP piles.

The average capacities determined by empirical relationships are shown graphically versus the interpretation of physical load test data. From this data shown in Figure 9 and Table 2, the compressive behavior of the ACIP pile can be studied, and Davisson's method for predicting ultimate capacity based on load test data can be compared. In most cases the pile was compressively loaded then unloaded and reloaded. When this loading information was available, it was graphically presented versus the elastic behavior criteria and Davisson's method, as shown in Appendix D. From the graphical data, it can be seen that the elastic equation (presented in

Chapter-2) does generally follow the compressive behavior of the ACIP pile during its first loading cycle. However, when the pile was re-loaded, the Davisson failure line generally followed the reloaded compressive behavior characteristics of the ACIP pile.

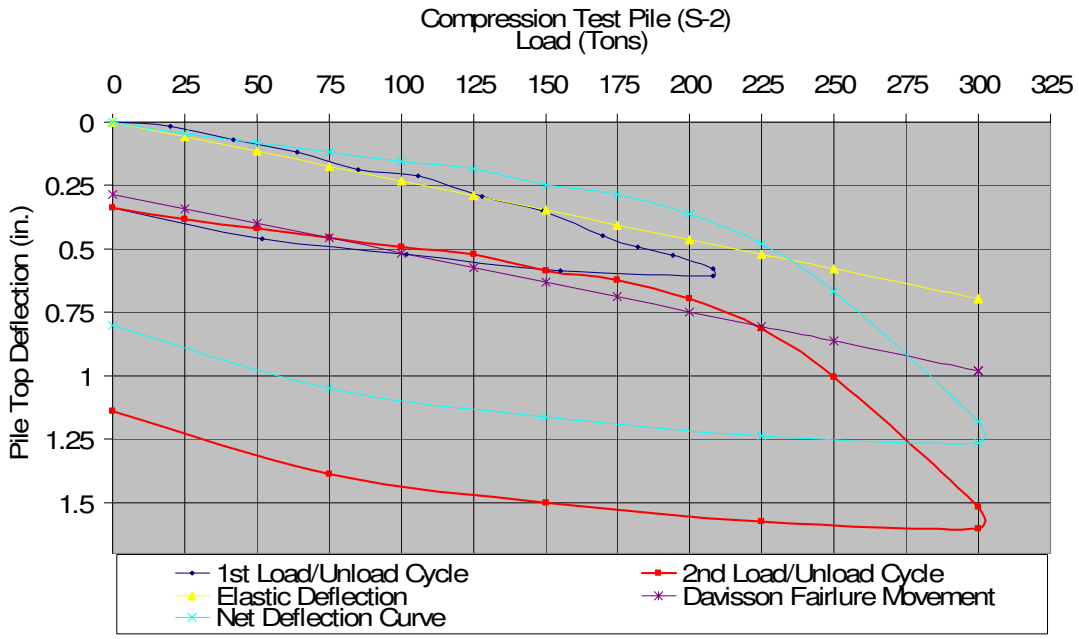

Figure 10-Load Deflection Plot Sample No. 2

Table 2-Load Test Data Sample No. 2, Test Pile No.1

Sample 2		**Compression Test**	
1st Load / Unload Cycle		2nd Load / Unload Cycle	
Applied Test Load (tons)	**Pile Top Deflection (in.)**	**Test Load (tons)**	**Pile Top Deflection (in.)**
0	0	0	0.337
20	0.018	25	0.383
42	0.071	50	0.418
64	0.118	75	0.455
85	0.189	100	0.492
106	0.213	125	0.52
128	0.291	150	0.587
149	0.35	175	0.622
170	0.447	200	0.697
182	0.491	225	0.815
194	0.526	250	1.003
208	0.579	300	1.516
208	0.606	300	1.602
155	0.586	225	1.574
102	0.522	150	1.502
52	0.461	75	1.387
0	0.337	0	1.137

CHAPTER 4 – DISCUSSION OF RESULTS

4.1 Results

The following sections describe the results of this study as they relate to the research question:

1. Will there be a difference between anticipated empirical capacity equations and interpreted physical load test data?
2. If there is a difference between anticipated empirical capacity equations and interpreted physical load test data, determine the significance of the variation between the two methods.
3. If there is a difference between anticipated empirical capacity equations and interpreted physical load test data, determine which methods provide the best fit relationship when compared to one another.
4. If there is a best fit relationship between interpreted physical load test data and anticipated empirical capacity equations, can an empirical method of predicting anticipated compressive capacity be determined to provide a better fit between methods?

The independent variable in the study is the method of analyzing data. The independent variable has the following fourteen levels: a) the ultimate pile capacity determined by skin friction only, b) the ultimate pile capacity determined skin friction only with adjusted earth pressure coefficients, c) the ultimate pile capacity determined by skin friction and tip bearing resistance based on Meyerhof's analysis, d) the ultimate pile capacity determined skin friction

with adjusted earth pressure coefficients and tip bearing resistance based on Meyerhof's analysis, e) the ultimate pile capacity determined by skin friction and tip bearing resistance based on Vesic's analysis, f) the ultimate pile capacity determined skin friction and tip bearing resistance based on Vesic's analysis and adjusted earth pressure coefficients, g) the ultimate pile capacity determined by skin friction and tip bearing resistance based on Janbu's analysis, h) the ultimate pile capacity determined by skin friction and tip bearing resistance based on Janbu's analysis and adjusted earth pressure coefficients, i) the ultimate pile capacity defined by Davisson's analysis of physical load test data, j) the ultimate pile capacity defined by Chin-Kondner's analysis of physical load test data at a net deflection of 0.25 inches, k) the ultimate pile capacity defined by Chin-Kondner's analysis of physical load test data at a deflection not to exceed 5% of the pile diameter, l) the ultimate pile capacity defined by the Army Corps of Engineers analysis of physical load test data at 0.25 inches of actual net deflection, m) the ultimate pile capacity defined by the Tangent method analysis of physical load test data, n) the ultimate capacity defined by Chin-Kondner's analysis of physical load test data without any net deflection criteria. The dependent variable in the study is the ultimate load capacity.

4.2 Analysis of Data

Data was analyzed using the chi squared method in SPSS. The results of this analysis are presented in Table-2.

Table 3-Chi-Squared & Eta Analysis of Data

Chi Squared Results (N=25)				
Analyzed Method	***Chi Squared***	***Significance (2-Tailed)***	***Degrees of Freedom***	***Eta Squared***
Skin Friction vs. Davisson Failure	46	0.205	24	0.322
Skin Friction vs. Chin Capacity (0.25 in)	46	0.349	24	0.287
Skin Friction vs. Chin Capacity (5% pile diameter)	44	0.514	24	0.34
Skin Friction vs. Army Corps	50	0.355	24	0.346
Skin Friction vs. Tangent Method	48	0.277	24	0.315
Skin Friction vs. Chin Ultimate (no deflection criteria)	50	0.281	24	0.664
Skin Friction Adjusted K's vs. Davisson Failure	44.57	0.215	24	0.157
Skin Friction Adjusted K's vs. Chin Capacity (0.25 in)	50	0.247	24	0.42
Skin Friction Adjusted K's vs. Chin Capacity (5% pile diameter)	41.33	0.544	24	0.154
Skin Friction Adjusted K's w/ Meyerhof vs. Army Corps	45.33	0.416	24	0.471
Skin Friction Adjusted K's vs. Tangent Method	47.33	0.264	24	0.445
Skin Friction Adjusted K's w/ Meyerhof vs. Chin Ultimate (no deflection criteria)	46	0.349	24	0.597
Skin Friction w/ Meyerhof vs. Davisson Failure	47	0.209	24	0.225
Skin Friction w/ Meyerhof vs. Chin Capacity (0.25 in)	50	0.185	24	0.646
Skin Friction w/ Meyerhof vs. Chin Capacity (5% pile diameter)	46	0.349	24	0.270

Chi Squared Results (N=25)				
Analyzed Method	***Chi Squared***	***Significance (2-Tailed)***	***Degrees of Freedom***	***Eta Squared***
Skin Friction w/ Meyerhof vs. Army Corps	50	0.247	24	0.677
Skin Friction w/ Meyerhof vs. Tangent Method	50	0.157	24	0.662
Skin Friction w/ Meyerhof vs. Chin Ultimate (no deflection criteria)	44	0.268	24	0.384
Skin Friction Adjusted K's w/ Meyerhof vs. Davisson Failure	48	0.21	24	0.303
Skin Friction Adjusted K's w/ Meyerhof vs. Chin Capacity (0.25 in)	50	0.185	24	0.646
Skin Friction Adjusted K's w/ Meyerhof vs. Chin Capacity (5% pile diameter)	48	0.432	24	0.357
Skin Friction Adjusted K's w/ Meyerhof vs. Army Corps	48	0.392	24	0.718
Skin Friction Adjusted K's w/ Meyerhof vs. Tangent Method	50	0.247	24	0.662
Skin Friction Adjusted K's w/ Meyerhof vs. Chin Ultimate (no deflection criteria)	48	0.314	24	0.327
Skin Friction w/ Vesic vs. Davisson Failure	50	0.134	24	0.190
Skin Friction w/ Vesic vs. Chin Capacity (0.25 in)	46	0.31	24	0.638
Skin Friction w/ Vesic vs. Chin Capacity (5% pile diameter)	50	0.355	24	0.226
Skin Friction w/ Vesic vs. Army Corps	46	0.389	24	0.673
Skin Friction w/ Vesic vs. Tangent Method	50	0.215	24	0.655
Skin Friction w/ Vesic vs. Chin Ultimate (no deflection criteria)	50	0.247	24	0.423
Skin Friction Adjusted K's w/ Vesic vs. Davisson Failure	44	0.232	24	0.319
Skin Friction w/ Vesic vs. Chin Capacity (0.25 in)	48	0.314	24	0.681

Chi Squared Results (N=25)				
Analyzed Method	***Chi Squared***	***Significance (2-Tailed)***	***Degrees of Freedom***	***Eta Squared***
Skin Friction Adjusted K's w/ Vesic vs. Chin Capacity (5% pile diameter)	46	0.472	24	0.358
Skin Friction Adjusted K's w/ Vesic vs. Army Corps	46	0.431	24	0.708
Skin Friction Adjusted K's w/ Vesic vs. Tangent Method	45.33	0.335	24	0.694
Skin Friction Adjusted K's w/ Vesic vs. Chin Ultimate (no deflection criteria)	46	0.349	24	0.311
Skin Friction w/ Janbu vs. Davisson Failure	46	0.238	24	0.023
Skin Friction w/ Janbu vs. Chin Capacity (0.25 in)	47.33	0.378	24	0.549
Skin Friction w/ Janbu vs. Chin Capacity (5% pile diameter)	44	0.556	24	0.046
Skin Friction w/ Janbu vs. Army Corps	50	0.394	24	0.592
Skin Friction w/ Janbu vs. Tangent Method	48	0.314	24	0.57
Skin Friction w/ Janbu vs. Chin Ultimate (no deflection criteria)	50	0.318	24	0.517
Skin Friction Adjusted K's w/ Janbu vs. Davisson Failure	50	0.185	24	0.17
Skin Friction w/ Janbu vs. Chin Capacity (0.25 in)	50	0.318	24	0.617
Skin Friction Adjusted K's w/ Janbu vs. Chin Capacity (5% pile diameter)	50	0.433	24	0.204
Skin Friction Adjusted K's w/ Janbu vs. Army Corps	48	0.432	24	0.652
Skin Friction Adjusted K's w/ Janbu vs. Tangent Method	50	0.281	24	0.634
Skin Friction Adjusted K's w/ Janbu vs. Chin Ultimate (no deflection criteria)	50	0.318	24	0.429

The Chi-Square, degrees of freedom, significance level, and ETA are presented in Table 4.1. An examination of Table 4.1 suggests no significant difference exists between the mean of any of the empirical relationships of anticipating the compressive load capacity of the pile compared to the interpretation of the physical load test data at the .05 level with the following results: (a) Skin Friction vs. Davisson Failure, χ^2 (24, N = 25) = 46, p = .205, (b) Skin Friction vs. Chin Capacity (.25 in.), χ^2 (24, N = 25) = 46, p = .349, (c) Skin Friction vs. Chin Capacity (5% pile diameter), χ^2 (24, N = 25) = 44, p = .514, (d) Skin Friction vs. Army Corps, χ^2 (24, N = 25) = 50, p = .355, (e) Skin Friction vs. Tangent Method, χ^2 (24, N = 25) = 48, p = .277, (f) Skin Friction vs. Chin Ultimate (no deflection criteria), χ^2 (24, N = 25) = 50, p = .281, (g) Skin Friction Adjusted K's vs. Davisson Failure, χ^2 (24, N = 25) = 44.57, p = .215, (h) Skin Friction Adjusted K's vs. Chin Capacity (0.25 in), χ^2 (24, N = 25) = 50, p = .247, (i) Skin Friction Adjusted K's vs. Chin Capacity (5% pile diameter), χ^2 (24, N = 25) = 41.33, p = .544, (j) Skin Friction Adjusted K's w/ Meyerhof vs. Army Corps, χ^2 (24, N = 25) = 45.33, p = .416, (k) Skin Friction Adjusted K's vs. Tangent Method, χ^2 (24, N = 25) = 47.33, p = .264, (l) Skin Friction Adjusted K's w/ Meyerhof vs. Chin Ultimate (no deflection criteria), χ^2 (24, N = 25) = 46, p = .349, (m) Skin Friction w/ Meyerhof vs. Davisson Failure, χ^2 (24, N = 25) = 47, p = .225, (n) Skin Friction w/ Meyerhof vs. Chin Capacity (0.25 in), χ^2 (24, N = 25) = 50, p = .646, (o) Skin Friction w/ Meyerhof vs. Chin Capacity (5% pile diameter), χ^2 (24, N = 25) = 46, p = .270, (p) Skin Friction w/ Meyerhof vs. Army Corps, χ^2 (24, N = 25) = 50, p = .677, (q) Skin Friction w/ Meyerhof vs. Tangent Method, χ^2 (24, N = 25) = 50, p = .662, (r) Skin Friction w/ Meyerhof vs. Chin Ultimate (no deflection criteria), χ^2 (24, N = 25) = 44, p = .384, (s) Skin Friction Adjusted

K's vs. Davisson Failure, $\chi^2(24, N = 25) = 42.57$, $p = .303$, (t) Skin Friction w/ Meyerhof vs. Chin Capacity (0.25 in), $\chi^2(24, N = 25) = 50$, $p = .646$, (u) Skin Friction Adjusted K's w/ Meyerhof vs. Chin Capacity (5% pile diameter), $\chi^2(24, N = 25) = 48$, $p = .357$, (v) Skin Friction Adjusted K's w/ Meyerhof vs. Army Corps, $\chi^2(24, N = 25) = 48$, $p = .718$, (w) Skin Friction Adjusted K's w/ Meyerhof vs. Tangent Method, $\chi^2(24, N = 25) = 50$, $p = .662$, (x) Skin Friction Adjusted K's w/ Meyerhof vs. Chin Ultimate (no deflection criteria), χ^2 (24, N =25) = 48, $p =$ .327, (y) Skin Friction w/ Vesic vs. Davisson Failure, $\chi^2(24, N = 25) = 50$, $p = .190$, (z) Skin Friction w/ Vesic vs. Chin Capacity (0.25 in), $\chi^2(24, N = 25) = 46$, $p = .638$, (aa) Skin Friction w/ Vesic vs. Chin Capacity (5% pile diameter), $\chi^2(24, N = 25) = 50$, $p = .226$, (bb) Skin Friction w/ Vesic vs. Army Corps, $\chi^2(24, N = 25) = 46$, $p = .673$, (cc) Skin Friction w/ Vesic vs. Tangent Method, $\chi^2(24, N = 25) = 50$, $p = .655$, (dd) Skin Friction w/ Vesic vs. Chin Ultimate (no deflection criteria), $\chi^2(24, N = 25) = 50$, $p = .423$, (ee) Skin Friction Adjusted K's w/ Vesic vs. Davisson Failure, $\chi^2(24, N = 25) = 44$, $p = .319$, (ff) Skin Friction w/ Vesic vs. Chin Capacity (0.25 in), $\chi^2(24, N = 25) = 48$, $p = .681$, (gg) Skin Friction Adjusted K's w/ Vesic vs. Chin Capacity (5% pile diameter), $\chi^2(24, N = 25) = 46$, $p = .358$, (hh) Skin Friction Adjusted K's w/ Vesic vs. Army Corps, $\chi^2(24, N = 25) = 46$, $p = .708$, (ii) Skin Friction Adjusted K's w/ Vesic vs. Tangent Method, $\chi^2(24, N = 25) = 45.33$, $p = .694$, (jj) Skin Friction Adjusted K's w/ Vesic vs. Chin Ultimate (no deflection criteria), $\chi^2(24, N = 25) = 46$, $p = .311$, (kk) Skin Friction w/ Janbu vs. Davisson Failure, $\chi^2(24, N = 25) = 46$, $p = .023$, (ll) Skin Friction w/ Janbu vs. Chin Capacity (0.25 in), $\chi^2(24, N = 25) = 47.33$, $p = .549$, (mm) Skin Friction

w/ Janbu vs. Chin Capacity (5% pile diameter), χ^2(24, N = 25) = 44, p = .046, (nn) Skin Friction w/ Janbu vs. Army Corps, χ^2(24, N = 25) = 50, p = .592, (oo) Skin Friction w/ Janbu vs. Tangent Method, χ^2(24, N = 25) = 48, p = .570, (pp) Skin Friction w/ Janbu vs. Chin Ultimate (no deflection criteria), χ^2 (24, N = 25) = 50, p = .517, (qq) Skin Friction Adjusted K's w/ Janbu vs. Davisson Failure, χ^2(24, N = 25) = 50, p = .170, (rr) Skin Friction w/ Janbu vs. Chin Capacity (0.25 in), χ^2(24, N = 25) = 50, p = .617, (ss) Skin Friction Adjusted K's w/ Janbu vs. Chin Capacity (5% pile diameter), χ^2(24, N = 25) = 50, p = .204, (tt) Skin Friction Adjusted K's w/ Janbu vs. Army Corps, χ^2(24, N = 25) = 48, p = .652, (uu) Skin Friction Adjusted K's w/ Janbu vs. Tangent Method, χ^2(24, N = 25) = 50, p = .634, and (vv) Skin Friction Adjusted K's w/ Janbu vs. Chin Ultimate (no deflection criteria), χ^2(24, N = 25) = 50, p = .429.

The results of the eta squared test produced values which ranged from 0.017 to 0.718 as shown in Table 4.1. The eta values produced for each independent load test and empirical method of determining capacity were summed and averaged to determine which empirical method produced the most reliable results. The following Table-3 provides the average eta squared value obtained when analyzing the anticipated capacity versus the interpretation of load test results:

Table 4-Eta Squared Values for Empirical Methods of Determining Ultimate Capacity

Averaged Eta-Squared Values For Anticipated Compressive Load Capacity vs. Interpretation of Load Test Results	
Method of Calculating Expected Compressive Capacity	***Eta-Squared Value***
Skin Friction Variable K's	0.374
Skin Friction Constant K's	0.379
Meyerhof Variable K's	0.477
Meyerhof Constant K's	0.517
Vesic Variable K's	0.468
Vesic Constant K's	0.512
Janbu Variable K's	0.383
Janbu Constant K’s	0.451

From the results provided by averaging the eta squared values, it was determined that the Meyerhof point bearing capacity equation in conjunction with the skin friction resistance with adjusted K-values, shows that a “Moderate Association” (as defined by Table 3.1) exists between the anticipated capacity when comparing versus the interpretation of load test data.

4.3 Chapter Summary

The data analysis and results were described in this chapter. Quantitative data were collected from 25 independent samples and were analyzed using Chi-Square in order to compare the mean scores of the dependent variables and determine if a predictive relationship exists.

The null hypothesis and the alternative hypothesis were investigated for a) the ultimate pile capacity determined by skin friction only, b) the ultimate pile capacity determined skin

friction only with adjusted earth pressure coefficients, c) the ultimate pile capacity determined by skin friction and tip bearing resistance based on Meyerhof's analysis, d) the ultimate pile capacity determined by skin friction with adjusted earth pressure coefficients and tip bearing resistance based on Meyerhof's analysis, e) the ultimate pile capacity determined by skin friction and tip bearing resistance based on Vesic's analysis, f) the ultimate pile capacity determined skin by friction and tip bearing resistance based on Vesic's analysis and adjusted earth pressure coefficients, g) the ultimate pile capacity determined by skin friction and tip bearing resistance based on Janbu's analysis, h) the ultimate pile capacity determined by skin friction and tip bearing resistance based on Janbu's analysis and adjusted earth pressure coefficients, i) the ultimate pile capacity defined by Davisson's analysis of physical load test data, j) the ultimate pile capacity defined by Chin-Kondner's analysis of physical load test data at a net deflection of 0.25 inches, k) the ultimate pile capacity defined by Chin-Kondner's analysis of physical load test data at a deflection not to exceed 5% of the pile diameter, l) the ultimate pile capacity defined by the Army Corps of Engineers analysis of physical load test data at 0.25 inches of actual net deflection, m) the ultimate pile capacity defined by the Tangent method analysis of physical load test data, n) the ultimate capacity defined by Chin-Kondner's analysis of physical load test data without any net deflection criteria. No significance was found in any of the 48 tests; therefore, the null hypothesis for each chi-square test could not be rejected.

The averaged eta squared values for each method of predicting compressive capacities of ACIP piles were compared to all of the methods of interpretation of load test data, which provided results that ranged from 0.374 to 0.539. These results show that a "Moderately Small Association" to "Moderate Association" exists between the methods for predicting the compressive capacity of ACIP piles and all of the results provided by the interpretation of load

test data. Therefore, a relationship can be drawn that identifies which anticipated method of determining compressive capacities of ACIP piles in cohesionless soils produce the more reliable results. From this analysis, the Meyerhof point bearing capacity in conjunction with the skin friction resistance equation and incorporating adjusted K-values produce an eta squared value which shows the greatest association between physical load test data and empirical methods of determining compressive capacities of ACIP piles in cohesionless soils.

CHAPTER 5 - CONCLUSIONS

5.1 Summary

The purpose of this study was to examine current methods used to predict the ultimate capacity of Augered Cast-In-Place piles, and if possible, determine a better empirical relationship between anticipated capacities versus physical load test data. This study analyzed the fundamental reactions of a pile while resisting compressive forces. The methods used in this study are commonly used in practice today to anticipate the ultimate compression capacity of piles. The methods used included (a) skin friction, (b) Meyerhof's point bearing capacity, (c) Janbu's point bearing capacity, and (d) Vesic's point bearing capacity. Variations of constant and variable lateral earth pressure coefficients were examined and applied to the skin friction capacities to determine if a better relationship exists between anticipated versus actual load test results. Also, the point bearing methods, as mentioned previously were combined with the skin friction capacities with and without the adjusted lateral earth pressure coefficients. This was performed to statistically prove if a relationship existed between the six empirical methods and the eight interpretations of physical load test data methods.

A total of 48 combinations were studied to determine which method of empirically method of predicting the ultimate capacity which most closely related to the methods of analyzing physical load test data based on studies performed by (a) Davisson, (b) Chin, (c) Tangent Method, and (d) Army Corp's of Engineers suggested 0.25inches of net deflection criteria. From this analysis using SPSS software, the averages of each empirical method versus the interpretation of all physical load test data methods was performed. The results of this study

showed that increasing the lateral earth pressure coefficients, resulted in increased skin friction capacity and provided a slightly better relationship with load test data. However, it was shown in Chapter 4 that this small increase in probability is magnified when summed with the point bearing tip capacities. This was true since the load test data consistently produced greater compressive capacities than the methods of predicting capacity provided.

The review of literature on Augered Cast-In-Place piles provided an overview of many possible variables that could influence the anticipated capacities and the interpretation of physical load test data for predicting ultimate capacities of piles. Some areas which presented variations with the empirical predicted capacities included the point bearing capacity equations which were utilized in this study. The capacities provided by the point bearing analysis sometimes varied over 80%. In some cases, this was an increase in pile compression ultimate capacity of over 120 tons. With this type of variation with the empirical methods, it makes it difficult to determine if a better empirical relationship exists. The empirical methods used in this study, when compared to the methods for interpreting load test data were analyzed and it was determined, that the combination of skin friction with adjusted lateral earth pressure coefficients and Meyerhof's method for predicting point bearing resistance provided the most reliable data. When this method was compared to skin friction with in-situ lateral earth pressure coefficients, the statistical analysis showed that Meyerhof's method along with the skin friction resistance based on in-situ lateral earth pressure coefficients was less accurate than when adjusting the lateral earth pressure coefficients. The lateral earth pressure coefficients were adjusted based on the theory that the constant pressure during the grouting of the ACIP pile densifies the soil surrounding the shaft of the pile during the radial displacement of soil and injection of

pressurized gout. Therefore, a constant value of two was used for the lateral earth pressure coefficient. If the relationship were drawn out further and based on predicted results from this study, the lateral earth pressure coefficient may be increased further and this could provide a more reliable prediction of compressive capacity of ACIP piles.

The presentation of this information, along with the results of the study, has provided a base to discuss the ways that ACIP pile load behaviors under compressive loading can be further predicted more accurately. With the increasing size of super structures along the gulf coast, it is feasible to believe that the use of ACIP piles may only continue to become more popular with the construction of deep foundations. Based on the findings of this study, it was discovered that Davisson's interpretation of physical load test data is quite conservative. However, it was determined both statistically and through literature review that Chin's method for ultimate capacity provided results which are quite larger than all other methods analyzed in this study. In addition, Chin's method no longer be an approved method in the upcoming addition of the International Building Code for methods allowable to predict ultimate capacity. The International Building Code authorities recommend a factor of safety, i.e., the ultimate load divided by the factor of safety that will produce the allowable capacity, of three to six.

The quantitative research questions studied in this project were:

1. Will there be a difference between anticipated empirical capacity equations and interpreted physical load test data?

2. If there is a difference between anticipated empirical capacity equations and interpreted physical load test data, determine the significance of the variation between the two methods.
3. If there is a difference between anticipated empirical capacity equations and interpreted physical load test data, determine which methods provide the best fit relationship when compared to one another.
4. If there is a best fit relationship between interpreted physical load test data and anticipated empirical capacity equations, can an empirical method of predicting anticipated compressive capacity be determined to provide a better fit between methods?

Based on the analysis of this research, there is a no significant difference between the anticipated empirical capacity equations and the interpreted physical load test methods. This lack of significant difference may be due to the uncertainty in the soil conditions, the limited soil test data provided, the proficiency of sampling of soil techniques, the proficiency of testing the test pile, or the engineering formulas currently available. It is clear that the uncertainty in multiple variables lends a higher factor of safety to be applied to the ultimate capacity. These uncertainties in soil conditions and pile interactions with soil have historically led to the over design of pile foundations. These uncertainties have resulted in the conclusion that pile load tests should be utilized to design with a high confidence and lower factor of safety, thus providing a more efficient deep foundation design.

The interpreted physical load test data and the methods for predicting compressive capacities of ACIP piles were examined using the Eta-squared method to determine best fit relationships. It was determined that Meyerhof's method of determining point bearing capacity

of the pile in conjunction with skin friction statistically provide more accurate results when compared with the interpreted physical load test data. The anticipated compressive capacities of all 25 samples were re-calculated using an adjusted lateral earth pressure coefficient value of 2.0. Once this analysis was completed, the Eta-squared method was performed to analyze the interpreted physical load test data versus this constant lateral earth pressure value. The results concluded that the adjusted value did provide results which had a better fit than with the lower adjustable values based on SPT values. These results are shown in Table-2.

The ultimate capacities were not provided with the data for each sample, however, based on this study, the empirical methods used typically underestimate the compression capacity of ACIP in cohesionless soils and therefore provide an increased factor of safety. Consequently, when applying further factors of safety, it assures the engineer with a higher confidence that the ultimate capacity threshold of the pile interaction with the soil will most likely not be obtained.

The findings of this study may benefit the geotechnical engineering community by allowing them to predict with more reliability the behaviors of ACIP piles in cohesionless soil conditions. To further this study, more data would need to be gathered and analyzed. This study provides a better understanding of pile-soil interaction in cohesionless soils which may potentially allow engineers to design with more certainty the ACIP piles, needed to feasibly support the super-structure.

APPENDIX A
PILE CALCULATED AND INTERPRATED COMPRESSION CAPACITY SUMMARY TABLES

Table 5-Summary Table of Each Load Test Performed and Pile Criteria

Job I.D.	W.T. Depth (ft.)	Percent Granular	Percent Cohesive	Pile Diameter (in.)	Pile Length (ft.)	Pile Tip Elev. (ft.)	Load Test Method
1	27	100.0%	0.0%	14	52	-28	Quick
2	10	100.0%	0.0%	16	70	-67	Quick
3	8	100.0%	0.0%	16	65	-60	Quick
4	6	100.0%	0.0%	14	45	-40	Quick
5A -TP1	7	100.0%	0.0%	16	71.5	-59.75	Quick
5B- TP2	7	100.0%	0.0%	16	71.5	-59.75	Quick
5C- TP3	7	100.0%	0.0%	16	71.5	-59.75	Quick
6A- TP1	5	100.0%	0.0%	14	18.5	-5	Quick
6B- TP2	5	100.0%	0.0%	14	21.5	2	Quick
7	10	100.0%	0.0%	18	31	-11	Quick
8A- TP1	3	100.0%	0.0%	16	50	-44.5	Quick
8B- TP2	3	100.0%	0.0%	16	50	-44.5	Quick
9	10	100.0%	0.0%	14	50	-33	Quick
10A- TP1	3	100.0%	0.0%	16	80	Varies	Long
10B- TP2	3	100.0%	0.0%	16	80	Varies	Long
10C- TP3	3	100.0%	0.0%	16	80	Varies	Long
11	100	100.0%	0.0%	16	52	Varies	Long
12A- TP1	7	100.0%	0.0%	16	69	-55.5	Quick
12B- TP2	7	100.0%	0.0%	16	69	-55.5	Quick
12C- TP3	7	100.0%	0.0%	16	69	-55.5	Quick
13A- TP1	10	100.0%	0.0%	14	40	-26.5	Long
13B- TP2	10	100.0%	0.0%	14	55	-41.5	Long
13C- TP3	10	100.0%	0.0%	14	50	-36.5	Long
13D- TP4	10	100.0%	0.0%	14	80	-66.5	Long
13E- TP5	10	100.0%	0.0%	14	55	-41.5	Long

Table 6-Summary Table No. 1 of Load Test Samples and Empirical Methods to Predict Ultimate Compression Capacity

Job I.D.	Load Applied (Tons)	Allowable Deflection @ 5% pile diameter	Net Deflection (in.)	Ultimate Pile Capacity Friction (Q_{fs}) determined by Effective Stress Varying K's (tons)	Ultimate Pile Capacity Friction (Q_{fs}) determined by Effective Stress Constant K's (tons)
1	210	0.7	0.0095	239	264
2	300	0.8	0.8	154	174
3	300	0.8	0.455	409	454
4	210	0.7	0.556	136	136
5A	300	0.8	0.64	176	226
5B	300	0.8	0.42	208	247
5C	300	0.8	0.53	214	269
6A	190	0.7	0.573	31	36
6B	190	0.7	0.501	32	43
7	150	0.9	0.987	103	119
8A	150	0.8	0.44	127	136
8B	150	0.8	0.346	175	177
9	200	0.7	0.922	221	231
10A	300	0.8	1.006	290	299
10B	300	0.8	1.11	268	288
10C	300	0.8	1.089	66	71
11	131	0.8	0.094	177	246
12A	290	0.8	0.72	250	300
12B	290	0.8	0.77	249	302
12C	290	0.8	0.68	210	292
13A	218	0.7	0.7	115	138
13B	320	0.7	0.7	187	217
13C	320	0.7	0.7	163	192
13D	490	0.7	0.7	307	343
13E	320	0.7	0.7	187	217

Table 7-Summary Table No. 2 of Load Test Samples and Empirical Methods to Predict Ultimate Compression Capacity

Job I.D.	Ultimate Pile Capacity total (Q_{all}) determined by Effective Stress Varying K's (tons) w/ Meyerhof Point Capacity	Ultimate Pile Capacity total (Q_{all}) determined by Effective Stress Constant K's (tons) w/ Meyerhof Point Capacity	Ultimate Pile Capacity total (Q_{all}) determined by Effective Stress Varying K's (tons) w/ Vesic Point Capacity	Ultimate Pile Capacity total (Q_{all}) determined by Effective Stress Constant K's (tons) w/ Vesic Point Capacity
1	331	356	444	468
2	399	441	415	456
3	488	533	550	627
4	213	136	195	195
5A	294	349	245	295
5B	300	338	279	318
5C	294	356	306	362
6A	105	116	88	99
6B	114	126	98	109
7	188	204	219	231
8A	210	219	188	196
8B	265	267	253	255
9	369	379	334	345
10A	380	389	365	374
10B	358	378	310	330
10C	124	119	106	111
11	267	336	312	381
12A	345	345	351	400
12B	344	347	301	354
12C	294	376	317	399
13A	207	230	253	276
13B	279	309	269	299
13C	255	284	247	275
13D	399	435	389	425
13E	279	309	269	299

Table 8-Summary Table No. 3 of Load Test Samples and Empirical Methods to Predict Ultimate Compression Capacity

Job I.D.	Ultimate Pile Capacity total (Q_{all}) determined by Effective Stress Varying K's (tons) w/ Janbu Point Capacity	Ultimate Pile Capacity total (Q_{all}) determined by Effective Stress Constant K's (tons) w/ Janbu Point Capacity
1	402	426
2	393	434
3	479	525
4	181	181
5A	231	278
5B	265	304
5C	247	302
6A	71	82
6B	80	91
7	190	206
8A	174	182
8B	220	222
9	295	305
10A	349	351
10B	314	334
10C	89	94
11	225	294
12A	328	377
12B	326	379
12C	234	316
13A	146	169
13B	224	254
13C	204	233
13D	348	385
13E	229	259

Table 9-Summary Table No. 1 of Load Test Samples and Methods of Interpretation of Physical Load Test Data to Predict Ultimate Compression Capacity

Job I.D.	Davisson Failure Movement (in)	Davisson Failure Movement Applied Load (Tons) Ultimate Capacity	Chin Ultimate Capacity deflection @0.25 in Deflection (Tons)	Actual Pile Deflection (5% Method) (in) or Largest Deflection Obtained	Failure Ultimate Load (5% Deflection) (Tons)
1	0.66	177	162	0.7	143
2	0.92	275	158	0.8	279
3	0.85	300	143	0.8	203
4	0.68	210	146	0.7	210
5A	0.87	238	115	0.8	231
5B	0.82	300	135	0.77	302
5C	0.97	300	129	0.8	305
6A	0.4	168	129	0.7	171
6B	0.38	148	127	0.7	189
7	0.39	105	88	0.9	142
8A	0.52	141	79	0.61	152
8B	0.484	150	107	0.46	150
9	0.59	152	97	0.7	166
10A	1.006	300	199	0.8	233
10B	0.68	255	191	0.8	217
10C	1.08	300	191	0.8	220
11	0.21	131	146	0.46	150
12A	0.8	225	301	0.8	225
12B	0.95	300	131	0.8	288
12C	0.92	295	113	0.8	261
13A	0.64	218	109	0.7	218
13B	0.7	320	179	0.7	320
13C	0.7	320	193	0.7	320
13D	0.85	490	202	0.7	438
13E	0.7	320	101	0.7	320

Table 10-Summary Table No. 2 of Load Test Samples and Methods of Interpretation of Physical Load Test Data to Predict Ultimate Compression Capacity

Job I.D.	Capacity at 0.25 inches (Tons) ARMY CORPS	Ultimate Capacity of Pile Tangent Method (Tons)	Deflection of Pile Tangent Method (in.)	Q(ult) Tons from Chin
1	129	130	0.18	298
2	143	215	0.33	370
3	168	175	0.16	238
4	159	150	0.16	217
5A	114	112	0.2	400
5B	140	120	0.2	645
5C	138	150	0.31	545
6A	147	151	0.16	217
6B	132	100	0.11	324
7	98	90	0.13	196
8A	101	90	0.15	380
8B	93	80	0.18	303
9	93	111	0.14	286
10A	183	191	0.18	370
10B	182	203	0.26	358
10C	178	216	0.28	373
11	130	130	0.25	205
12A	131	111	0.15	356
12B	137	137	0.25	556
12C	120	135	0.25	526
13A	109	109	0.25	489
13B	172	172	0.25	592
13C	174	160	0.19	555
13D	217	217	0.25	770
13E	141	142	0.25	526

APPENDIX B
GENERALIZED SUBSURFACE PROFILE (GSP) FOR EACH TEST PILE LOCATION

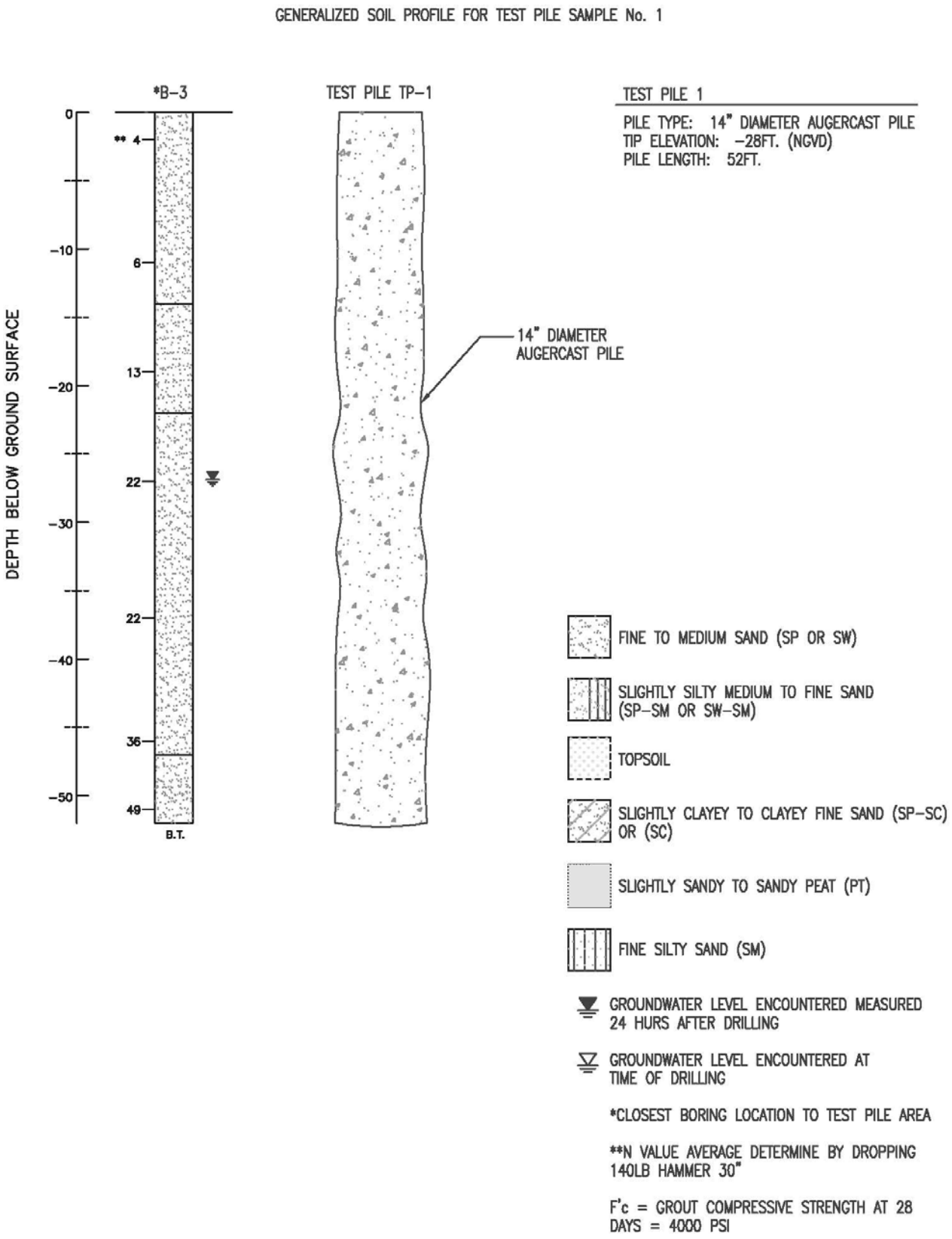

Figure 11-GSP Sample No. 1

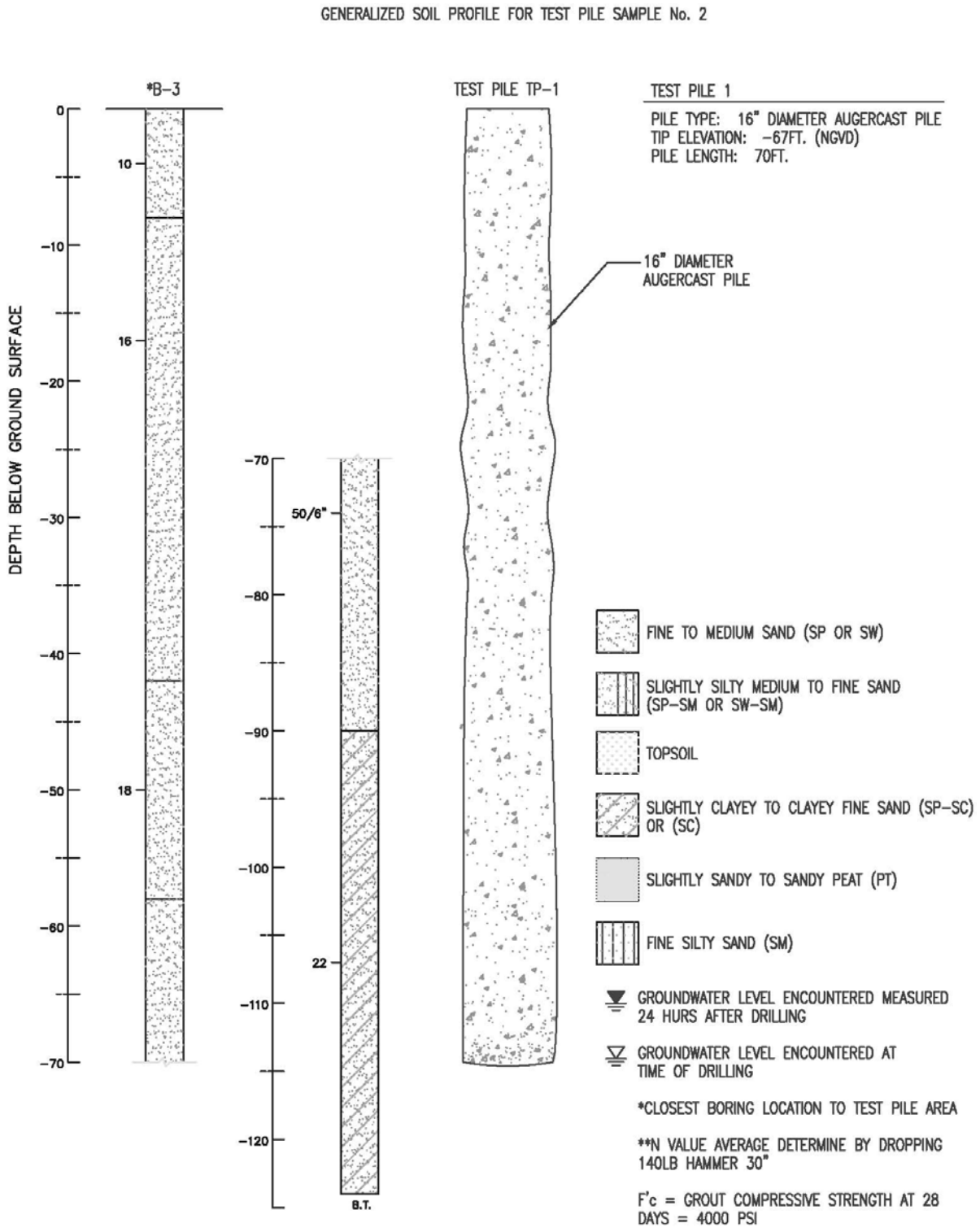

Figure 12-GSP Sample No. 2

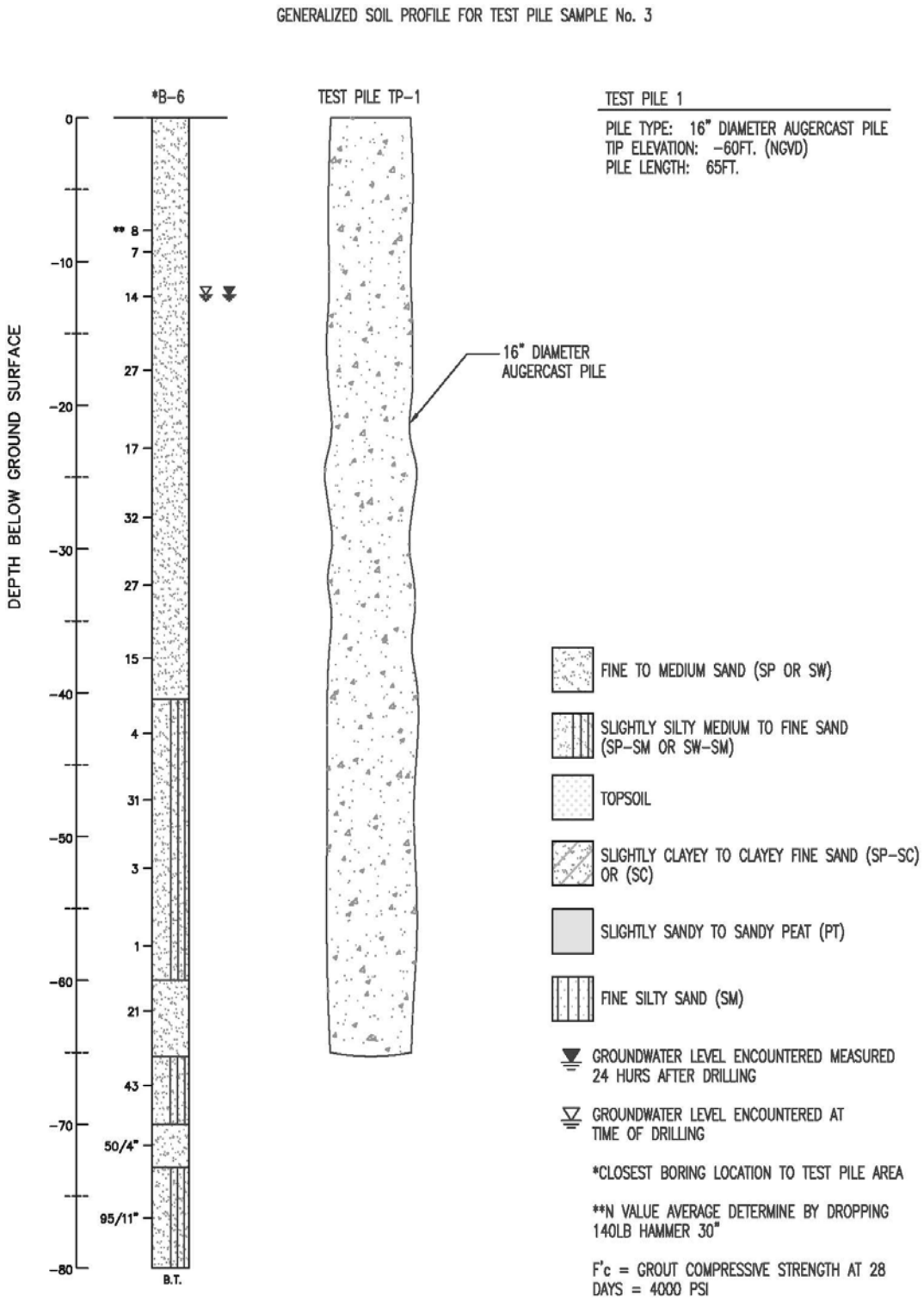

Figure 13-GSP Sample No. 3

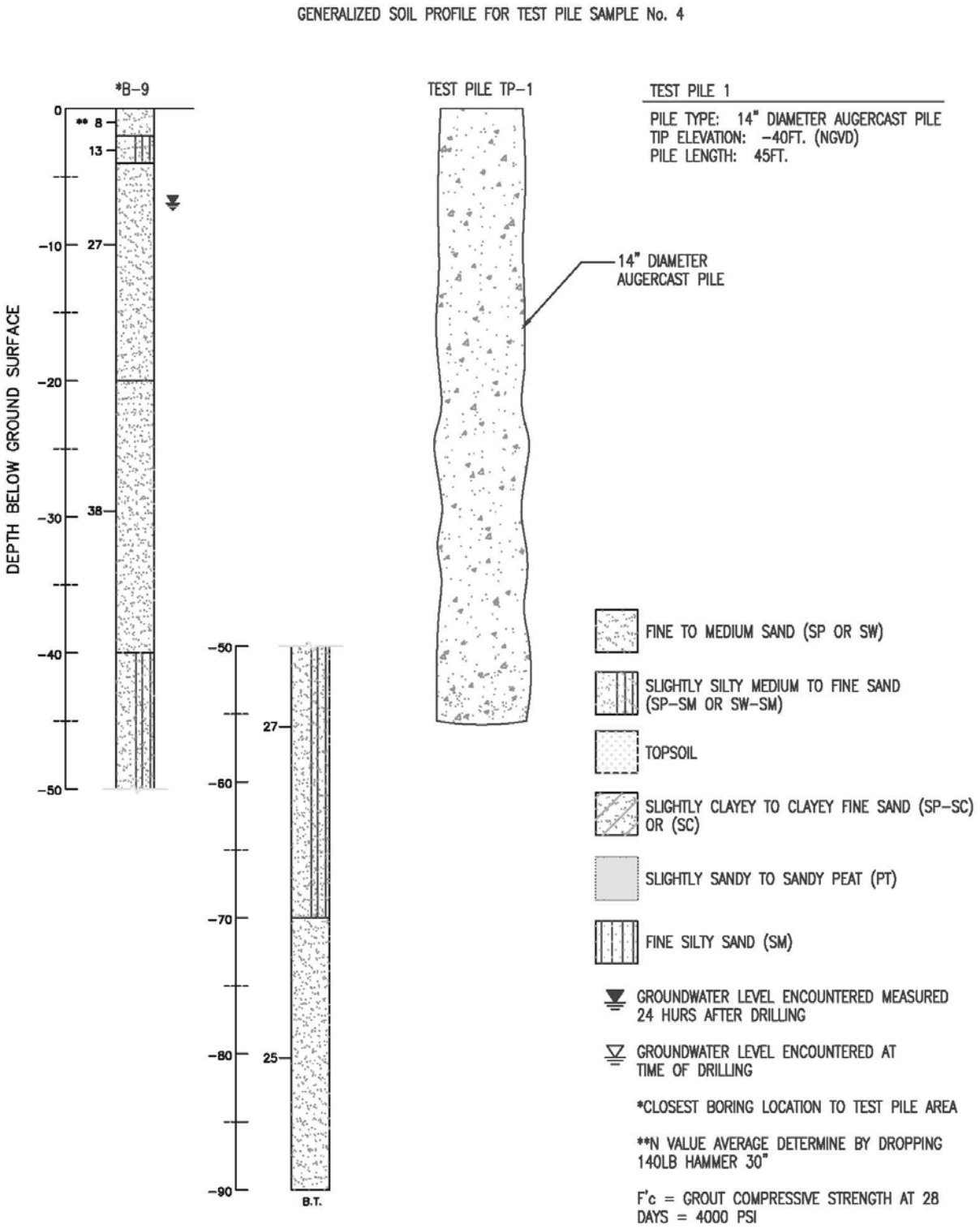

Figure 14-GSP Sample No. 4

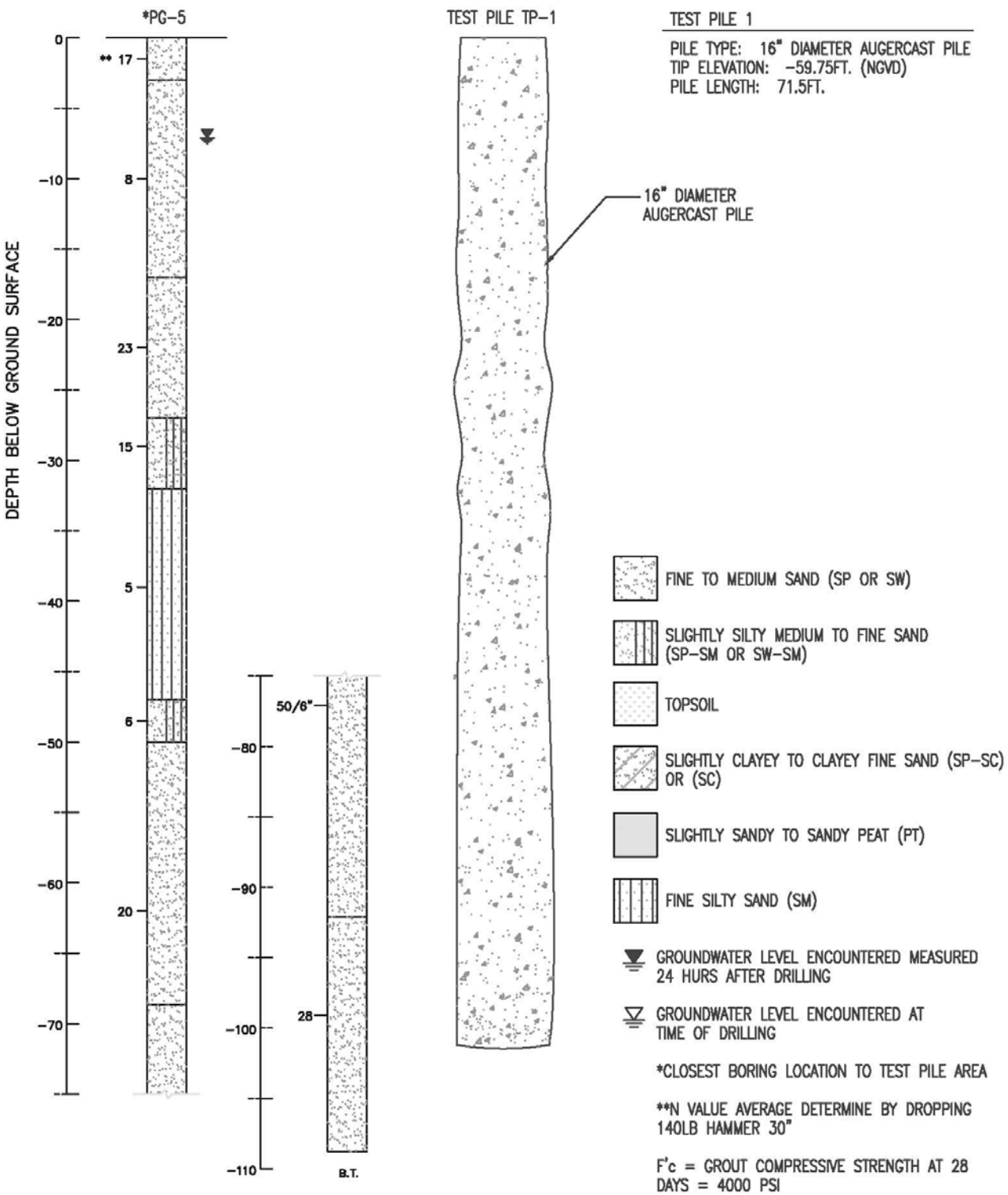

Figure 15-GSP Sample No. 5, Test Pile No. 1

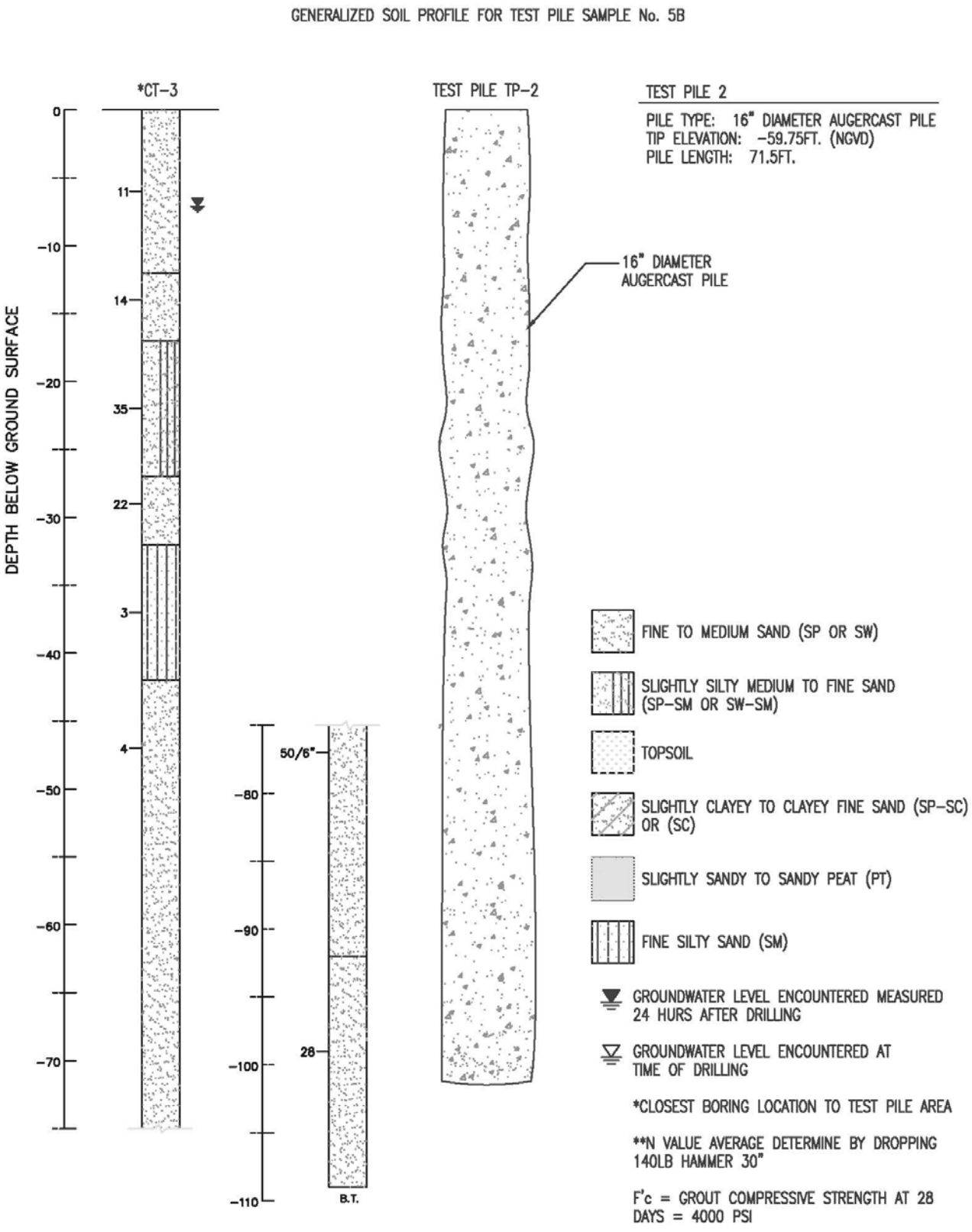

Figure 16-GSP Sample No. 5, Test Pile No. 2

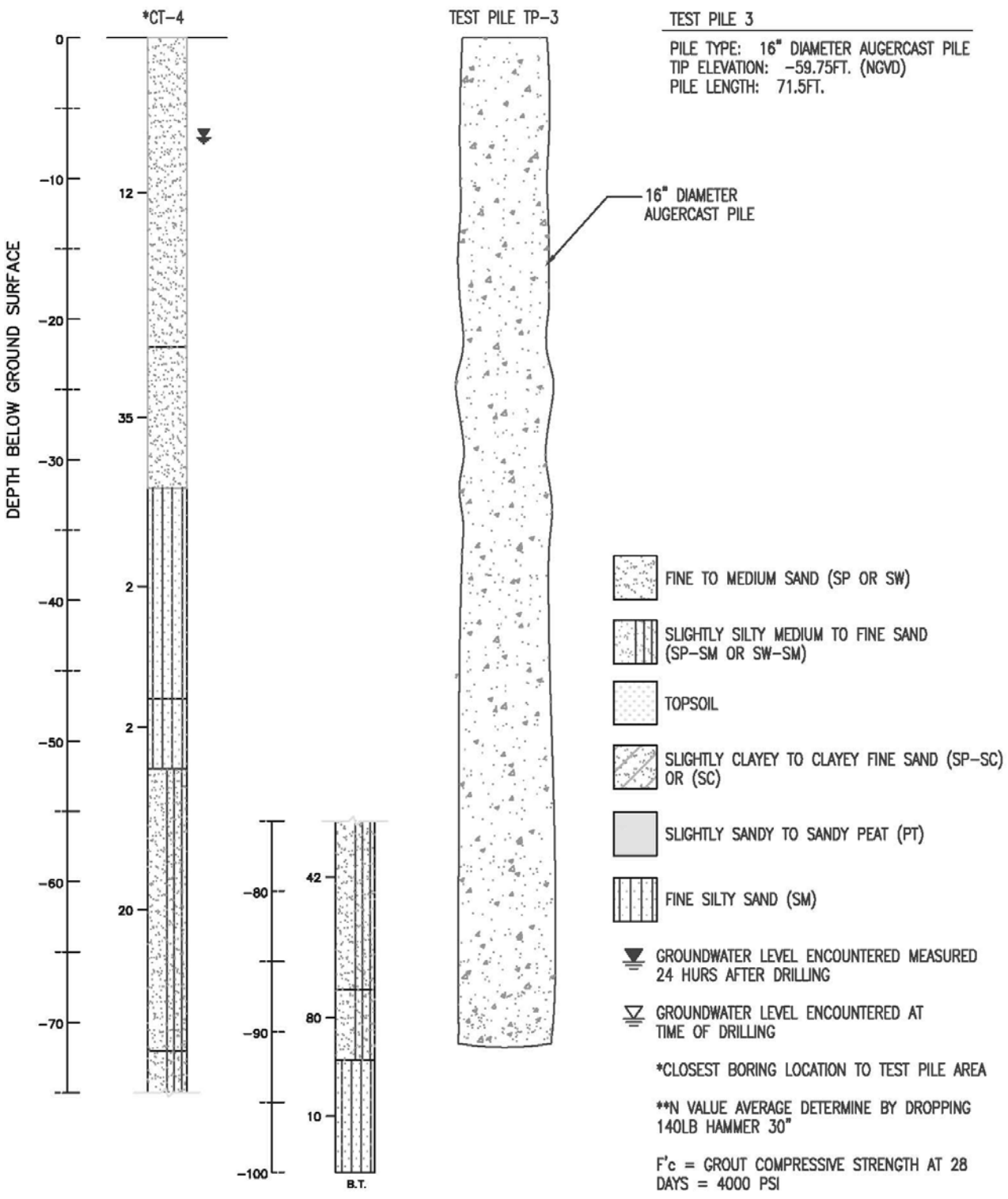

Figure 18-GSP Sample No. 5, Test Pile No. 3

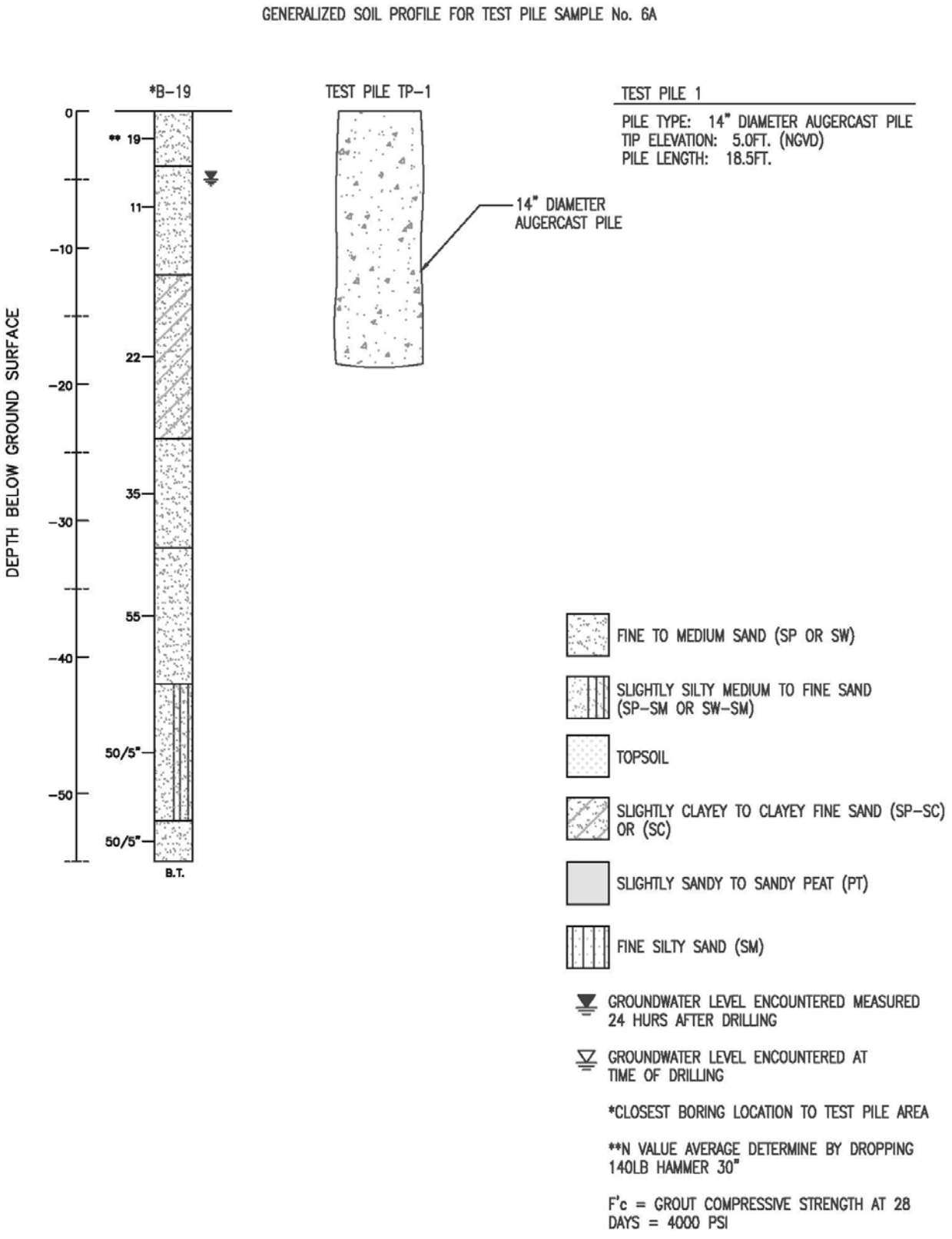

Figure 19-GSP Sample No 6 Test Pile No. 1

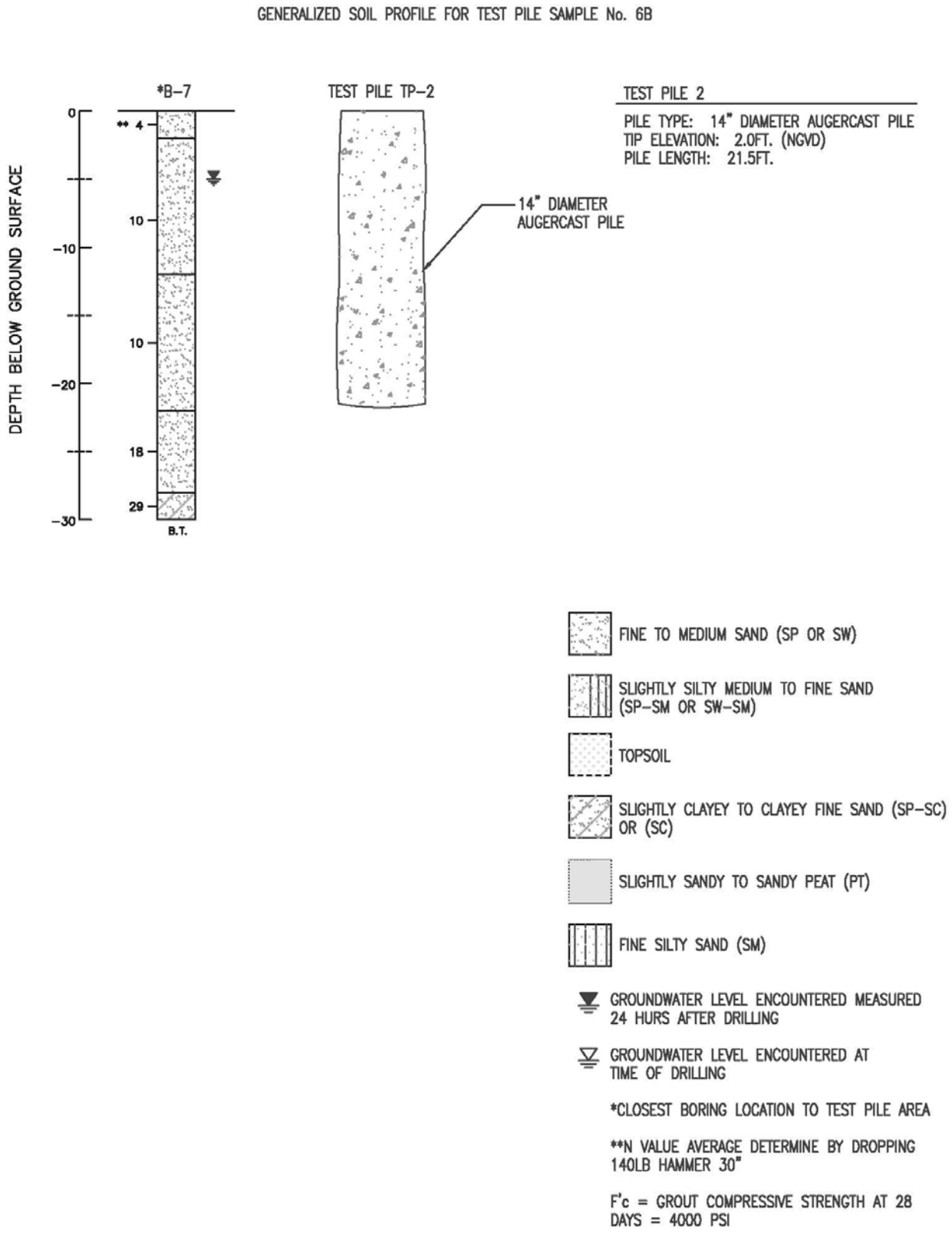

Figure 20-GSP Sample No. 6 Test Pile No. 2

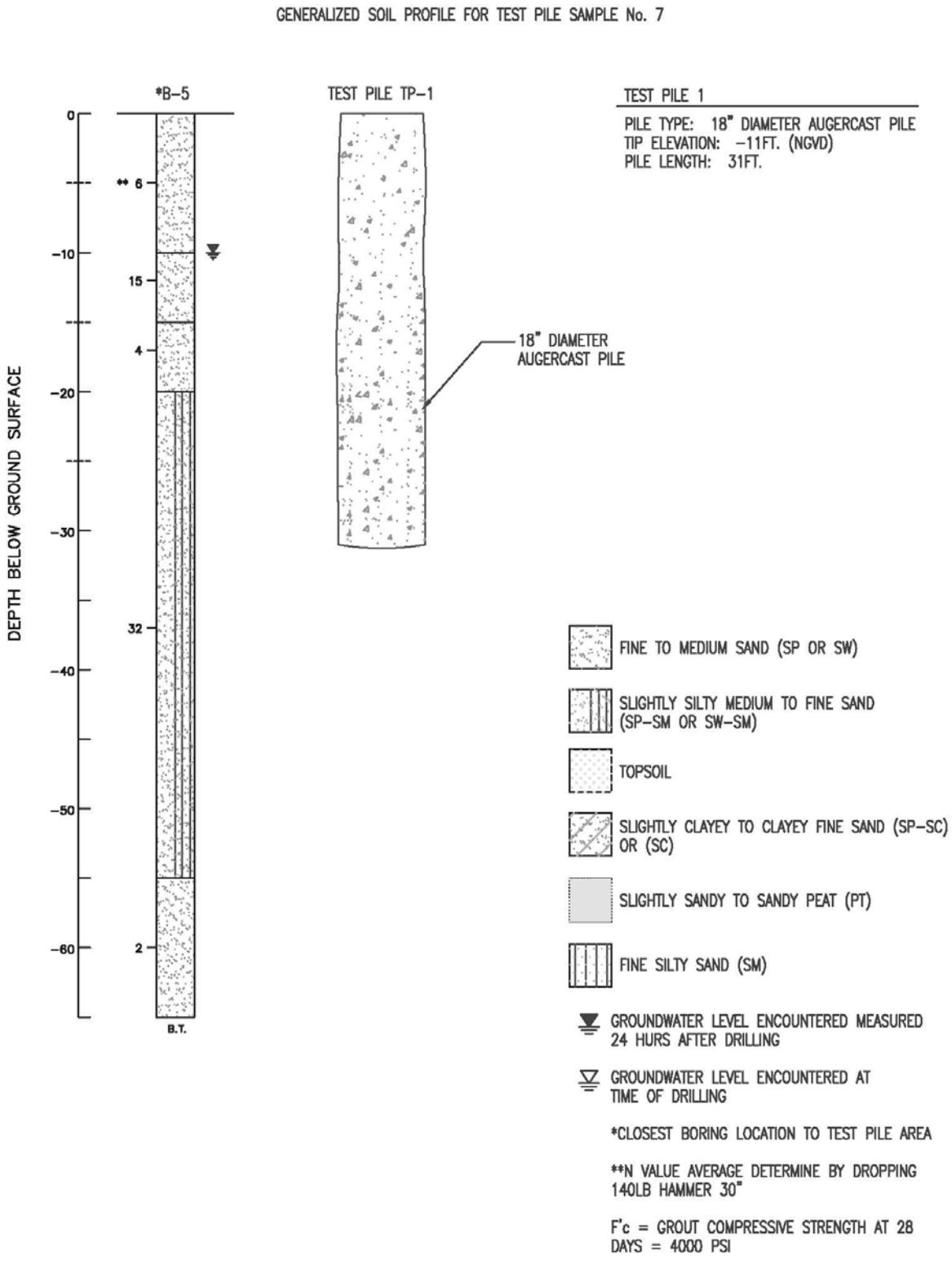

Figure 21-GSP Sample No. 7

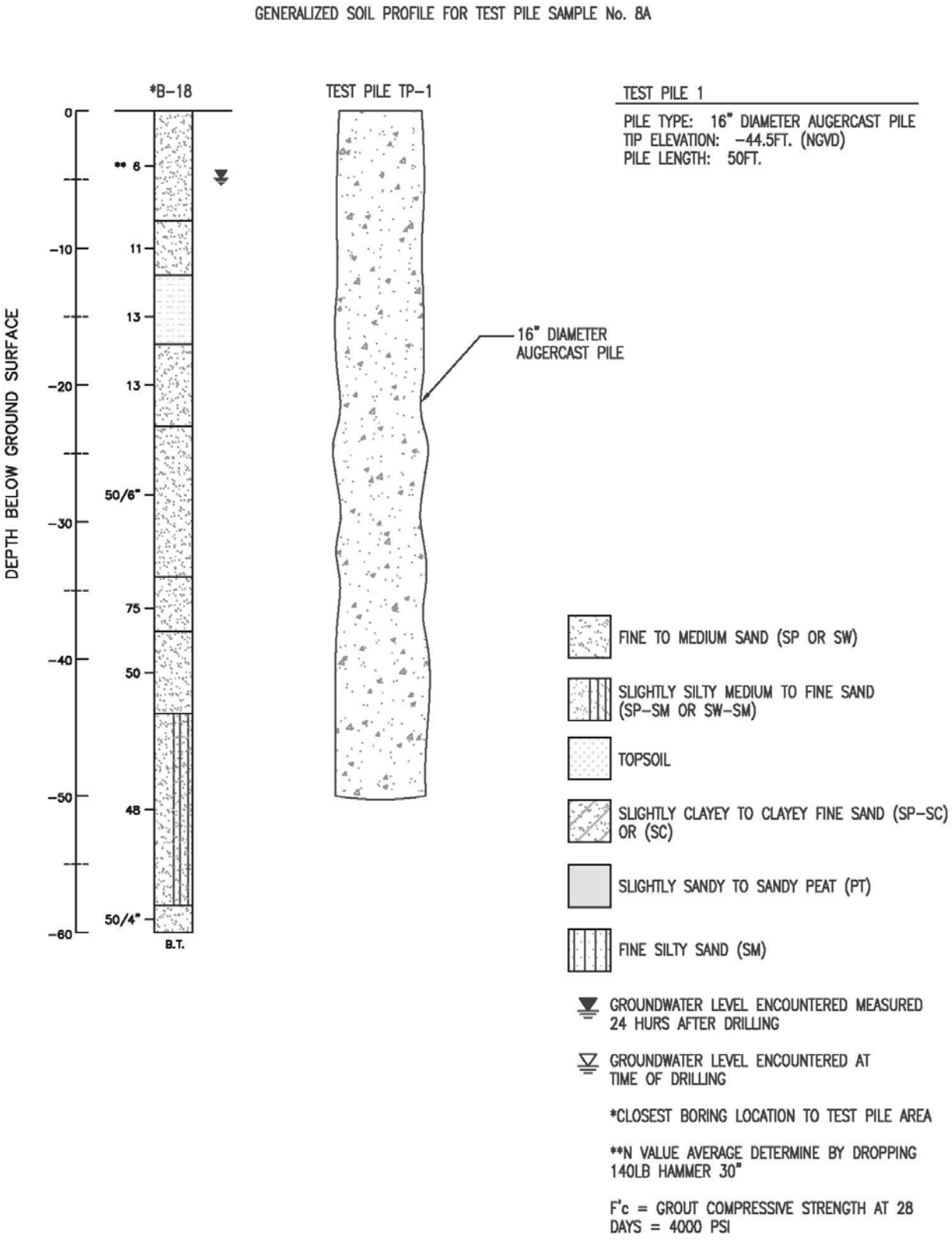

Figure 22-GSP Sample No. 8 & Test Pile No. 1

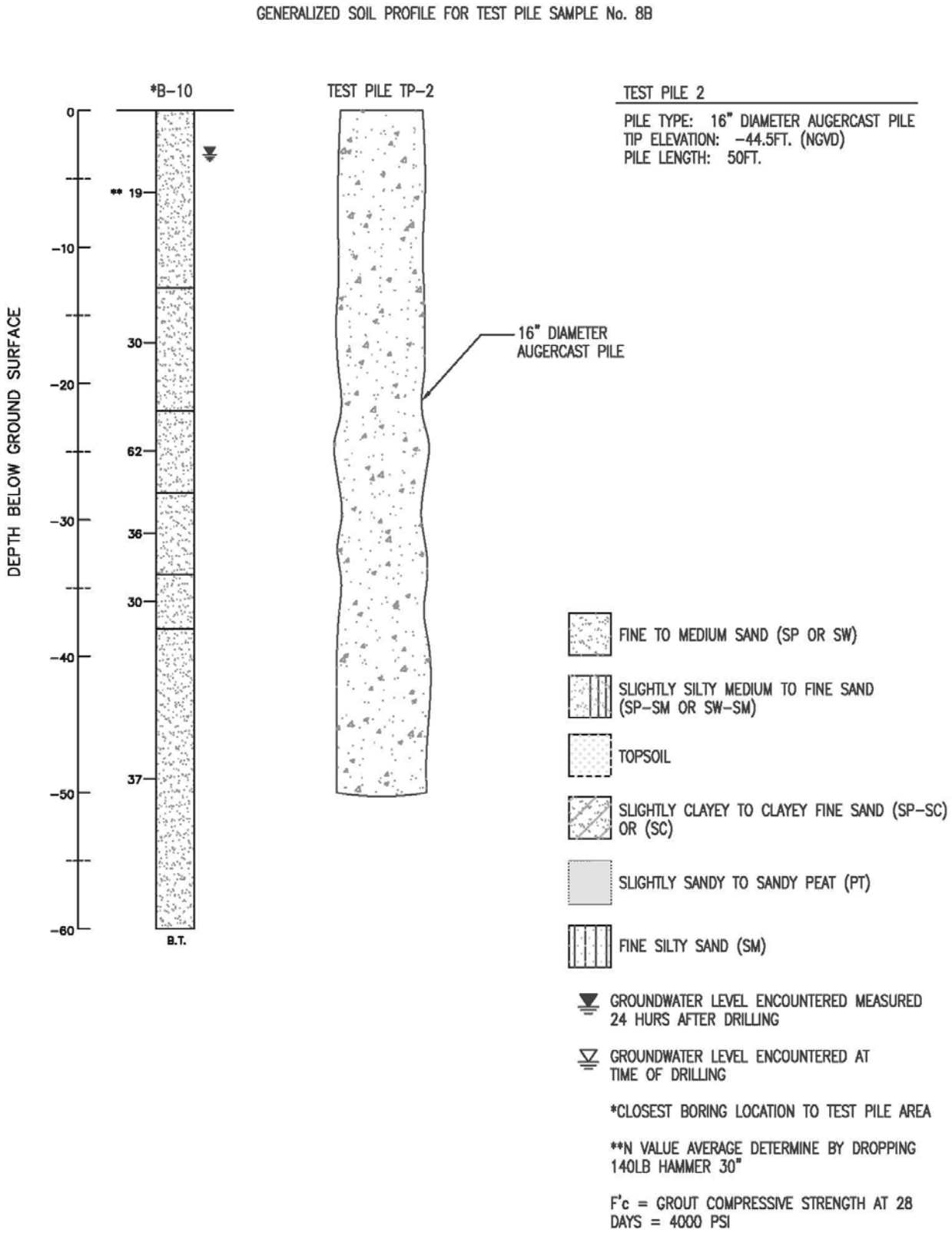

Figure 23-GSP Sample No. 8 & Test Pile No. 2

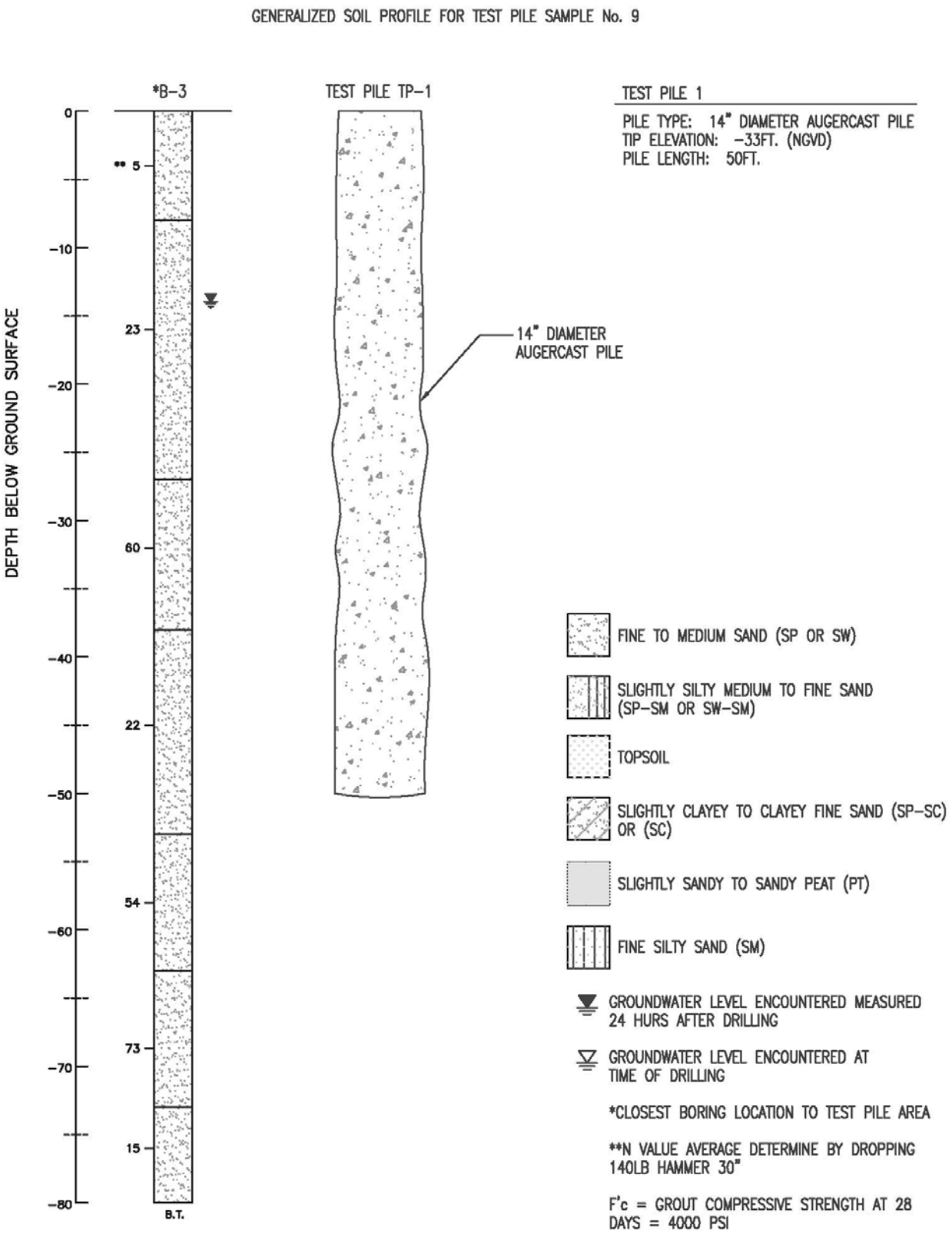

Figure 24-GSP Sample No. 9

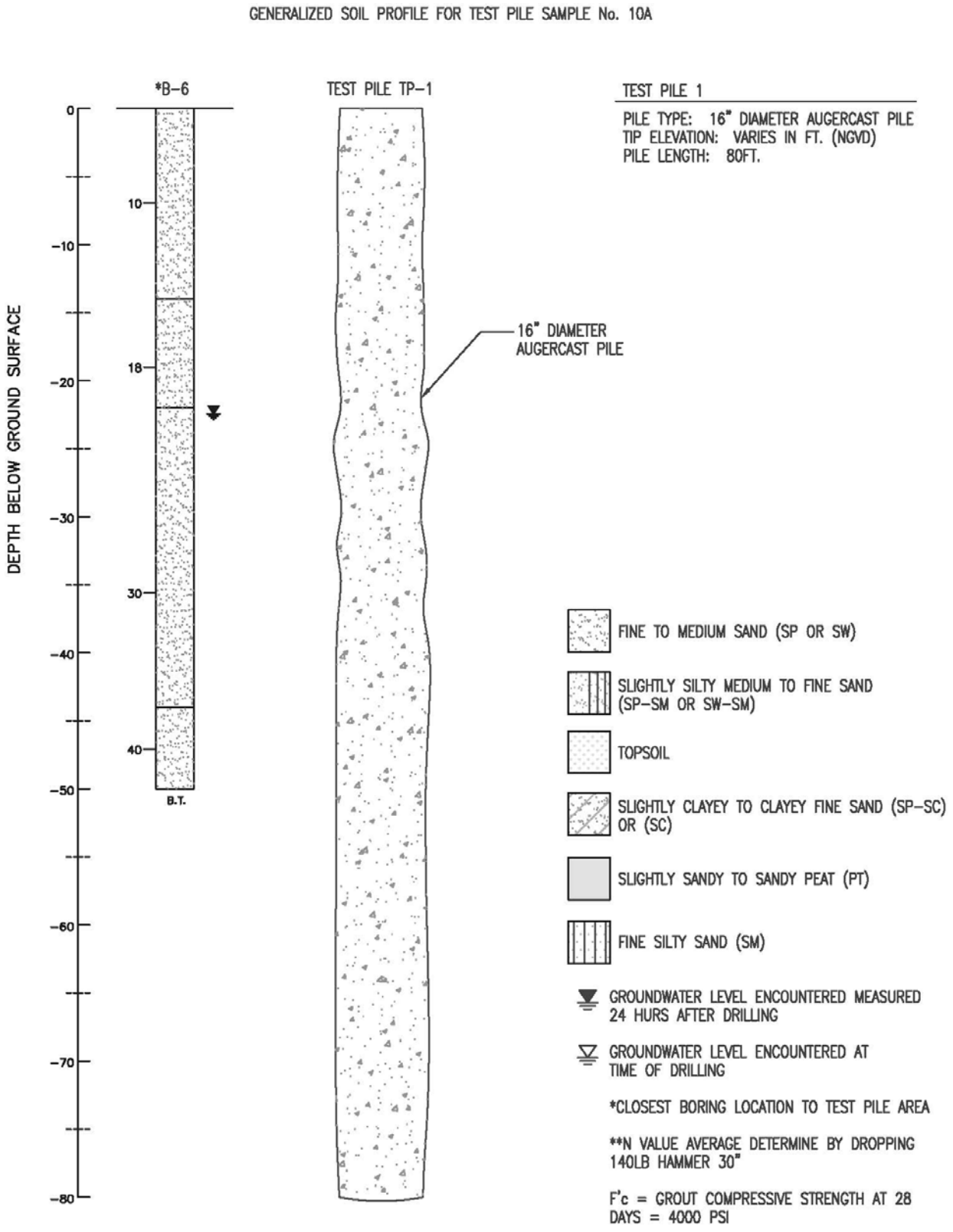

Figure 25-GSP Sample No. 10 & Test Pile No. 1,2,and 3

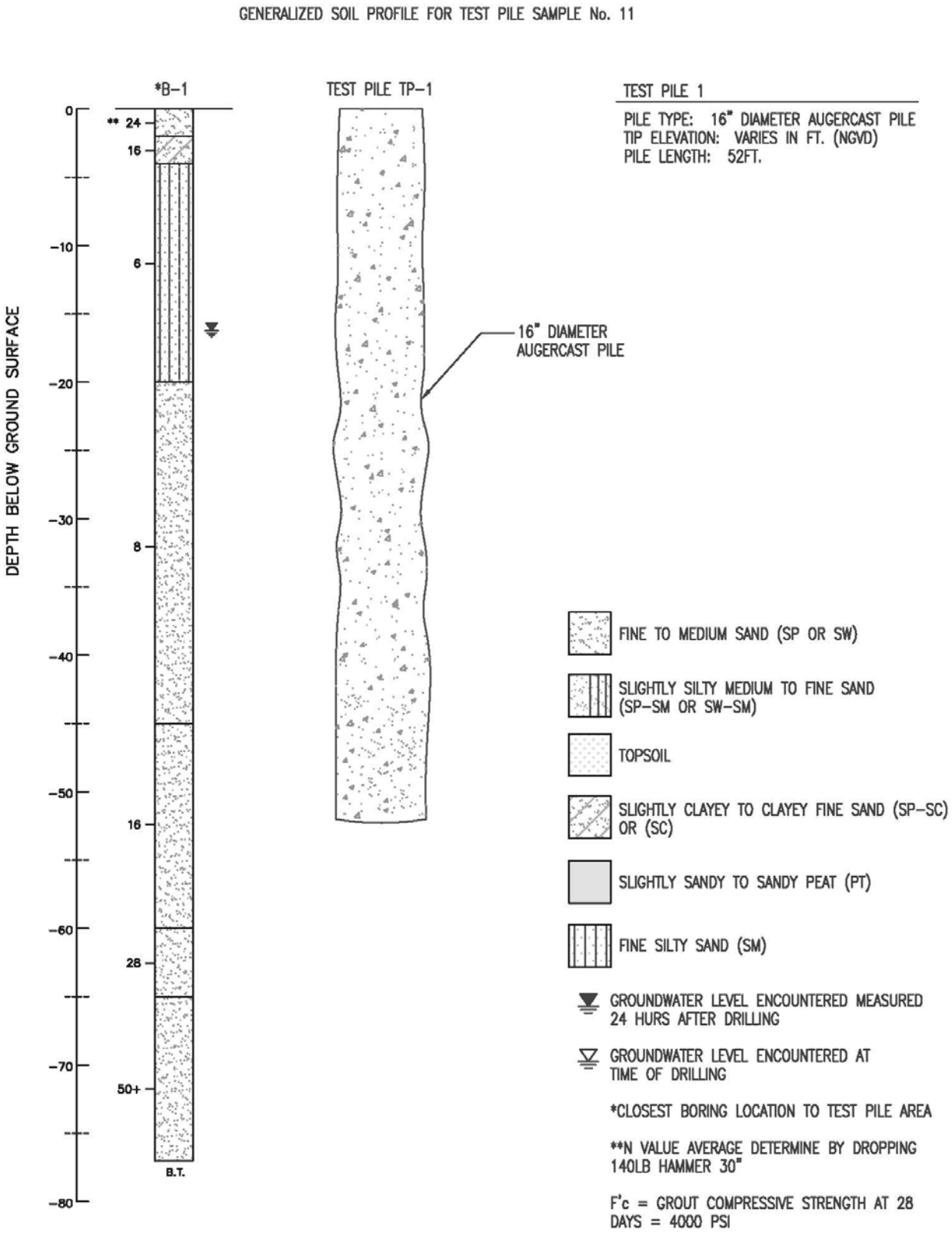

Figure 26-GSP Sample No. 11

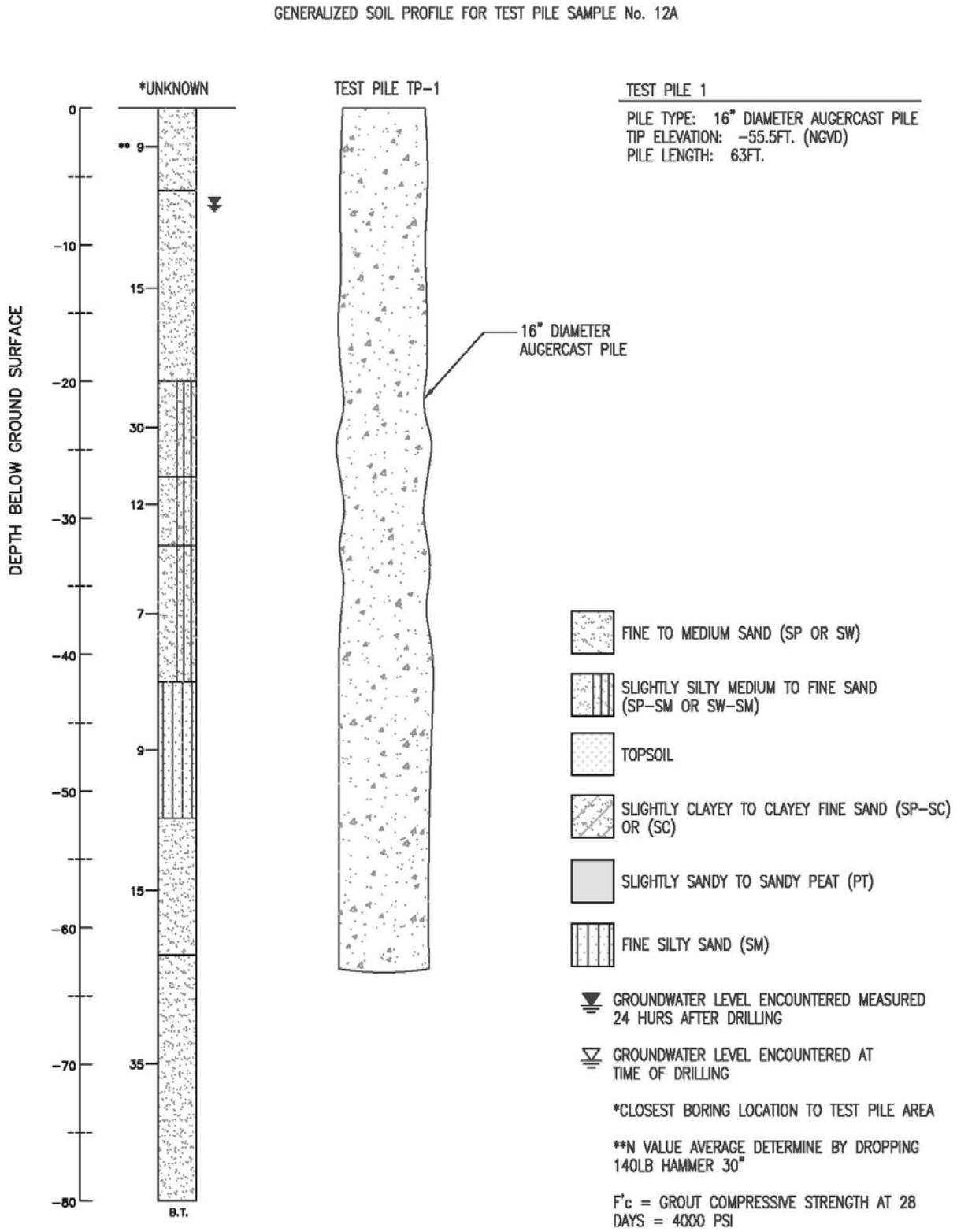

Figure 27-GSP Sample No. 12 & Test Pile No. 1

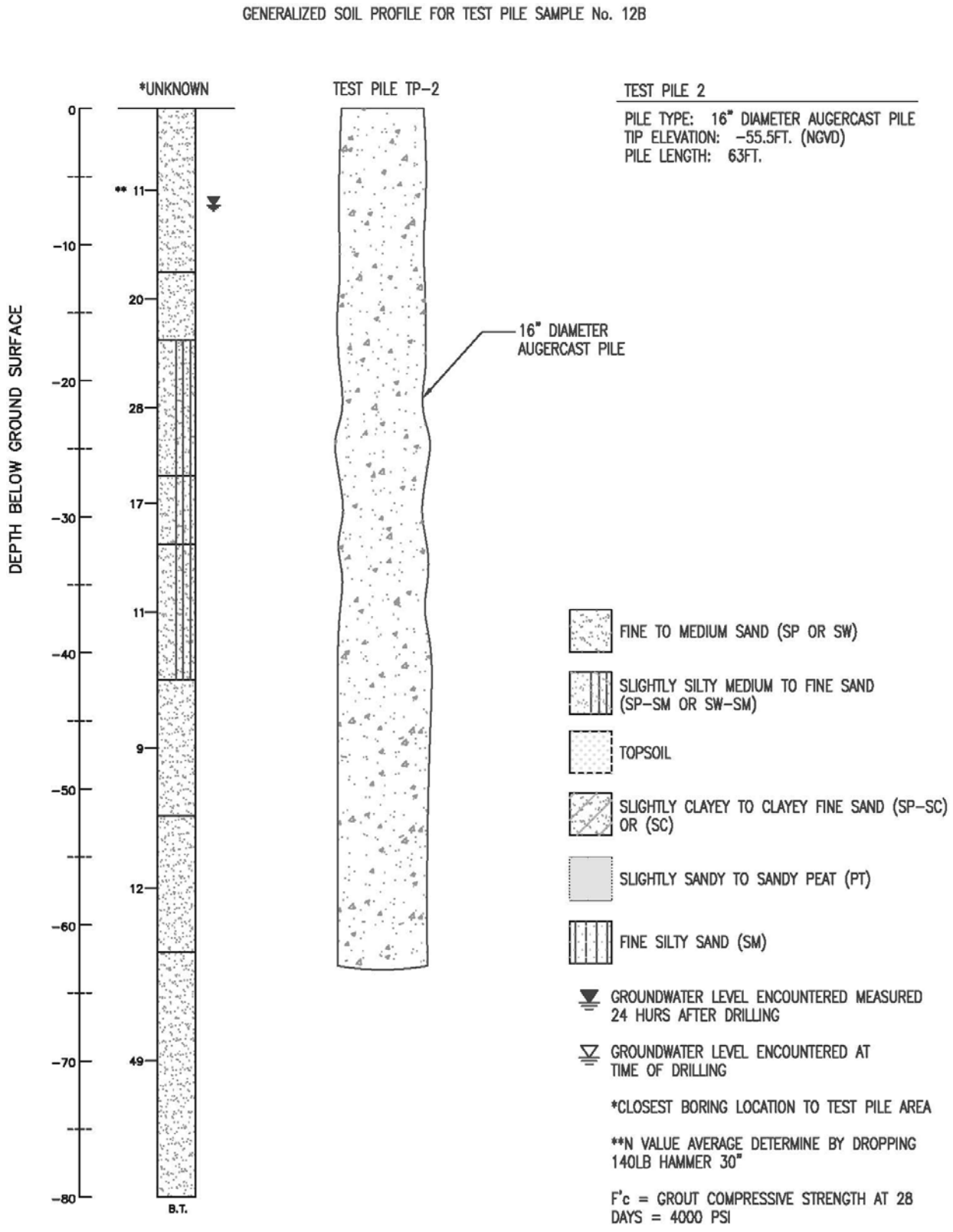

Figure 28-GSP Sample No. 12 & Test Pile No. 2

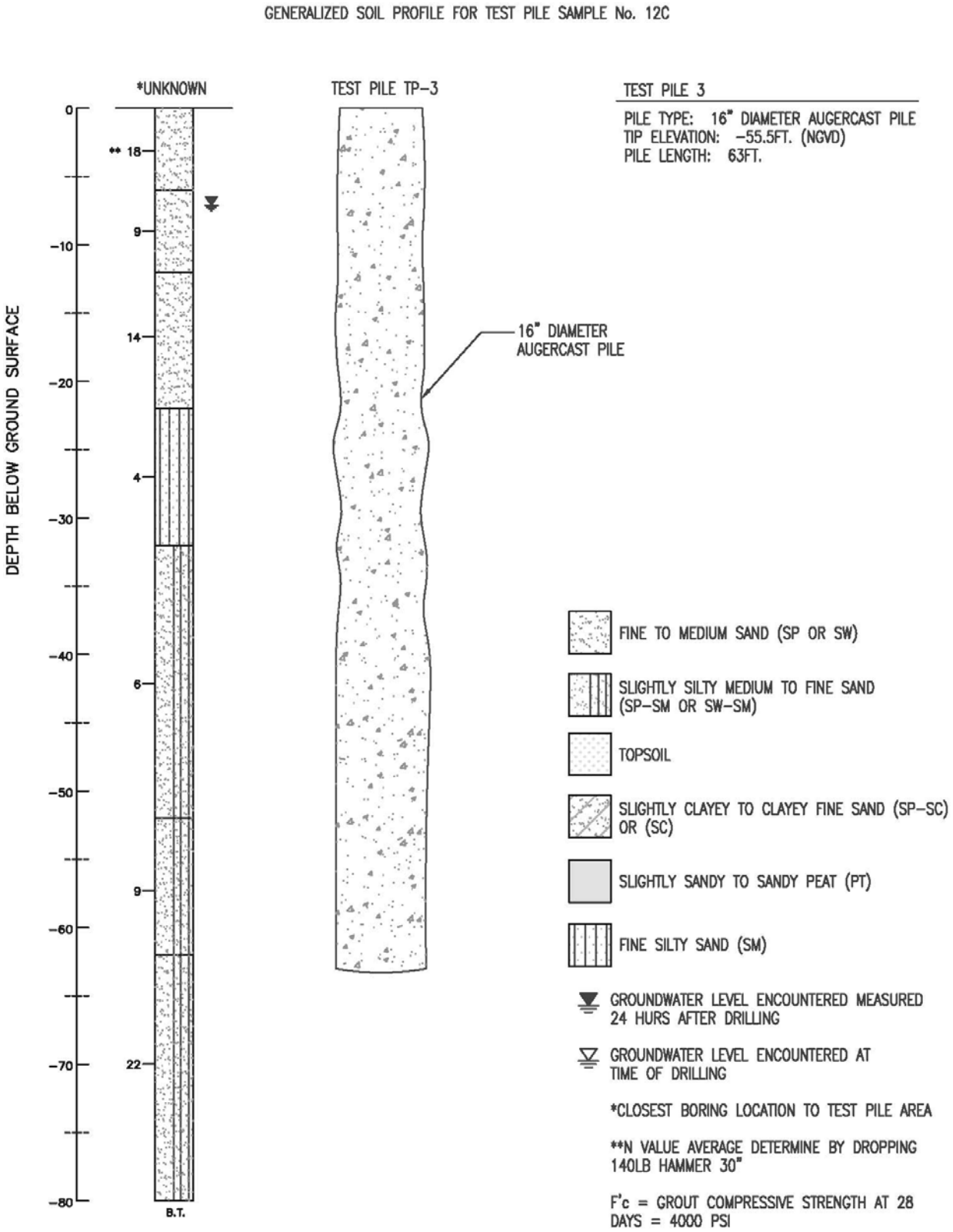

Figure 29-GSP Sample No. 12 & Test Pile No. 3

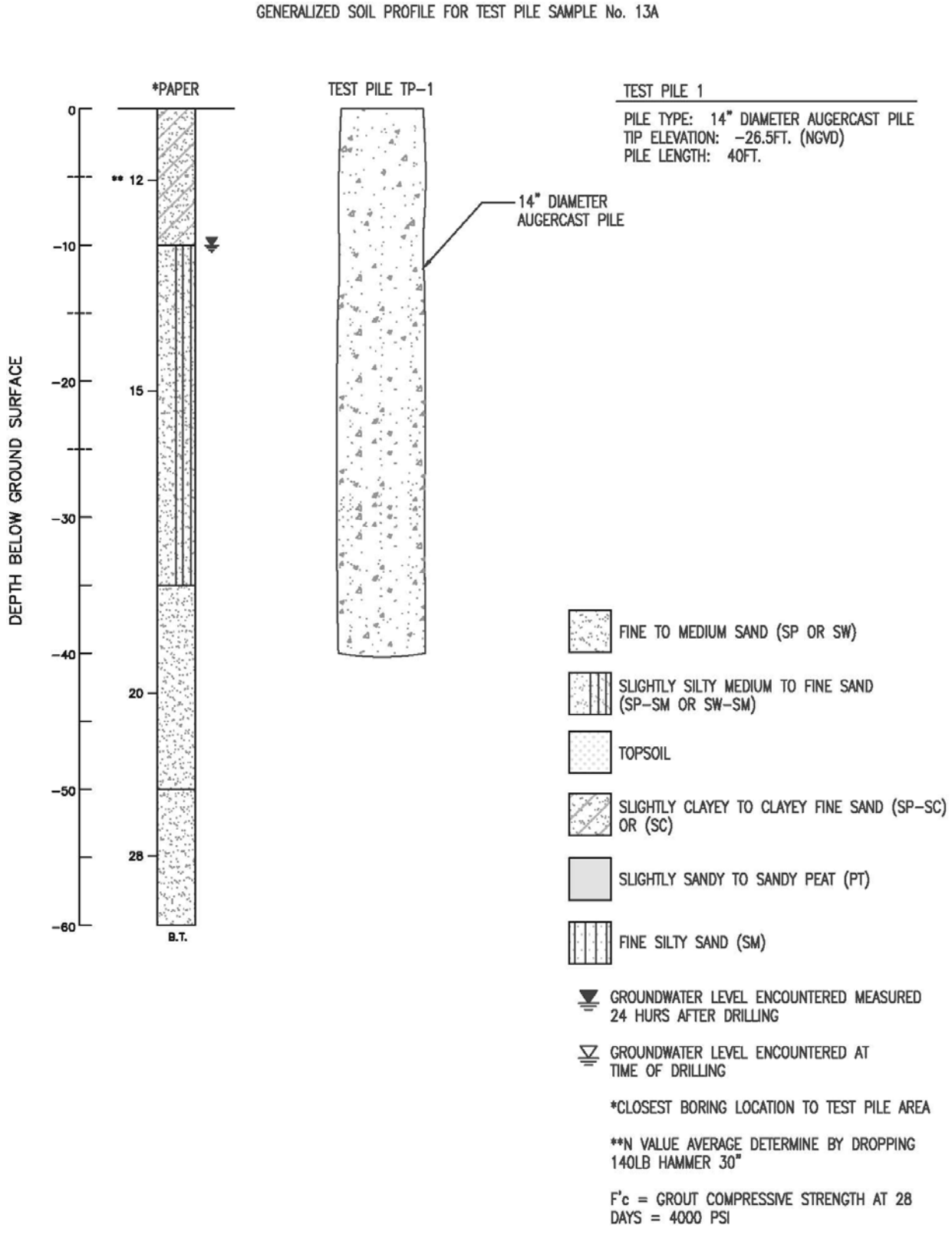

Figure 30-GSP Sample No. 13 & Test Pile No. 1

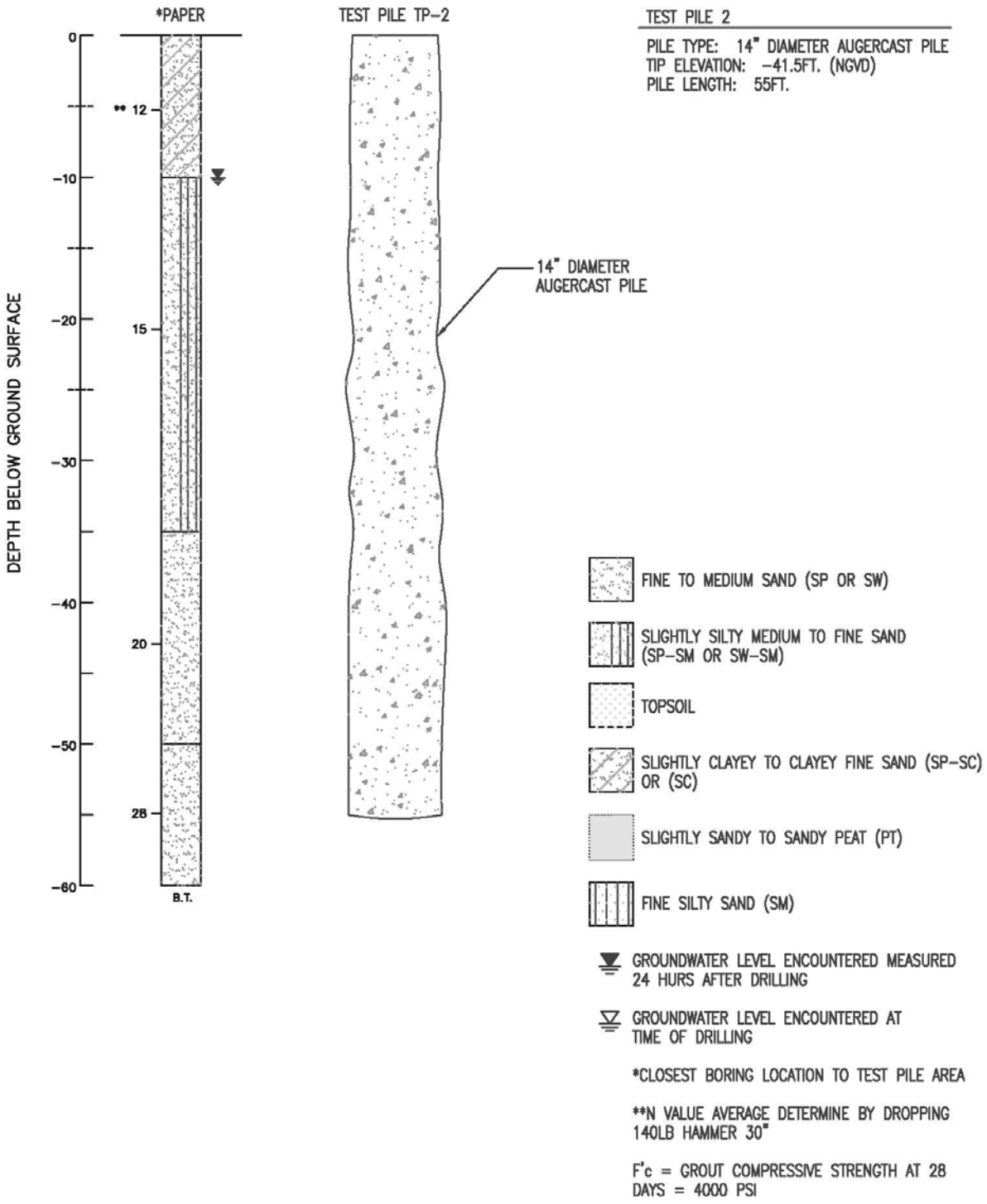

Figure 31-GSP Sample No. 13 & Test Pile No. 2

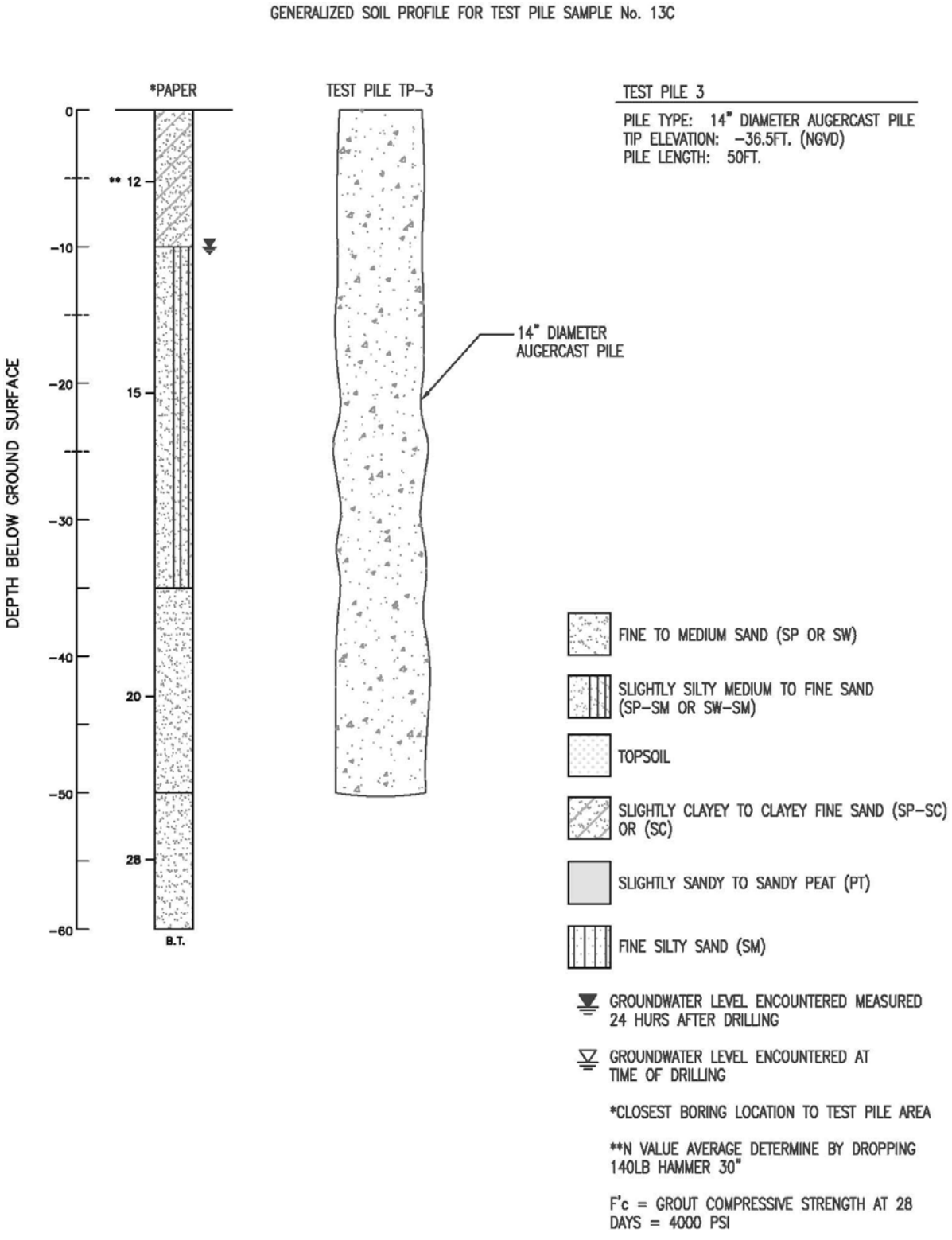

Figure 32-GSP Sample No. 13 & Test Pile No. 3

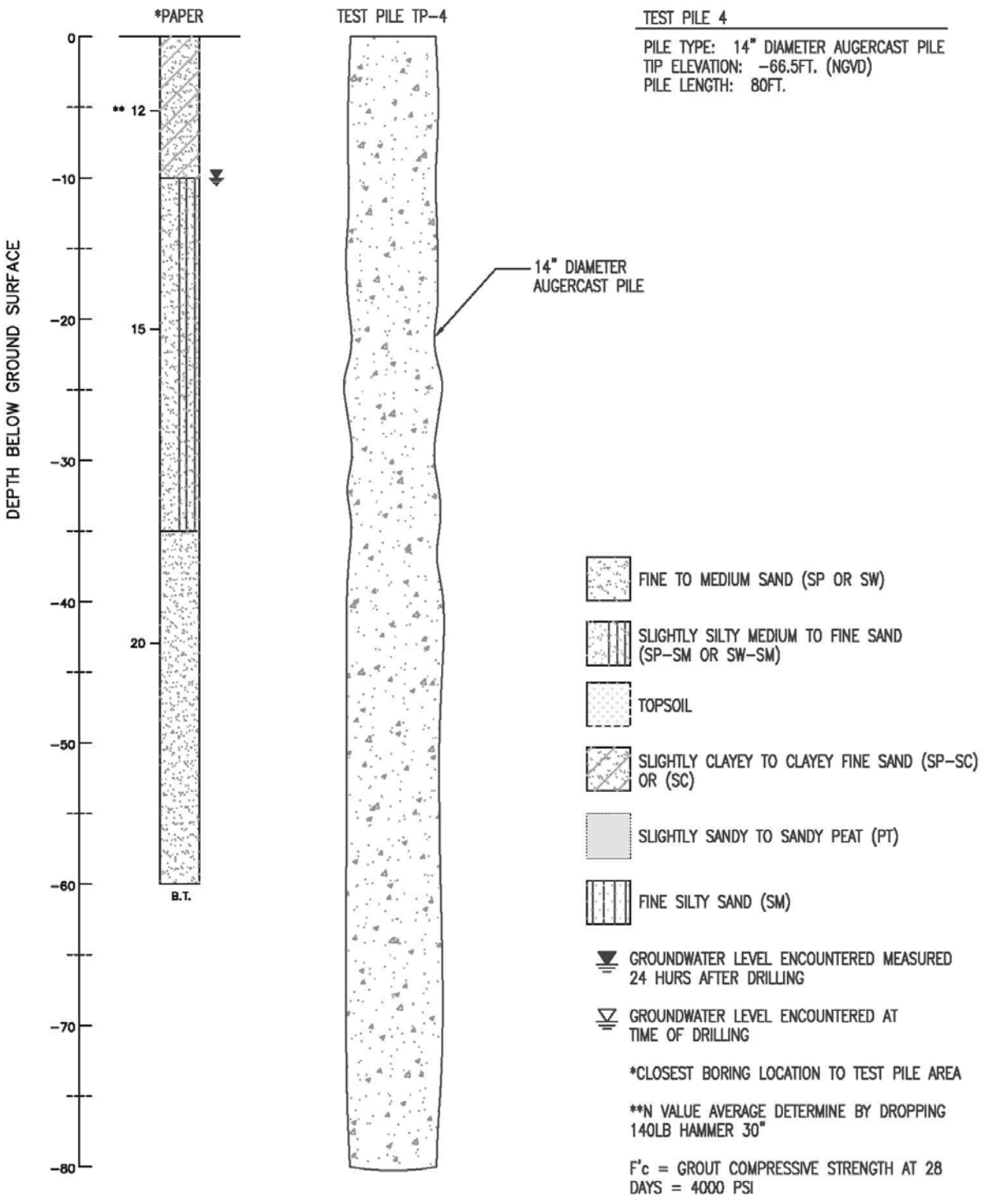

Figure 33-GSP Sample No. 13 & Test Pile No. 4

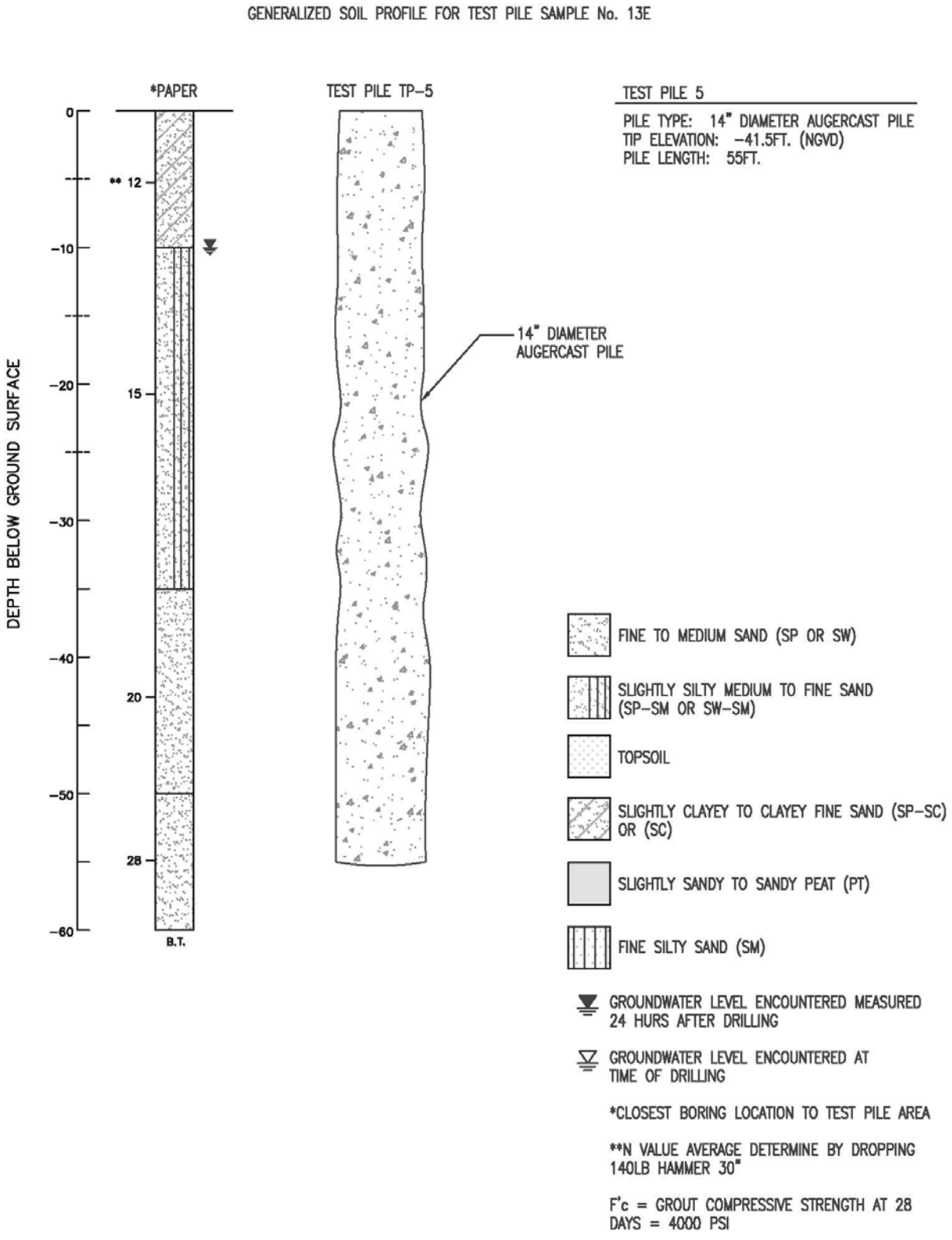

Figure 34-GSP Sample No. 13 & Test Pile No. 5

APPENDIX C
GENERAL PICTURES OF AUGERED CAST-IN-PLACE INSTALLATION PROCEDURES

Pictures of Augered Cast-In-Place Pile Placement and Procedures

Figure 35- Picture of hollow stem auger, crane, and leads after placement of grout pile.

Figure 36- Picture of installation of grout pile with hollow stem auger and crane.

Figure 37-Picture of auger removing soil to begin pumping of grout to cast pile.

Figure 38-Picture of ACIP pile butt's and steel reinforcement for large mat foundation.

APPENDIX D
LOAD DEFLECTION GRAPHS AND TABLES FOR EACH LOAD TEST PERFORMED

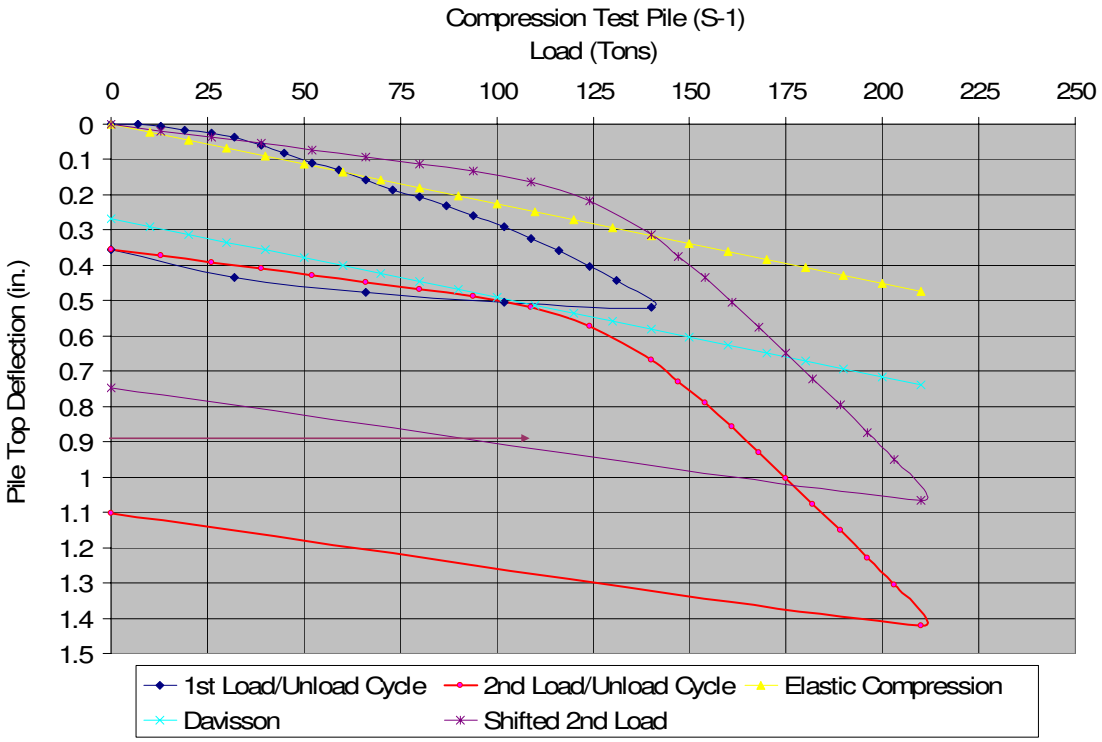

Figure 39-Load Deflection Plot Sample No. 1

Table 11-Load Test Data Sample No. 1, Test Pile No.1

Sample 1	**Compression Test**		
1st Load / Unload Cycle		2nd Load / Unload Cycle	
Applied Test Load (tons)	**Pile Top Deflection (in.)**	**Test Load (tons)**	**Pile Top Deflection (in.)**
0	0	0	0.355
7	0.0005	13	0.3735
13	0.006	26	0.391
19	0.017	39	0.409
26	0.025	52	0.429
32	0.036	66	0.449
39	0.0595	80	0.467
45	0.082	94	0.488
52	0.11	109	0.518
59	0.131	124	0.571
66	0.1575	140	0.669
73	0.185	147	0.729
80	0.207	154	0.789
87	0.232	161	0.8585
94	0.26	168	0.9295
102	0.2915	175	1.0025
109	0.324	182	1.0775
116	0.3585	189	1.151
124	0.403	196	1.229
131	0.4435	203	1.306
140	0.5195	210	1.4205
102	0.504	0	1.102
66	0.477	----	----
32	0.433	----	----
0	0.355	----	----

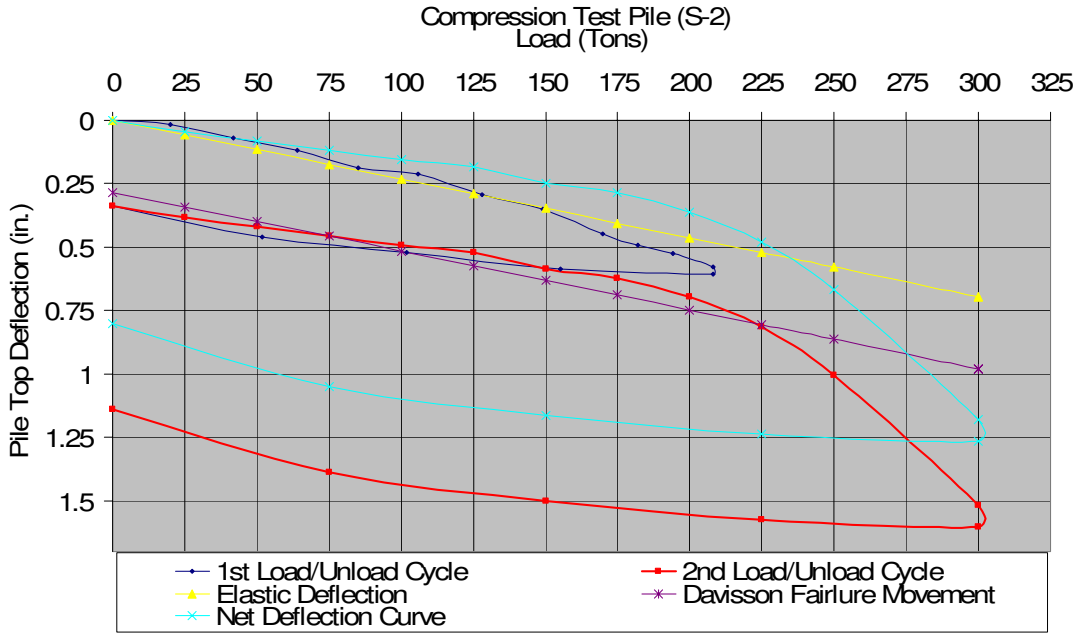

Figure 40-Load Deflection Plot Sample No. 2

Table 12-Load Test Data Sample No. 2, Test Pile No.1

Sample 2		**Compression Test**	
1st Load / Unload Cycle		2nd Load / Unload Cycle	
Applied Test Load (tons)	**Pile Top Deflection (in.)**	**Test Load (tons)**	**Pile Top Deflection (in.)**
0	0	0	0.337
20	0.018	25	0.383
42	0.071	50	0.418
64	0.118	75	0.455
85	0.189	100	0.492
106	0.213	125	0.52
128	0.291	150	0.587
149	0.35	175	0.622
170	0.447	200	0.697
182	0.491	225	0.815
194	0.526	250	1.003
208	0.579	300	1.516
208	0.606	300	1.602
155	0.586	225	1.574
102	0.522	150	1.502
52	0.461	75	1.387
0	0.337	0	1.137

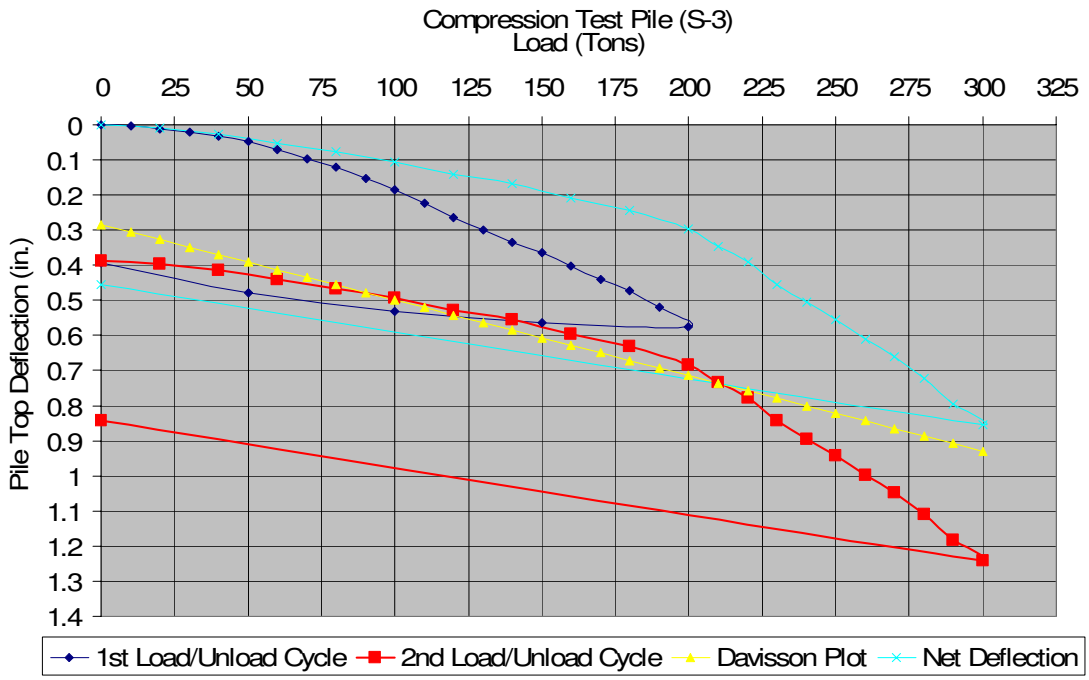

Figure 41-Load Deflection Plot Sample No. 3, Test Pile No.1

Table 13-Load Test Data Sample No. 3, Test Pile No.1

Sample 3	**Compression Test**		
1st Load / Unload Cycle		2nd Load / Unload Cycle	
Applied Test Load (tons)	**Pile Top Deflection (in.)**	**Test Load (tons)**	**Pile Top Deflection (in.)**
0	0	0	0.388
10	0.0025	20	0.3955
20	0.012	40	0.414
30	0.022	60	0.4415
40	0.032	80	0.4655
50	0.048	100	0.494
60	0.07	120	0.5285
70	0.096	140	0.5555
80	0.12	160	0.595
90	0.152	180	0.6315
100	0.185	200	0.685
110	0.2235	210	0.735
120	0.2645	220	0.777
130	0.299	230	0.8415
140	0.3345	240	0.894
150	0.3645	250	0.943
160	0.402	260	0.9975
170	0.44	270	1.0475
180	0.473	280	1.1105
190	0.519	290	1.1825
200	0.576	300	1.2425
150	0.563	0	0.843
100	0.53	----	----
50	0.4775	----	----
0	0.393	----	----

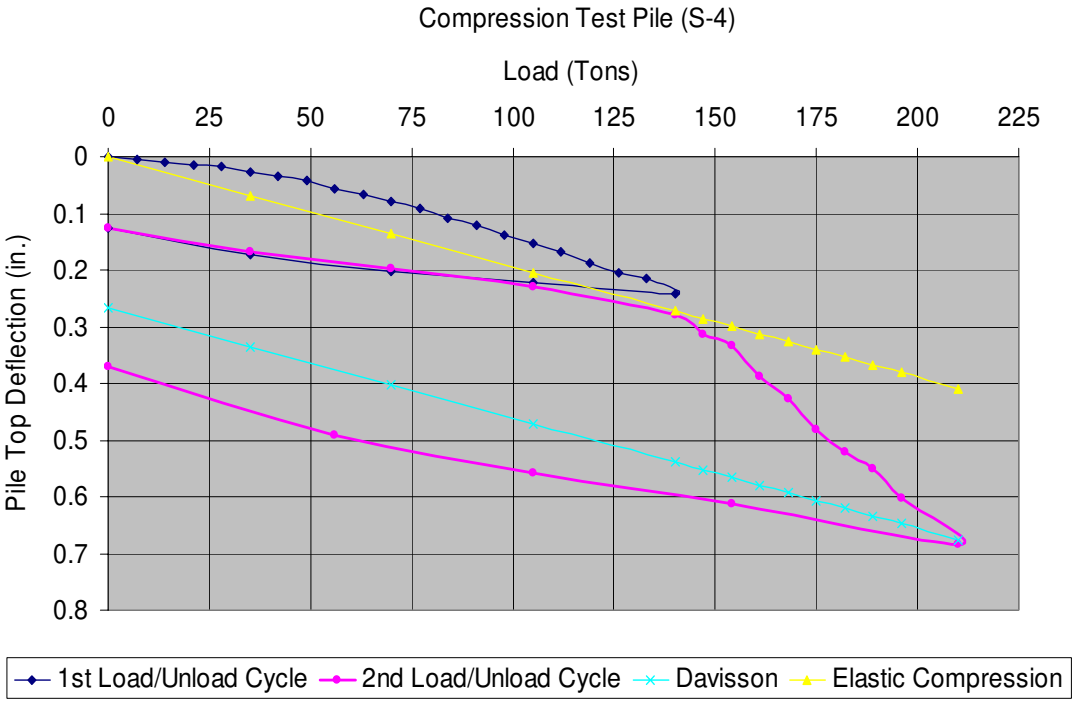

Figure 42-Load Deflection Plot Sample No. 4, Test Pile No.1

Table 14-Load Test Data Sample No. 4, Test Pile No.1

Sample 4	**Compression Test**		
1st Load / Unload Cycle		2nd Load / Unload Cycle	
Applied Test Load (tons)	**Pile Top Deflection (in.)**	**Test Load (tons)**	**Pile Top Deflection (in.)**
0	0	0	0.127
7	0.005	35	0.153
14	0.009	70	0.188
21	0.015	105	0.223
28	0.018	140	0.266
35	0.026	147	0.282
42	0.035	154	0.299
49	0.043	161	0.313
56	0.057	168	0.328
63	0.067	175	0.343
70	0.08	182	0.358
77	0.092	189	0.378
84	0.109	196	0.401
91	0.121	210	0.434
98	0.138	154	0.408
105	0.152	105	0.372
112	0.167	56	0.328
119	0.188	0	0.247
126	0.204	----	----
133	0.214	----	----
140	0.242	----	----
105	0.223	----	----
70	0.202	----	----
35	0.172	----	----
0	0.127	----	----

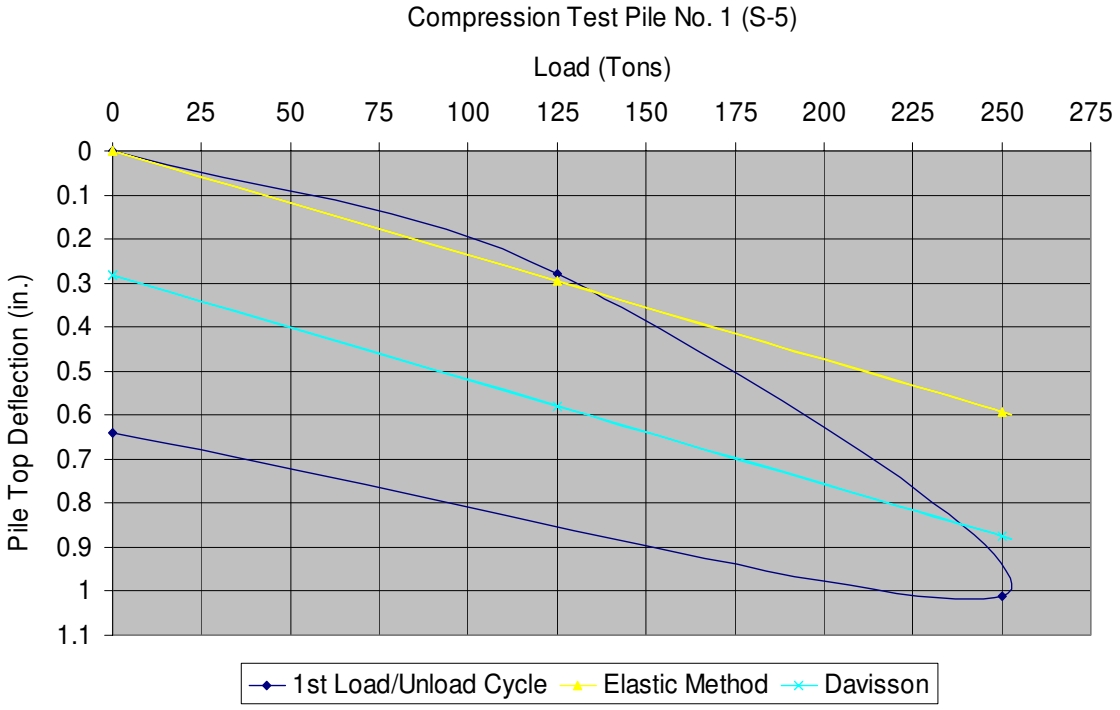

Figure 43-Load Deflection Plot Sample No. 5, Test Pile No. 1

Table 15-Load Test Data Sample No. 5, Test Pile No. 1

Sample 5 - Test Pile 1	**Compression Test**		
1st Load / Unload Cycle		2nd Load / Unload Cycle	
Applied Test Load (tons)	**Pile Top Deflection (in.)**	**Test Load (tons)**	**Pile Top Deflection (in.)**
0	0	N/A	N/A
125	0.28	N/A	N/A
250	1.01	N/A	N/A
0	0.64	N/A	N/A

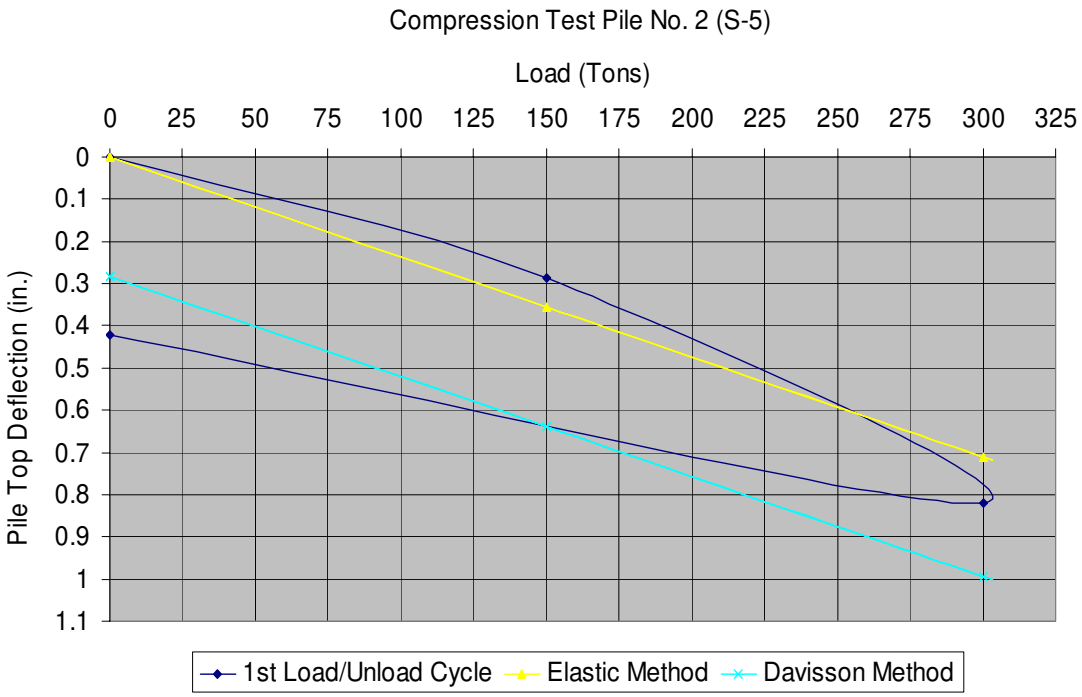

Figure 44-Load Deflection Plot Sample No. 5, Test Pile No. 2

Table 16-Load Test Data Sample No. 5, Test Pile No. 2

Sample 5 - Test Pile 2	**Compression Test**		
1st Load / Unload Cycle		2nd Load / Unload Cycle	
Applied Test Load (tons)	**Pile Top Deflection (in.)**	**Test Load (tons)**	**Pile Top Deflection (in.)**
0	0	N/A	N/A
150	0.285	N/A	N/A
300	0.82	N/A	N/A
0	0.42	N/A	N/A

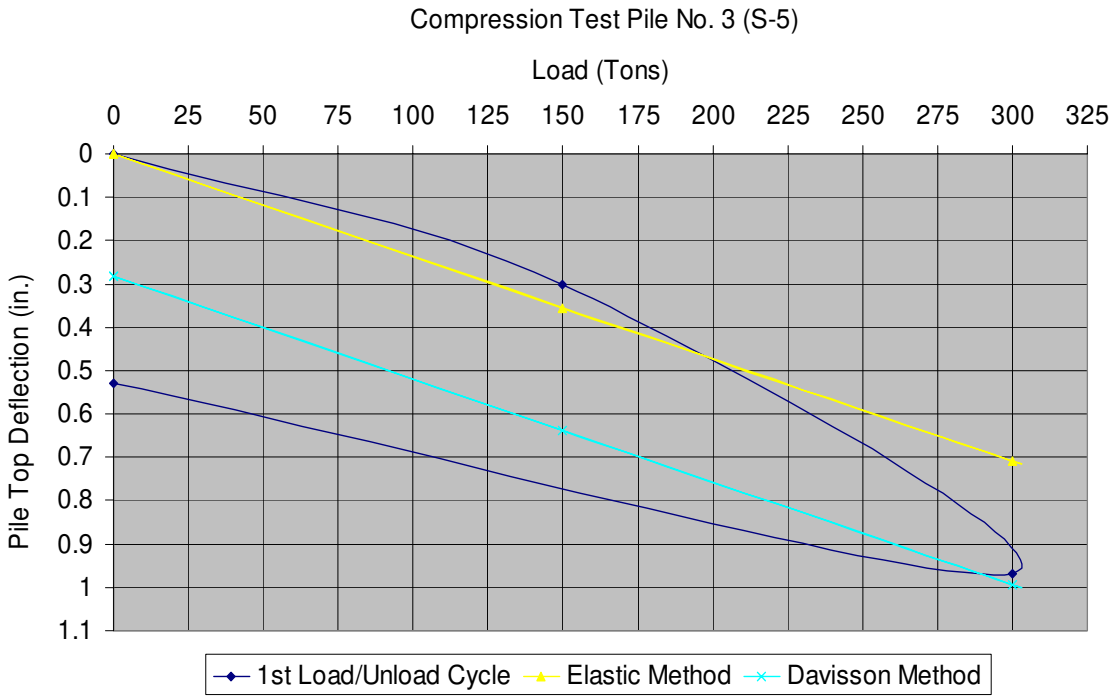

Figure 45-Load Deflection Plot Sample No. 5, Test Pile No. 3

Table 17-Load Test Data Sample No. 5, Test Pile No.3

Sample 5 - Test Pile 3	**Compression Test**		
1st Load / Unload Cycle		2nd Load / Unload Cycle	
Applied Test Load (tons)	**Pile Top Deflection (in.)**	**Test Load (tons)**	**Pile Top Deflection (in.)**
0	0	N/A	N/A
150	0.3	N/A	N/A
300	0.97	N/A	N/A
0	0.53	N/A	N/A

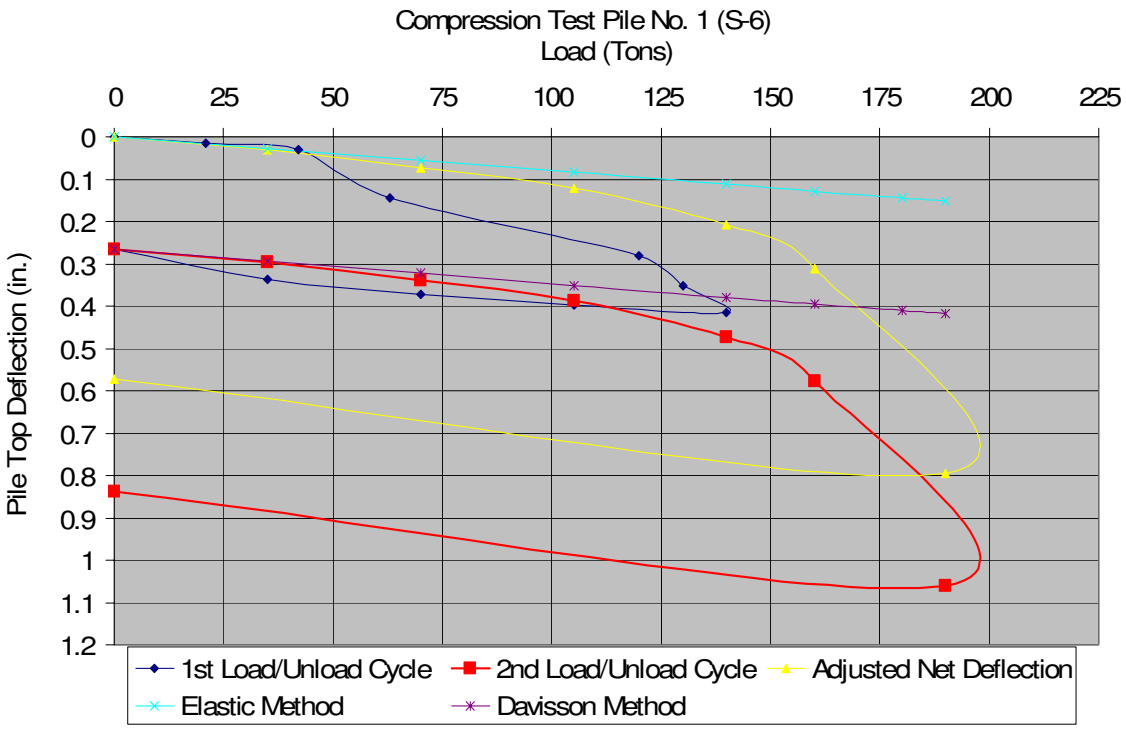

Figure 46-Load Deflection Plot Sample No. 6, Test Pile No. 1

Table 18-Load Test Data Sample No. 6, Test Pile No. 1

Sample 6 - Test Pile 1	**Compression Test**		
1st Load / Unload Cycle		2nd Load / Unload Cycle	
Applied Test Load (tons)	**Pile Top Deflection (in.)**	**Test Load (tons)**	**Pile Top Deflection (in.)**
0	0	0	0.266
21	0.014	35	0.297
42	0.0305	70	0.3385
63	0.144	105	0.3885
120	0.28	140	0.473
130	0.353	160	0.578
140	0.415	190	1.062
105	0.398	0	0.839
70	0.372	----	----
35	0.337	----	----
0	0.266	----	----

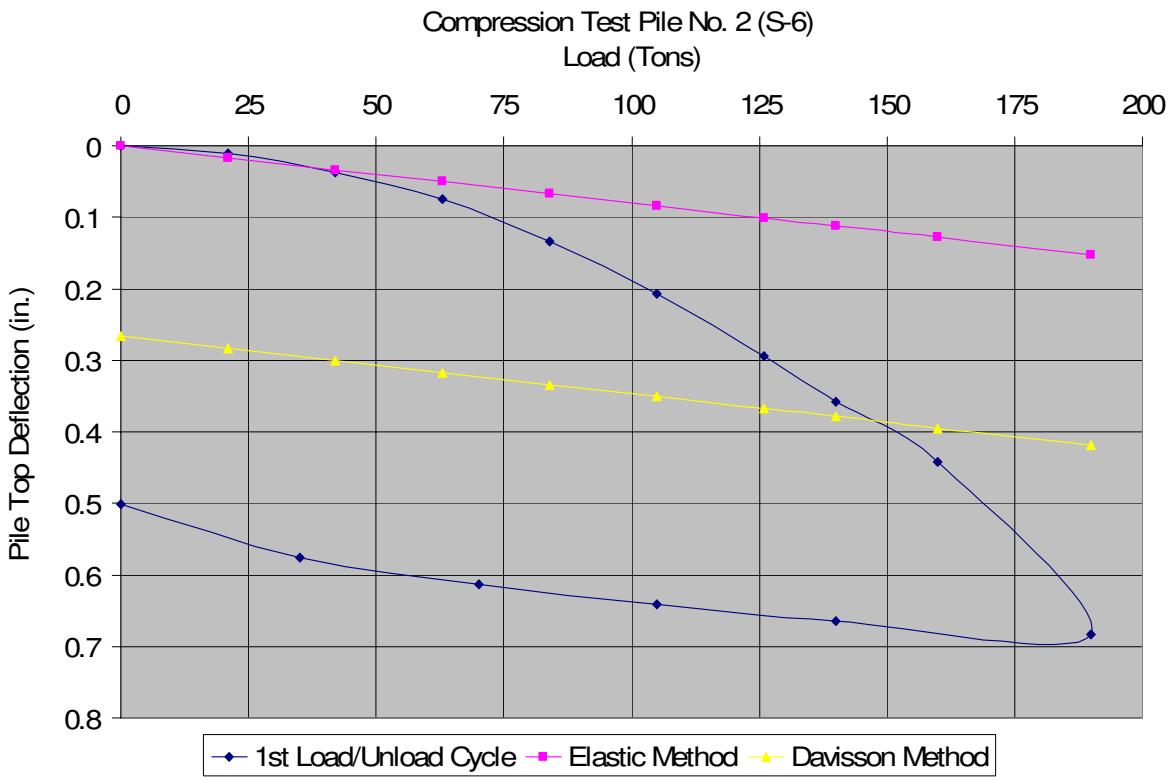

Figure 47-Load Deflection Plot Sample No. 6, Test Pile No. 2

Table 19-Load Test Data Sample No. 6, Test Pile No. 2

Sample 6 - Test Pile 2	**Compression Test**		
1st Load / Unload Cycle		2nd Load / Unload Cycle	
Applied Test Load (tons)	**Pile Top Deflection (in.)**	**Test Load (tons)**	**Pile Top Deflection (in.)**
0	0	N/A	N/A
21	0.0105	N/A	N/A
42	0.0375	N/A	N/A
63	0.075	N/A	N/A
84	0.1345	N/A	N/A
105	0.2075	N/A	N/A
126	0.2935	N/A	N/A
140	0.358	N/A	N/A
160	0.4415	N/A	N/A
190	0.6825	N/A	N/A
140	0.664	N/A	N/A
105	0.642	N/A	N/A
70	0.613	N/A	N/A
35	0.576	N/A	N/A
0	0.501	N/A	N/A

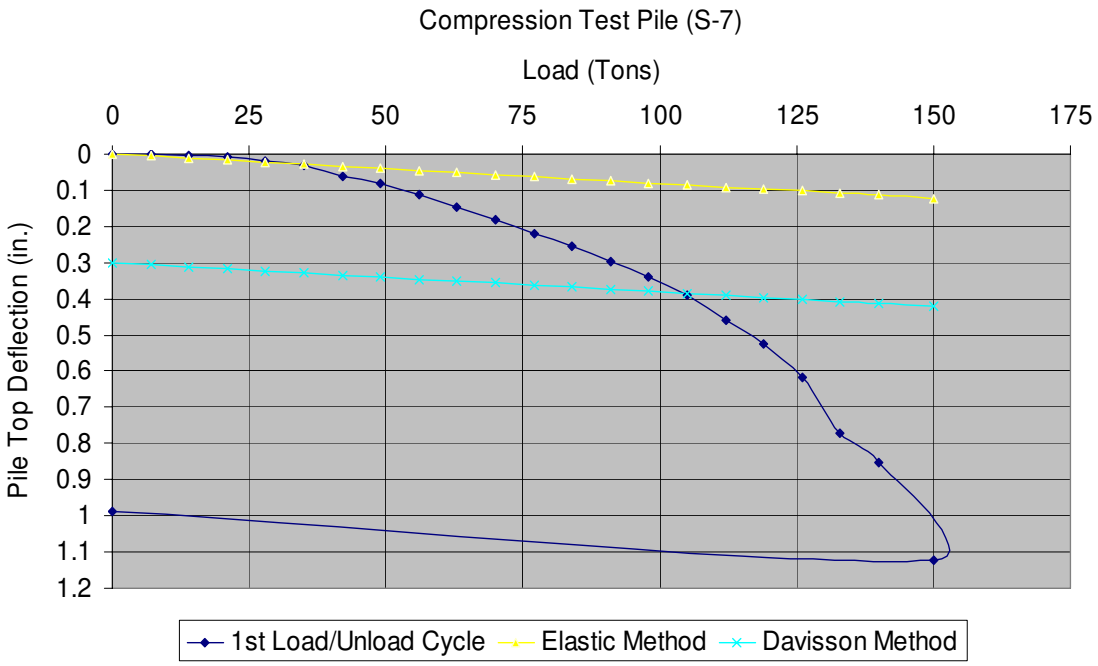

Figure 48-Load Deflection Plot Sample No. 7, Test Pile No.1

Table 20-Load Test Data Sample No. 7, Test Pile No.1

Sample 7 - Test Pile 1	**Compression Test**		
1st Load / Unload Cycle		2nd Load / Unload Cycle	
Applied Test Load (tons)	**Pile Top Deflection (in.)**	**Test Load (tons)**	**Pile Top Deflection (in.)**
0	0	N/A	N/A
7	0	N/A	N/A
14	0.002	N/A	N/A
21	0.008	N/A	N/A
28	0.02	N/A	N/A
35	0.032	N/A	N/A
42	0.06	N/A	N/A
49	0.082	N/A	N/A
56	0.111	N/A	N/A
63	0.146	N/A	N/A
70	0.181	N/A	N/A
77	0.219	N/A	N/A
84	0.253	N/A	N/A
91	0.296	N/A	N/A
98	0.34	N/A	N/A
105	0.388	N/A	N/A
112	0.46	N/A	N/A
119	0.526	N/A	N/A
126	0.617	N/A	N/A
133	0.77	N/A	N/A
140	0.854	N/A	N/A
150	1.123	N/A	N/A
0	0.987	N/A	N/A

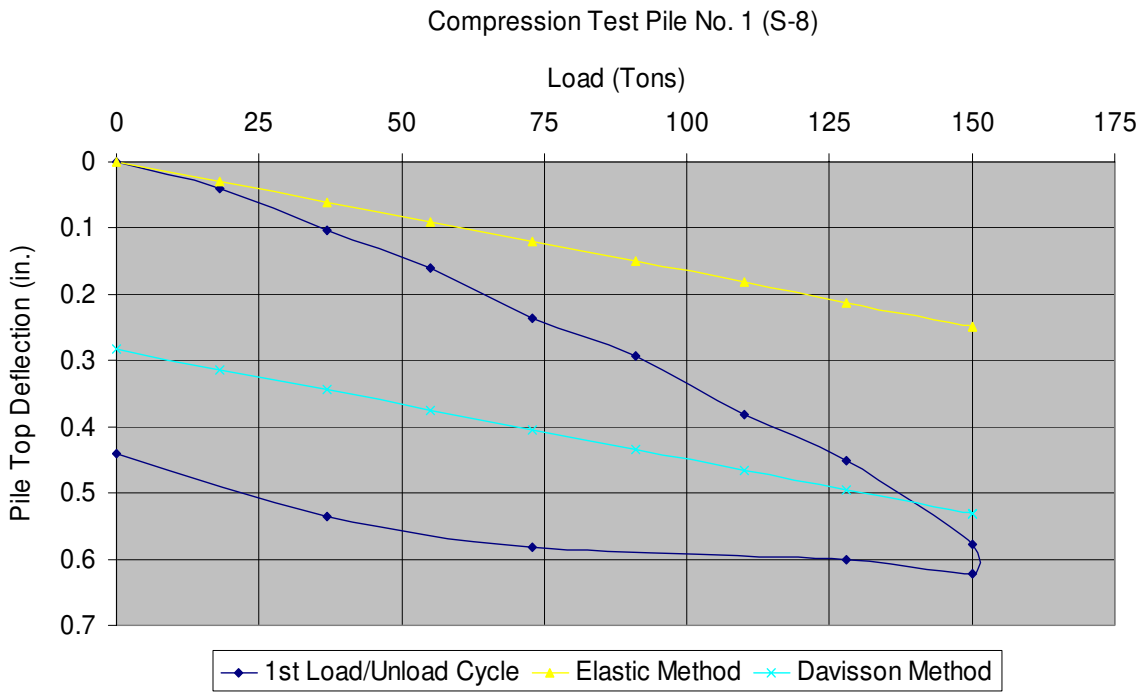

Figure 49-Load Deflection Plot Sample No. 8, Test Pile No. 1

Table 21-Load Test Data Sample No. 8, Test Pile No. 1

Sample 8 - Test Pile 1	**Compression Test**		
1st Load / Unload Cycle		2nd Load / Unload Cycle	
Applied Test Load (tons)	**Pile Top Deflection (in.)**	**Test Load (tons)**	**Pile Top Deflection (in.)**
0	0	N/A	N/A
18	0.041	N/A	N/A
37	0.103	N/A	N/A
55	0.161	N/A	N/A
73	0.237	N/A	N/A
91	0.293	N/A	N/A
110	0.381	N/A	N/A
128	0.452	N/A	N/A
150	0.578	N/A	N/A
150	0.621	N/A	N/A
128	0.6	N/A	N/A
73	0.581	N/A	N/A
37	0.535	N/A	N/A
0	0.44	N/A	N/A
98	0.34	N/A	N/A
105	0.388	N/A	N/A
112	0.46	N/A	N/A
119	0.526	N/A	N/A
126	0.617	N/A	N/A
133	0.77	N/A	N/A
140	0.854	N/A	N/A
150	1.123	N/A	N/A
0	0.987	N/A	N/A

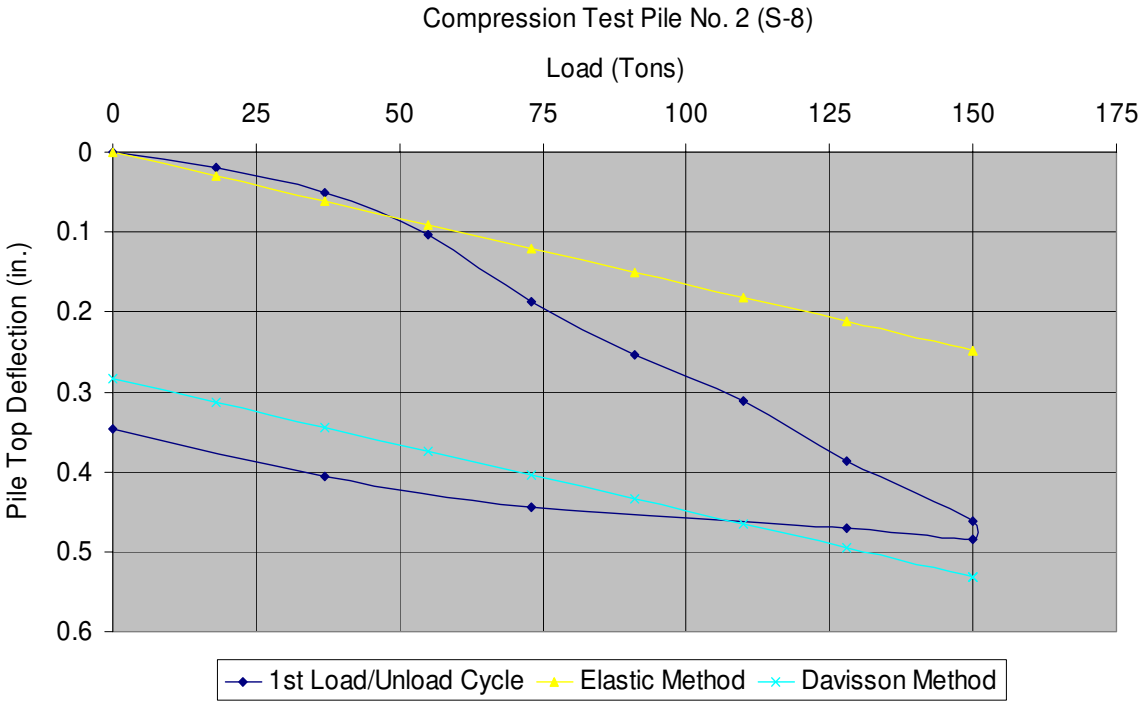

Figure 50-Load Deflection Plot Sample No. 8, Test Pile No. 2

Table 22-Load Test Data Sample No. 8, Test Pile No. 2

Sample 8 - Test Pile 2	**Compression Test**		
1st Load / Unload Cycle		2nd Load / Unload Cycle	
Applied Test Load (tons)	**Pile Top Deflection (in.)**	**Test Load (tons)**	**Pile Top Deflection (in.)**
0	0	N/A	N/A
18	0.0189	N/A	N/A
37	0.0502	N/A	N/A
55	0.104	N/A	N/A
73	0.188	N/A	N/A
91	0.254	N/A	N/A
110	0.312	N/A	N/A
128	0.387	N/A	N/A
150	0.462	N/A	N/A
150	0.484	N/A	N/A
128	0.47	N/A	N/A
73	0.445	N/A	N/A
37	0.405	N/A	N/A
0	0.346	N/A	N/A

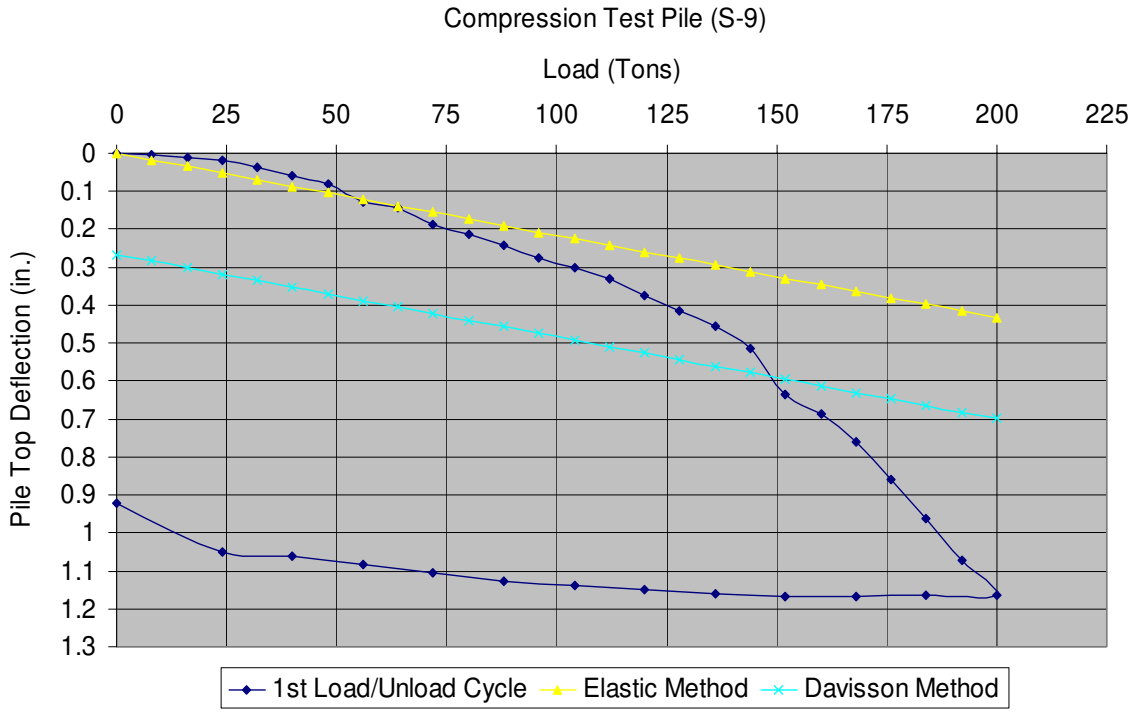

Figure 51-Load Deflection Plot Sample No. 9, Test Pile No.1

Table 23-Load Test Data Sample No. 9, Test Pile No.1

Sample 9	**Compression Test**		
1st Load / Unload Cycle		2nd Load / Unload Cycle	
Applied Test Load (tons)	**Pile Top Deflection (in.)**	**Test Load (tons)**	**Pile Top Deflection (in.)**
0	0	N/A	N/A
8	0.0035	N/A	N/A
16	0.0095	N/A	N/A
24	0.02	N/A	N/A
32	0.037	N/A	N/A
40	0.057	N/A	N/A
48	0.0815	N/A	N/A
56	0.127	N/A	N/A
64	0.145	N/A	N/A
72	0.1865	N/A	N/A
80	0.2115	N/A	N/A
88	0.2425	N/A	N/A
96	0.275	N/A	N/A
104	0.3005	N/A	N/A
112	0.332	N/A	N/A
120	0.3755	N/A	N/A
128	0.4145	N/A	N/A
136	0.4555	N/A	N/A
144	0.5125	N/A	N/A
152	0.635	N/A	N/A
160	0.686	N/A	N/A
168	0.76	N/A	N/A
176	0.8585	N/A	N/A
184	0.9635	N/A	N/A
192	1.0735	N/A	N/A
200	1.1645	N/A	N/A
184	1.165	N/A	N/A
168	1.1665	N/A	N/A
152	1.1685	N/A	N/A
136	1.162	N/A	N/A
120	1.151	N/A	N/A
104	1.14	N/A	N/A
88	1.1265	N/A	N/A
72	1.1065	N/A	N/A
56	1.083	N/A	N/A
40	1.0595	N/A	N/A
24	1.05	N/A	N/A
0	0.922	N/A	N/A

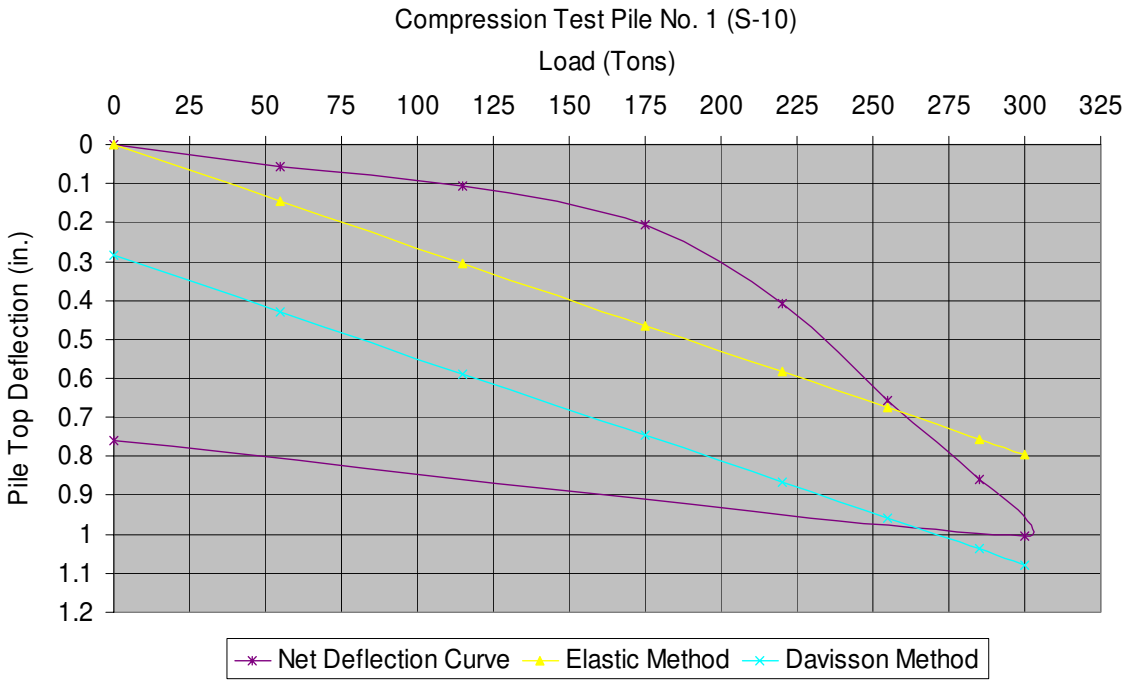

Figure 52-Load Deflection Plot Sample No 10, Test Pile No. 1

Table 24-Load Test Data Sample No. 10, Test Pile No. 1

Sample 10 - Test Pile 1	**Compression Test**		
1st Load / Unload Cycle		2nd Load / Unload Cycle	
Applied Test Load (tons)	**Pile Top Deflection (in.)**	**Test Load (tons)**	**Pile Top Deflection (in.)**
0	0	0	0.343
18	0.011	55	0.399
39	0.0649	115	0.451
57	0.121	175	0.549
80	0.203	220	0.751
100	0.283	255	1
122	0.395	285	1.201
140	0.507	300	1.349
107	0.543	0	1.102

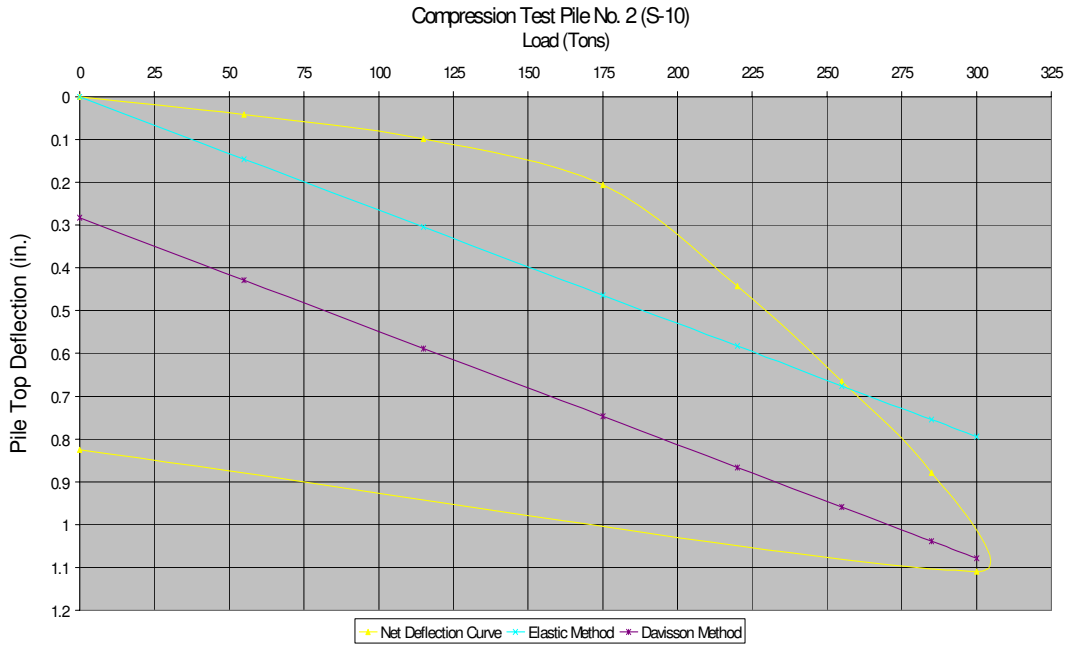

Figure 53-Load Deflection Plot No 10, Test Pile No. 2

Table 25-Load Test Data Sample No. 10, Test Pile No. 2

Sample 10 - Test Pile 2	**Compression Test**		
1st Load / Unload Cycle		2nd Load / Unload Cycle	
Applied Test Load (tons)	**Pile Top Deflection (in.)**	**Test Load (tons)**	**Pile Top Deflection (in.)**
0	0	0	0.379
18	0.014	55	0.421
39	0.056	115	0.477
57	0.138	175	0.585
80	0.22	220	0.821
100	0.307	255	1.045
122	0.421	285	1.258
140	0.532	300	1.489
107	0.511	0	1.204
71	0.489	----	----
28	0.382	----	----
0	0.379	----	----

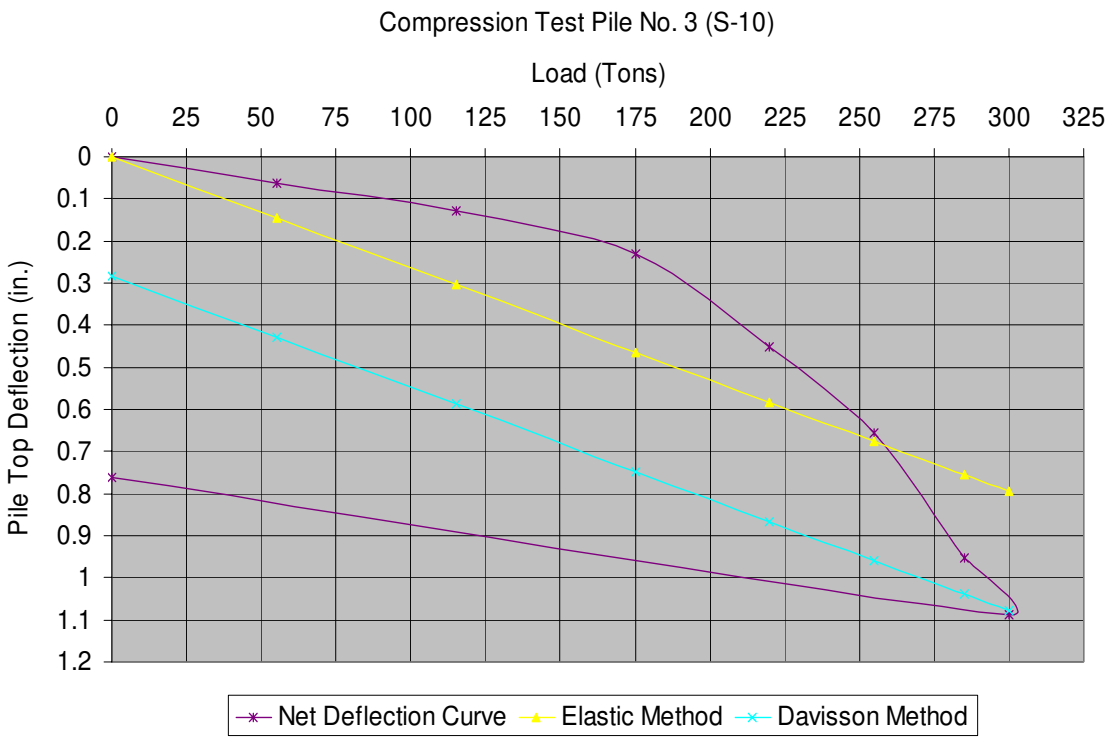

Figure 54-Load Deflection Plot No 10, Test Pile No. 3

Table 26-Load Test Data Sample No. 10, Test Pile No. 2

Sample 10 - Test Pile 3	**Compression Test**		
1st Load / Unload Cycle		2nd Load / Unload Cycle	
Applied Test Load (tons)	**Pile Top Deflection (in.)**	**Test Load (tons)**	**Pile Top Deflection (in.)**
0	0	0	0.349
18	0.011	55	0.412
39	0.0591	115	0.479
57	0.124	175	0.581
80	0.2	220	0.799
100	0.308	255	1.0034
122	0.4	285	1.303
140	0.473	300	1.438
107	0.498	0	1.109
71	0.461	----	----
28	0.422	----	----
0	0.349	----	----

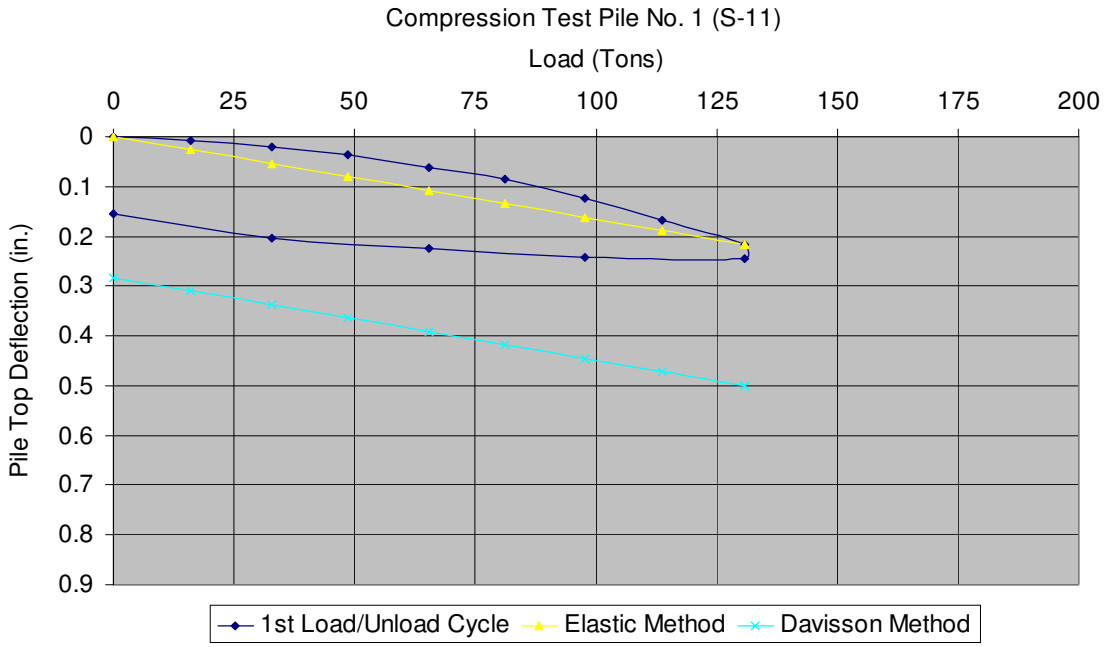

Figure 55-Load Deflection Plot Sample No. 11, Test Pile No.1

Table 27-Load Test Data Sample No. 11, Test Pile No.1

Sample 11 - Test Pile 1	**Compression Test**		
1st Load / Unload Cycle		2nd Load / Unload Cycle	
Applied Test Load (tons)	**Pile Top Deflection (in.)**	**Test Load (tons)**	**Pile Top Deflection (in.)**
0	0	N/A	N/A
16.1	0.0085	N/A	N/A
32.8	0.02	N/A	N/A
48.6	0.036	N/A	N/A
65.4	0.061	N/A	N/A
81.2	0.0845	N/A	N/A
97.8	0.124	N/A	N/A
113.7	0.1665	N/A	N/A
130.9	0.2175	N/A	N/A
130.9	0.244	N/A	N/A
97.8	0.242	N/A	N/A
65.4	0.2248	N/A	N/A
32.8	0.204	N/A	N/A
0	0.155	N/A	N/A

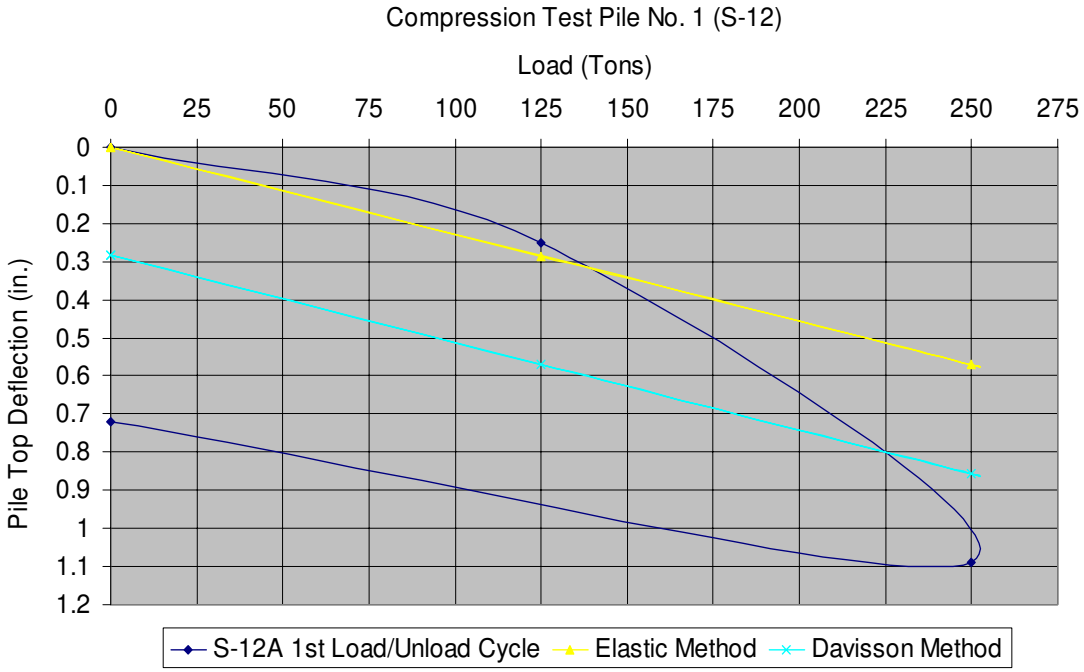

Figure 56-Load Deflection Plot Sample No. 12, Test Pile No. 1

Table 28-Load Test Data Sample No. 12, Test Pile No. 1

Sample 12 - Test Pile 1	**Compression Test**		
1st Load / Unload Cycle		2nd Load / Unload Cycle	
Applied Test Load (tons)	**Pile Top Deflection (in.)**	**Test Load (tons)**	**Pile Top Deflection (in.)**
0	0	N/A	N/A
125	0.25	N/A	N/A
250	1.09	N/A	N/A
0	0.72	N/A	N/A

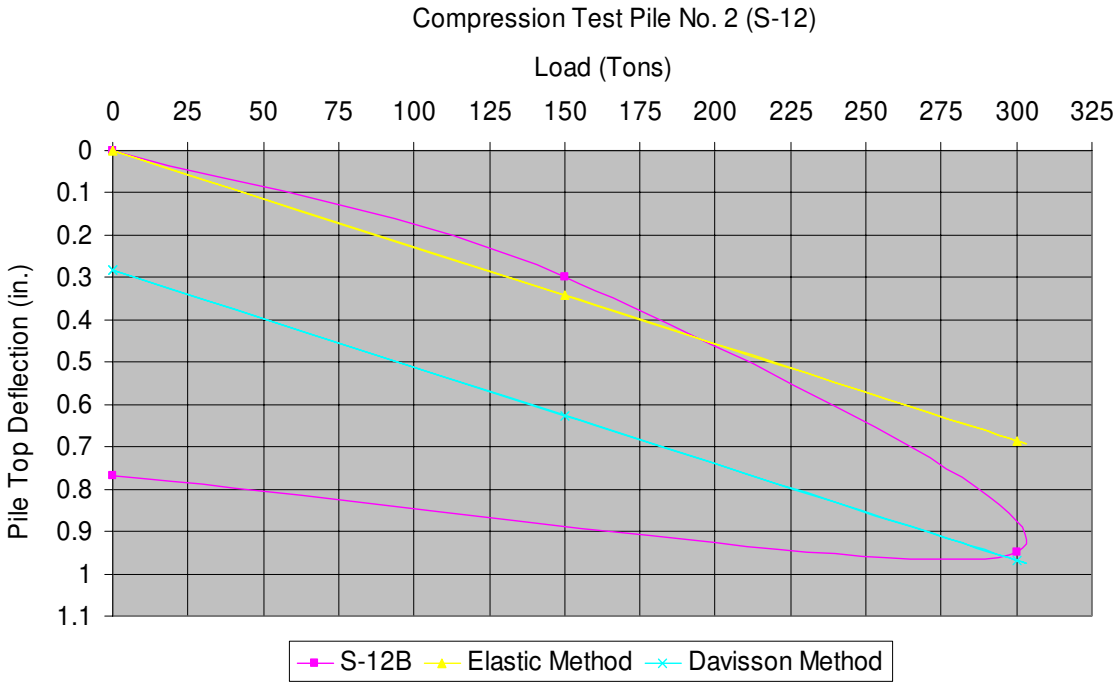

Figure 57-Load Deflection Plot Sample No. 12, Test Pile No. 2

Table 29-Load Test Data Sample No. 12, Test Pile No. 2

Sample 12 - Test Pile 2	**Compression Test**		
1st Load / Unload Cycle		2nd Load / Unload Cycle	
Applied Test Load (tons)	**Pile Top Deflection (in.)**	**Test Load (tons)**	**Pile Top Deflection (in.)**
0	0	N/A	N/A
150	0.3	N/A	N/A
300	0.95	N/A	N/A
0	0.77	N/A	N/A

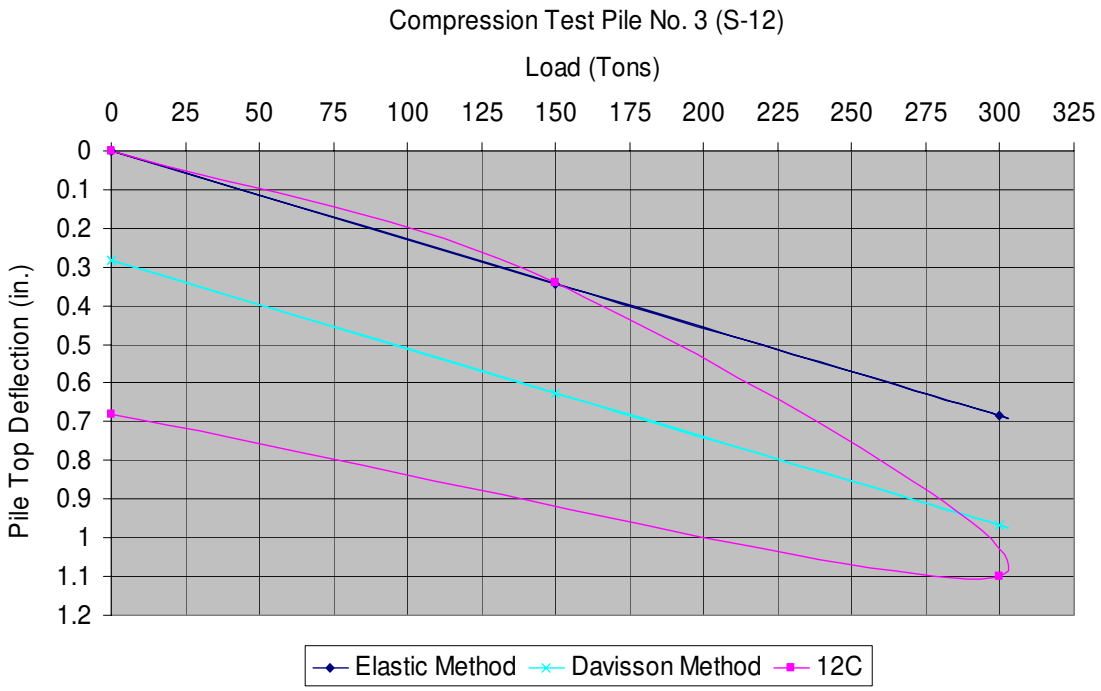

Figure 58-Load Deflection Plot Sample No. 12, Test Pile No. 3

Table 30-Load Test Data Sample No. 12, Test Pile No. 3

Sample 12 - Test Pile 3	**Compression Test**		
1st Load / Unload Cycle		2nd Load / Unload Cycle	
Applied Test Load (tons)	**Pile Top Deflection (in.)**	**Test Load (tons)**	**Pile Top Deflection (in.)**
0	0	N/A	N/A
150	0.339	N/A	N/A
300	1.1	N/A	N/A
0	0.68	N/A	N/A

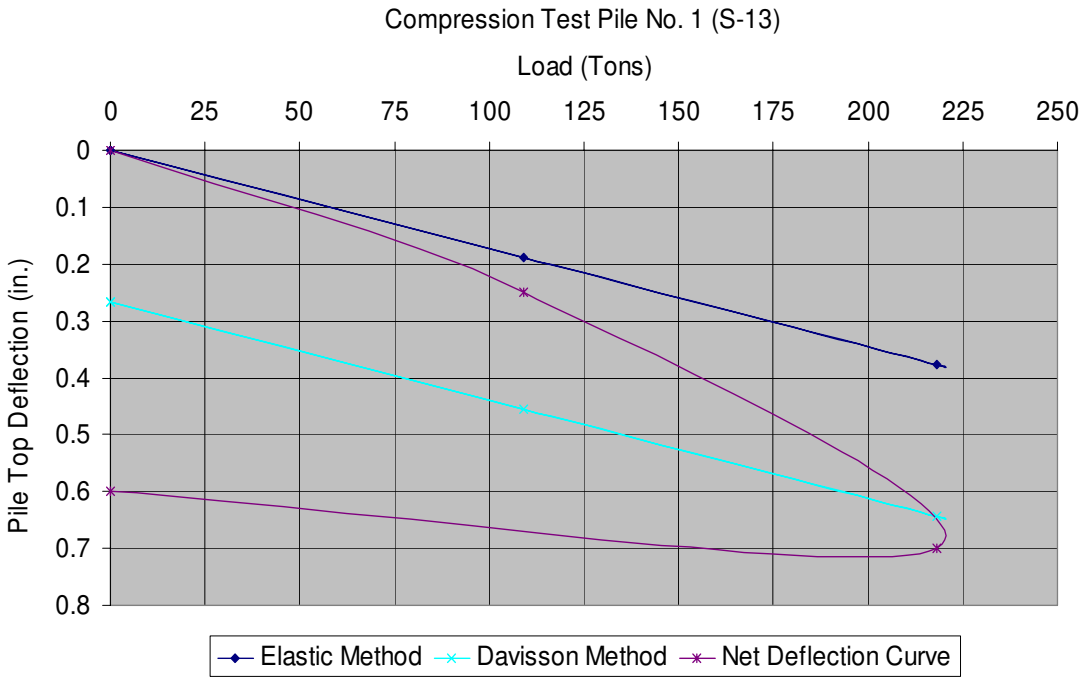

Figure 59-Load Deflection Plot Sample No. 13, Test Pile No. 1

Table 31- Load Test Data Sample No. 13, Test Pile No. 1

Sample 13 - Test Pile 1	**Compression Test**		
1st Load / Unload Cycle		2nd Load / Unload Cycle	
Applied Test Load (tons)	**Pile Top Deflection (in.)**	**Test Load (tons)**	**Pile Top Deflection (in.)**
0	0	N/A	N/A
109	0.25	N/A	N/A
218	0.7	N/A	N/A
0	0.6	N/A	N/A

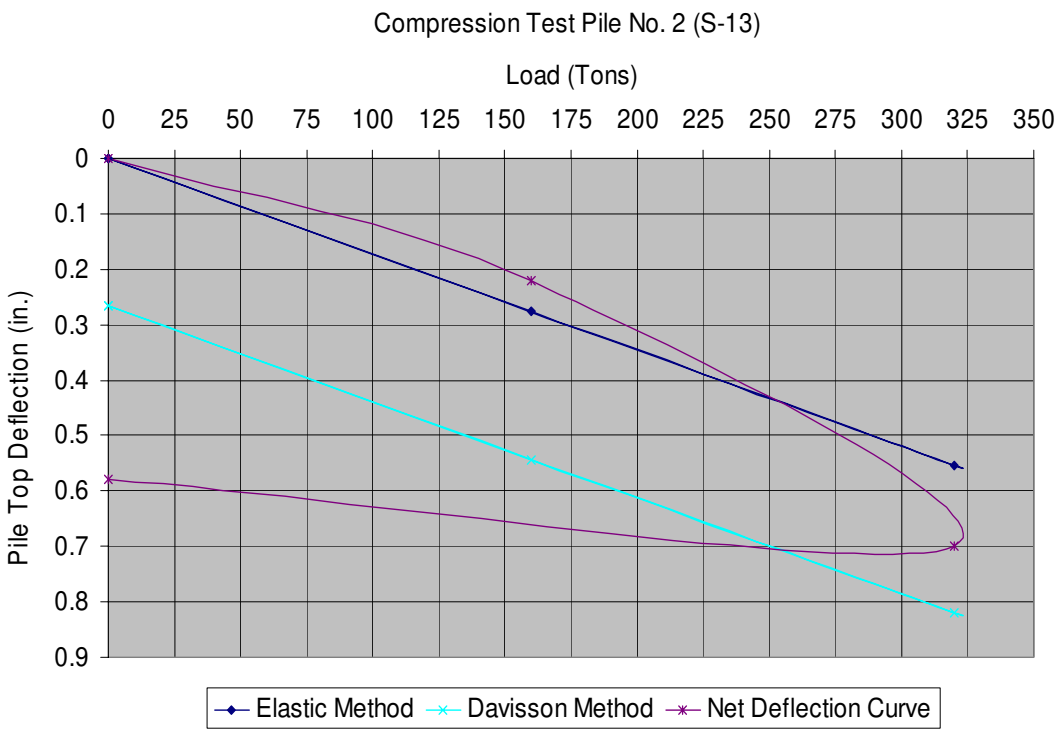

Figure 60-Load Deflection Plot Sample No. 13, Test Pile No. 2

Table 32- Load Test Data Sample No. 13, Test Pile No. 2

Sample 13 - Test Pile 2	**Compression Test**		
1st Load / Unload Cycle		2nd Load / Unload Cycle	
Applied Test Load (tons)	**Pile Top Deflection (in.)**	**Test Load (tons)**	**Pile Top Deflection (in.)**
0	0	N/A	N/A
160	0.22	N/A	N/A
320	0.7	N/A	N/A
0	0.58	N/A	N/A

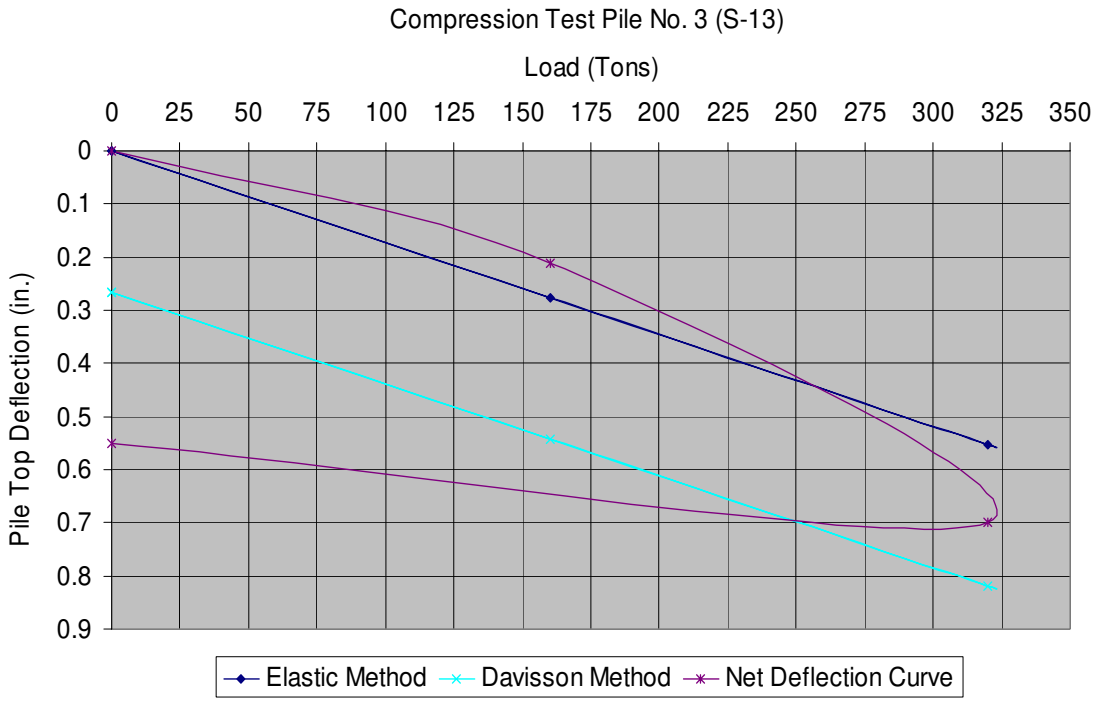

Figure 61-Load Deflection Plot Sample No. 13, Test Pile No. 3

Table 33- Load Test Data Sample No. 13, Test Pile No. 3

Sample 13 - Test Pile 3	**Compression Test**		
1st Load / Unload Cycle		2nd Load / Unload Cycle	
Applied Test Load (tons)	**Pile Top Deflection (in.)**	**Test Load (tons)**	**Pile Top Deflection (in.)**
0	0	N/A	N/A
160	0.21	N/A	N/A
320	0.7	N/A	N/A
0	0.55	N/A	N/A

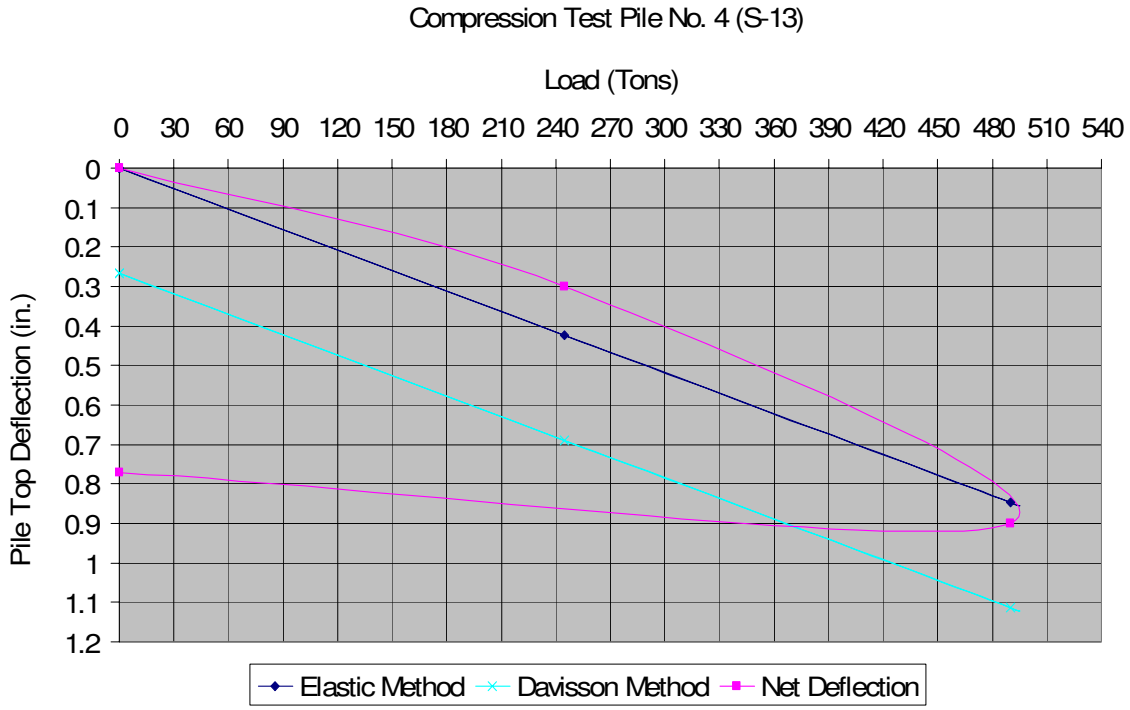

Figure 62-Load Deflection Plot Sample No. 13, Test Pile No. 4

Table 34- Load Test Data Sample No. 13, Test Pile No. 4

Sample 13 - Test Pile 4	**Compression Test**		
1st Load / Unload Cycle		2nd Load / Unload Cycle	
Applied Test Load (tons)	**Pile Top Deflection (in.)**	**Test Load (tons)**	**Pile Top Deflection (in.)**
0	0	N/A	N/A
245	0.3	N/A	N/A
490	0.9	N/A	N/A
0	0.77	N/A	N/A

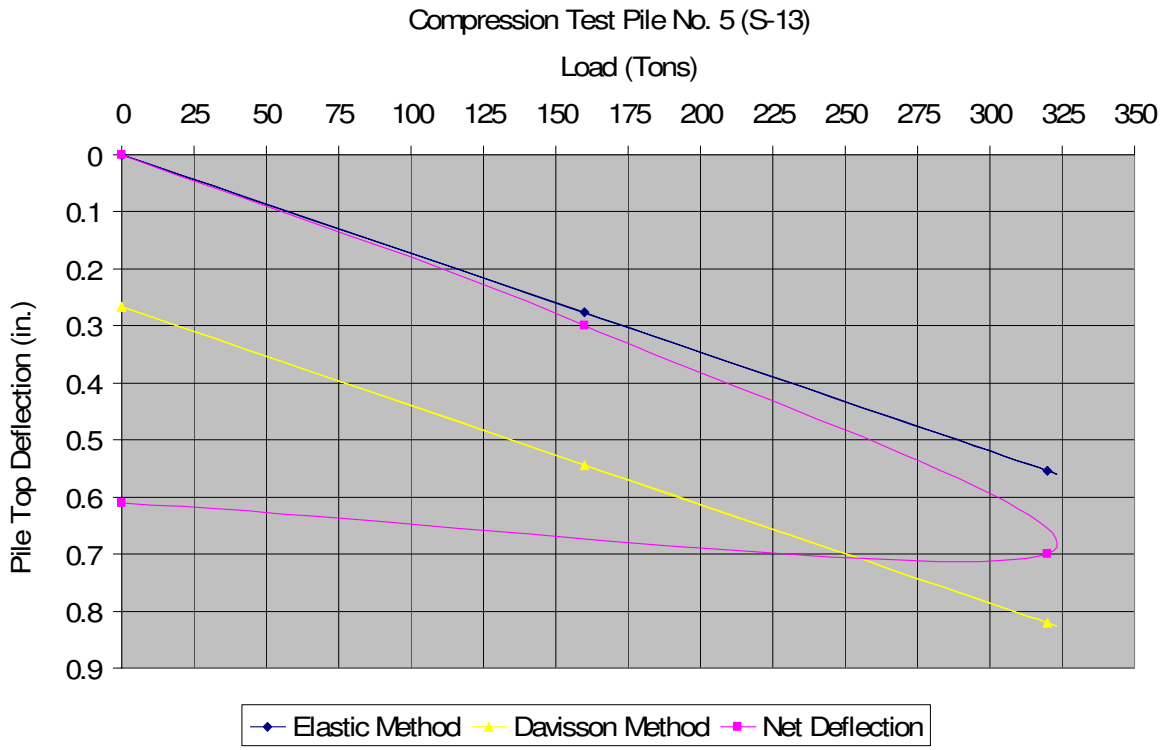

Figure 63-Load Deflection Plot Sample No. 13, Test Pile No. 5

Table 35- Load Test Data Sample No. 13, Test Pile No. 5

Sample 13 - Test Pile 5	**Compression Test**		
1st Load / Unload Cycle		2nd Load / Unload Cycle	
Applied Test Load (tons)	**Pile Top Deflection (in.)**	**Test Load (tons)**	**Pile Top Deflection (in.)**
0	0	N/A	N/A
160	0.3	N/A	N/A
320	0.7	N/A	N/A
0	0.61	N/A	N/A

APPENDIX E
CHIN-KONDNER'S METHOD FOR INTERPRATATION OF PHYSICAL LOAD TEST DATA CURVES AND LOADING INFORMATION

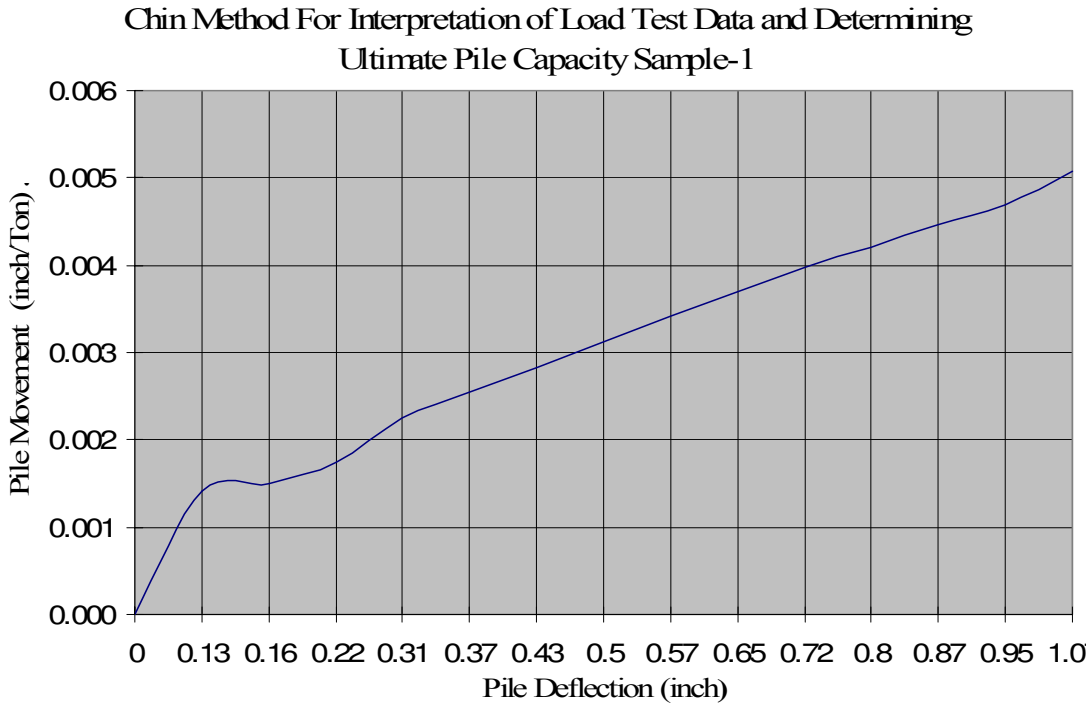

Figure 64-Chin's Method for Interpretation of Load Test Data Sample No. 1

Table 36-Chin's Load Test Data Sample No. 1

Compression Test - Sample No. 1		
Load / Unload Cycle		
Load Applied	**Pile Top Deflection Divided by Load Applied**	**Pile Top Deflection**
0	0.00000	0.00000
94	0.00141	0.13300
109	0.00150	0.16300
124	0.00174	0.21600
140	0.00224	0.31400
147	0.00254	0.37400
154	0.00282	0.43400
161	0.00313	0.50350
168	0.00342	0.57450
175	0.00370	0.64750
182	0.00397	0.72250
189	0.00421	0.79600
196	0.00446	0.87400
203	0.00468	0.95100
210	0.00507	1.06550
0	0.00000	0.74700

Chin's Method for Interpretation of Load Test Data

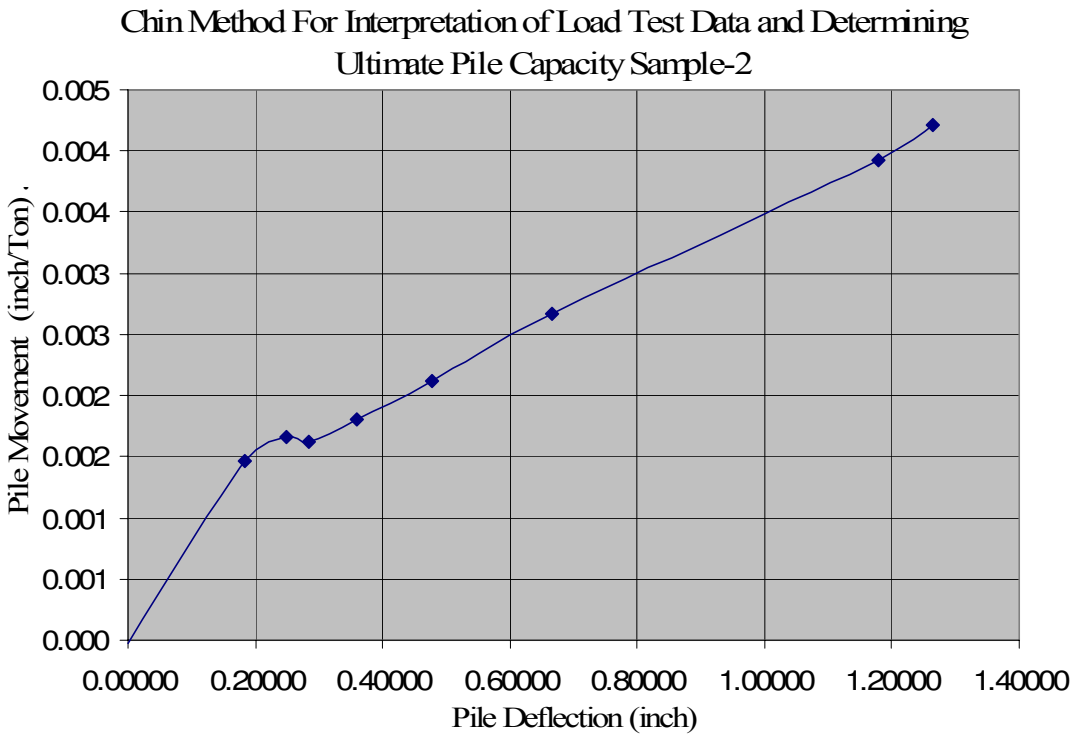

Figure 65-Chin's Method for Interpretation of Load Test Data Sample No. 2

Table 37-Chin's Load Test Data Sample No. 2

Compression Test - Sample No. 2		
Load / Unload Cycle		
Load Applied	**Pile Top Deflection Divided by Load Applied**	**Pile Top Deflection**
0	0.00000	0.00000
125	0.00146	0.18300
150	0.00167	0.25000
175	0.00163	0.28500
200	0.00180	0.36000
225	0.00212	0.47800
250	0.00266	0.66600
300	0.00393	1.17900
300	0.00422	1.26500

Chin's Method for Interpretation of Load Test Data

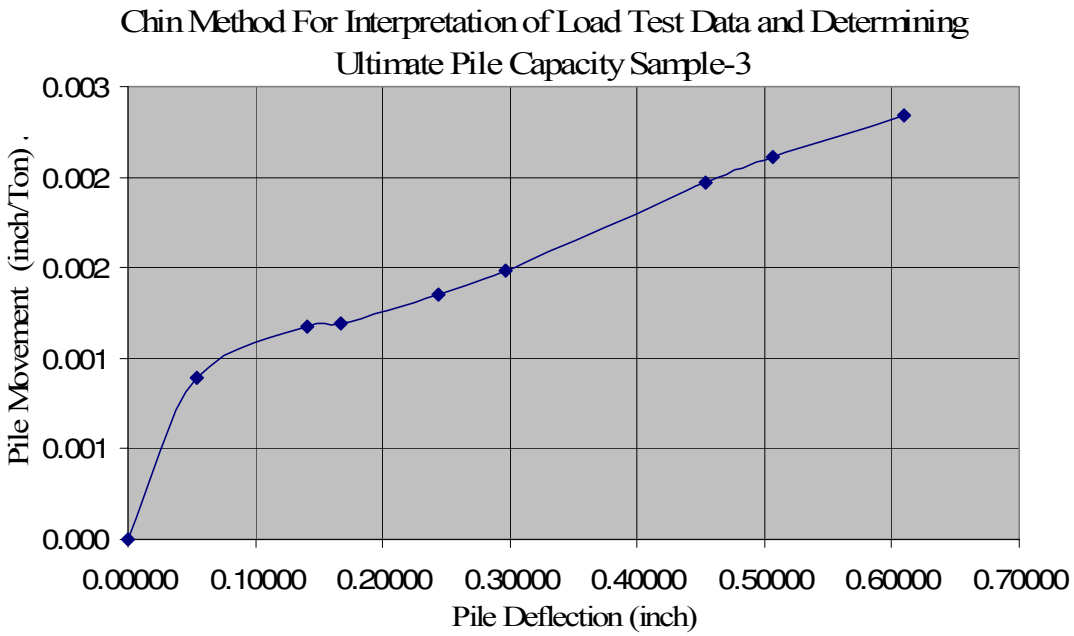

Figure 66-Chin's Method for Interpretation of Load Test Data Sample No. 3

Table 38-Chin's Load Test Data Sample No. 3

Compression Test - Sample No. 3		
Load / Unload Cycle		
Load Applied	**Pile Top Deflection Divided by Load Applied**	**Pile Top Deflection**
0	0.00000	0.00000
60	0.00089	0.05350
120	0.00117	0.14050
140	0.00120	0.16750
180	0.00135	0.24350
200	0.00149	0.29700
230	0.00197	0.45350
240	0.00211	0.50600
260	0.00234	0.60950
270	0.00244	0.65950
280	0.00258	0.72250
290	0.00274	0.79450
300	0.00285	0.85450

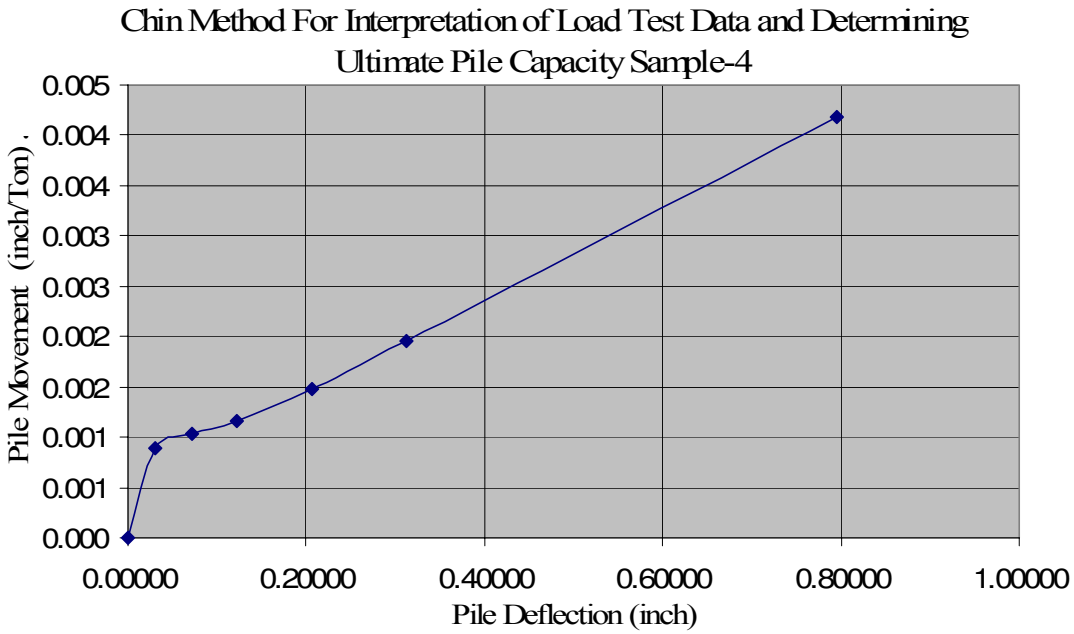

Figure 67-Chin's Method for Interpretation of Load Test Data Sample No. 4

Table 39-Chin's Load Test Data Sample No. 4

Compression Test - Sample No. 4		
Load / Unload Cycle		
Load Applied	**Pile Top Deflection Divided by Load Applied**	**Pile Top Deflection**
0	0.00000	0.00000
35	0.00089	0.03100
70	0.00104	0.07250
105	0.00117	0.12250
140	0.00148	0.20700
160	0.00195	0.31200
190	0.00419	0.79600

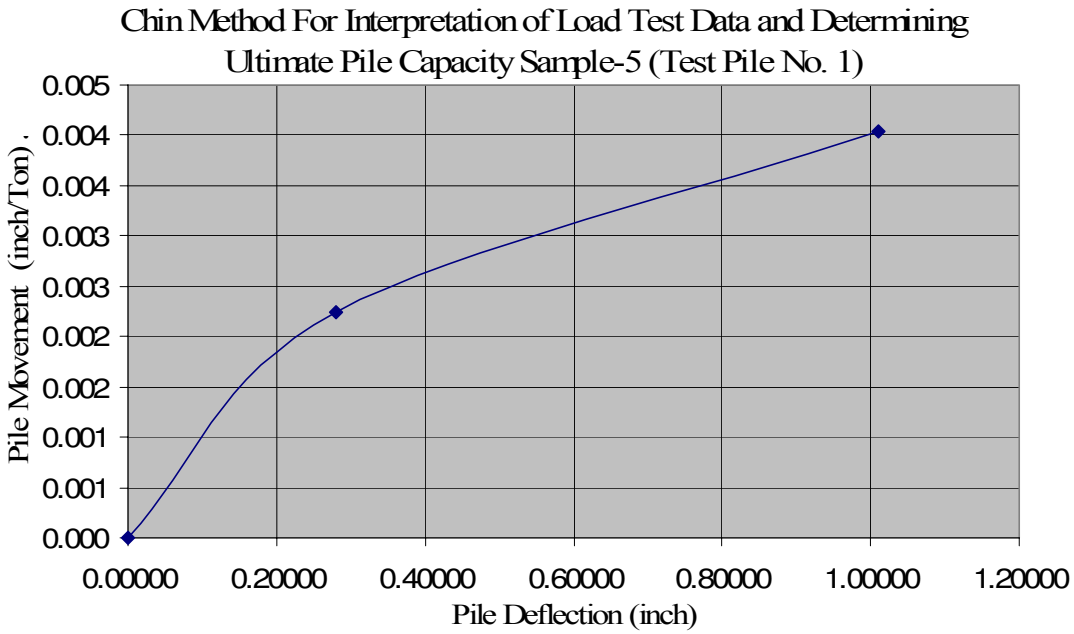

Figure 68-Chin's Method for Interpretation of Load Test Data Sample No. 5, Test Pile No. 1

Table 40-Chin's Load Test Data Sample No. 5, Test Pile No. 1

Compression Test - Sample No. 5 (Test Pile No. 1)		
Load / Unload Cycle		
Load Applied	**Pile Top Deflection Divided by Load Applied**	**Pile Top Deflection**
0	0.00000	0.00000
125	0.00224	0.28000
250	0.00404	1.01000

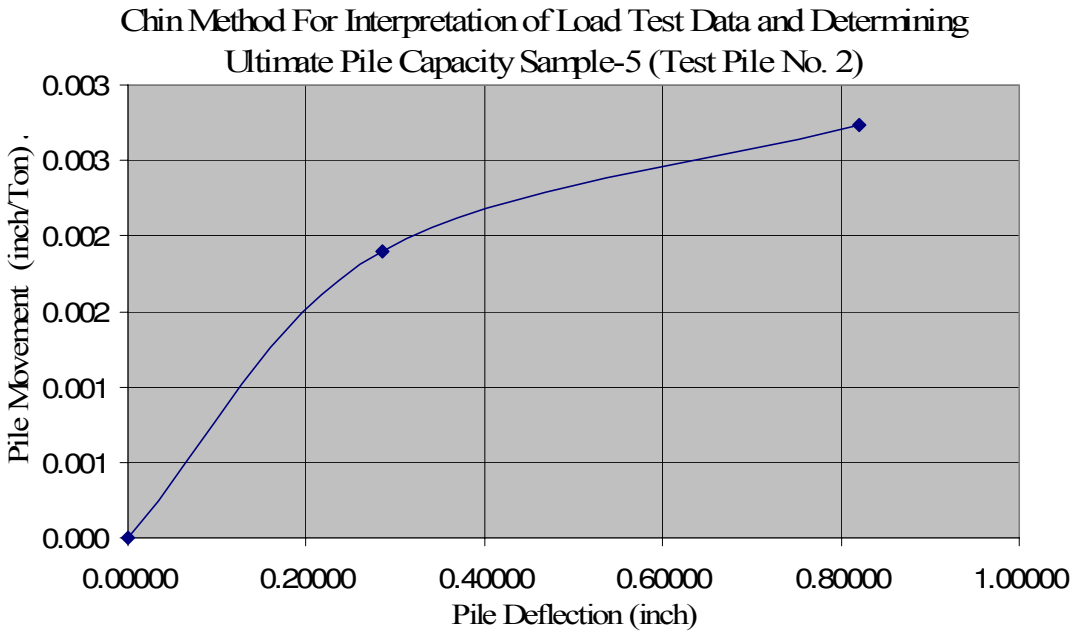

Figure 69-Chin's Method for Interpretation of Load Test Data Sample No. 5, Test Pile No. 2

Table 41-Chin's Load Test Data Sample No. 5, Test Pile No. 2

Compression Test - Sample No. 5 (Test Pile No. 2)		
Load / Unload Cycle		
Load Applied	**Pile Top Deflection Divided by Load Applied**	**Pile Top Deflection**
0	0.00000	0.00000
150	0.00190	0.28500
300	0.00273	0.82000

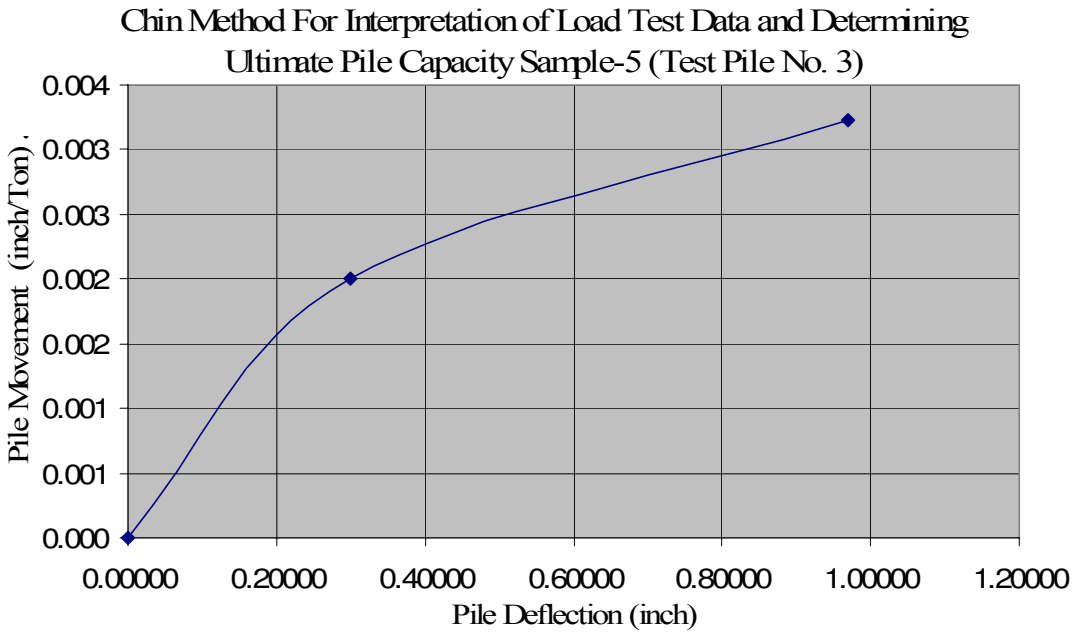

Figure 70-Chin's Method for Interpretation of Load Test Data Sample No. 5, Test Pile No. 3

Table 42-Chin's Load Test Data Sample No. 5, Test Pile No. 3

Compression Test - Sample No. 5 (Test Pile No. 3)		
Load / Unload Cycle		
Load Applied	**Pile Top Deflection Divided by Load Applied**	**Pile Top Deflection**
0	0.00000	0.00000
150	0.00200	0.30000
300	0.00323	0.97000

Chin's Method for Interpretation of Load Test Data

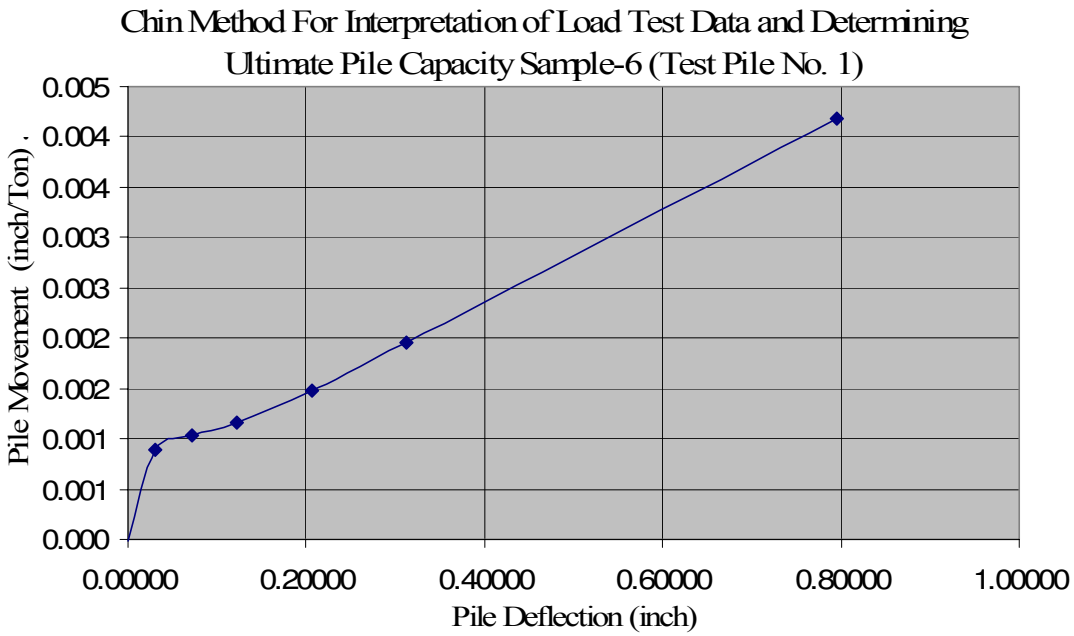

Figure 71-Chin's Method for Interpretation of Load Test Data Sample No. 6, Test Pile No. 1

Table 43-Chin's Load Test Data Sample No. 6, Test Pile No. 1

Compression Test - Sample No. 6 (Test Pile No. 1)		
Load / Unload Cycle		
Load Applied	**Pile Top Deflection Divided by Load Applied**	**Pile Top Deflection**
0	0.00000	0.00000
35	0.00089	0.03100
70	0.00104	0.07250
105	0.00117	0.12250
140	0.00148	0.20700
160	0.00195	0.31200
190	0.00419	0.79600

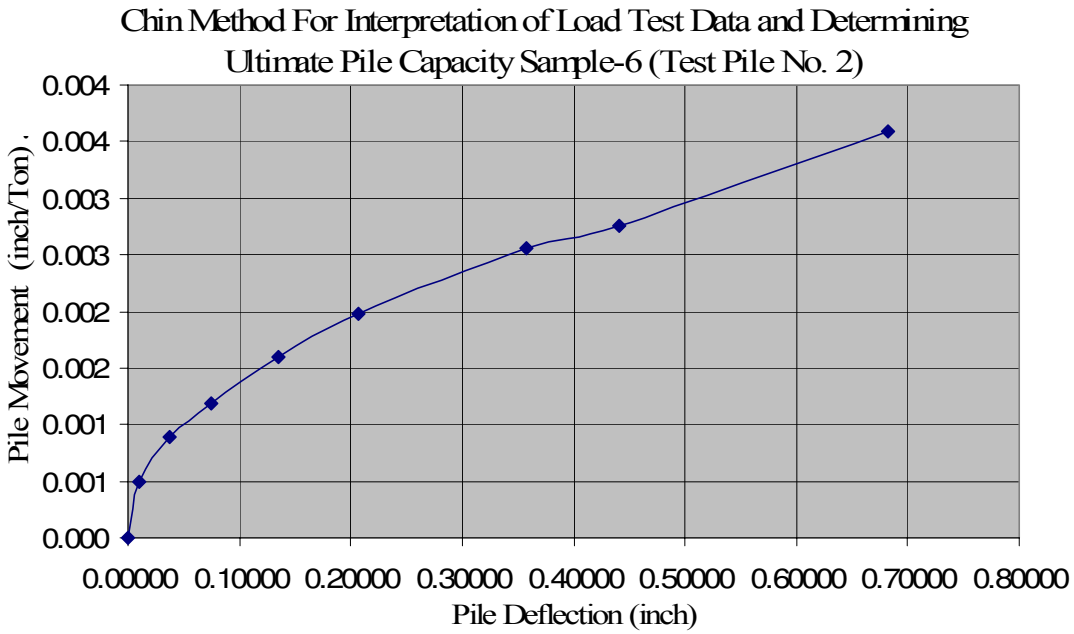

Figure 72-Chin's Method for Interpretation of Load Test Data Sample No. 6, Test Pile No. 2

Table 44-Chin's Load Test Data Sample No. 6, Test Pile No. 2

Compression Test - Sample No. 6 (Test Pile No. 2)		
Load / Unload Cycle		
Load Applied	**Pile Top Deflection Divided by Load Applied**	**Pile Top Deflection**
0	0.00000	0.00000
21	0.00050	0.01050
42	0.00089	0.03750
63	0.00119	0.07500
84	0.00160	0.13450
105	0.00198	0.20750
140	0.00256	0.35800
160	0.00276	0.44150
190	0.00359	0.68250

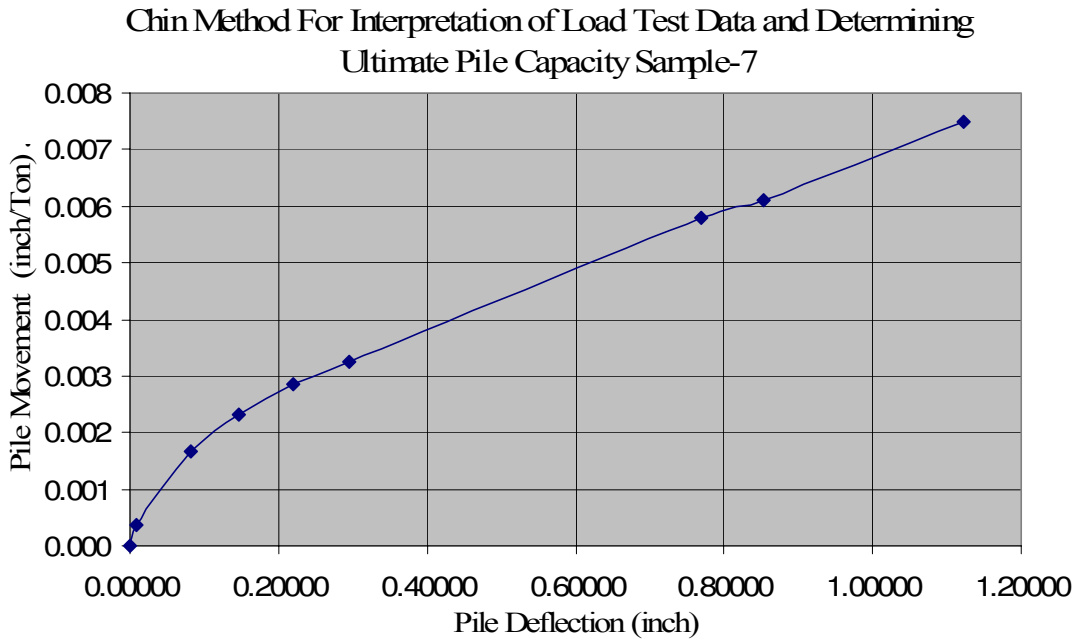

Figure 73-Chin's Method for Interpretation of Load Test Data Sample No. 7

Table 45-Chin's Load Test Data Sample No. 7

Compression Test - Sample No. 7		
Load / Unload Cycle		
Load Applied	**Pile Top Deflection Divided by Load Applied**	**Pile Top Deflection**
0	0.00000	0.00000
21	0.00038	0.00800
49	0.00167	0.08200
63	0.00232	0.14600
77	0.00284	0.21900
91	0.00325	0.29600
133	0.00579	0.77000
140	0.00610	0.85400
150	0.00749	1.12300

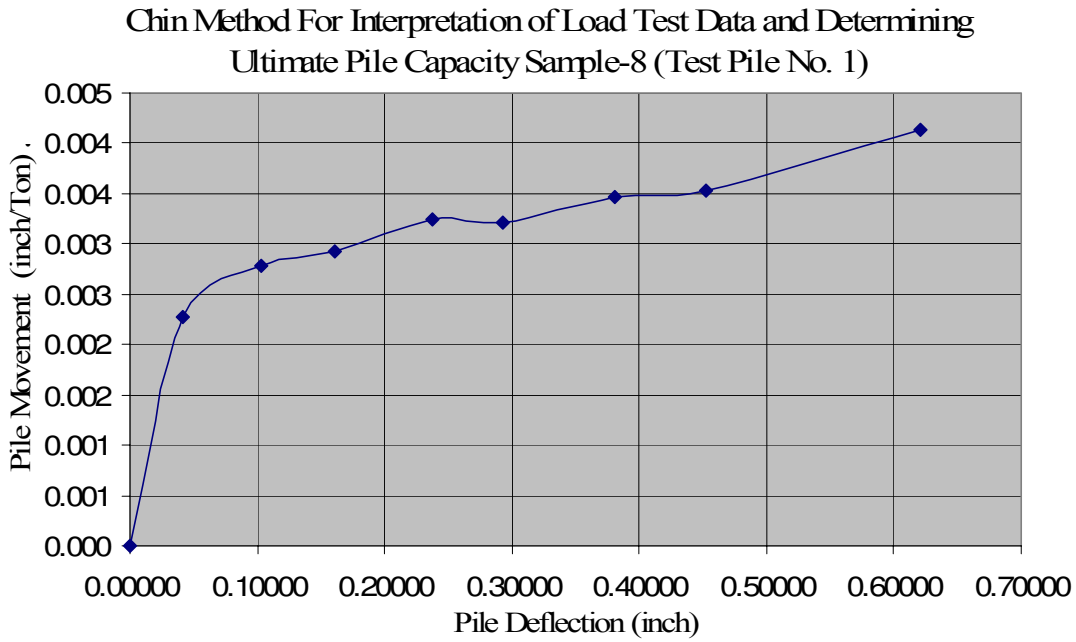

Figure 74-Chin's Method for Interpretation of Load Test Data Sample No. 8, Test Pile No. 1

Table 46-Chin's Load Test Data Sample No. 8, Test Pile No. 1

Compression Test - Sample No. 8 (Test Pile No. 1)		
Load / Unload Cycle		
Load Applied	**Pile Top Deflection Divided by Load Applied**	**Pile Top Deflection**
0	0.00000	0.00000
18	0.00228	0.04100
37	0.00278	0.10300
55	0.00293	0.16100
73	0.00325	0.23700
91	0.00322	0.29300
110	0.00346	0.38100
128	0.00353	0.45200
150	0.00414	0.62100

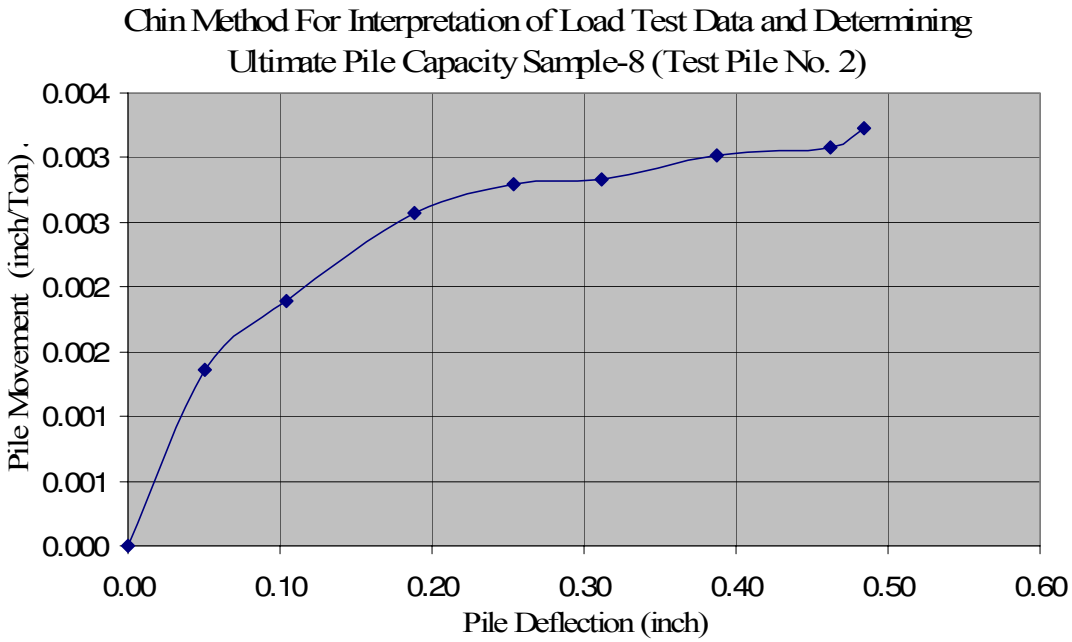

Figure 75-Chin's Method for Interpretation of Load Test Data Sample No. 8, Test Pile No. 2

Table 47-Chin's Load Test Data Sample No. 8, Test Pile No. 2

Compression Test - Sample No. 8 (Test Pile No. 2)		
Load / Unload Cycle		
Load Applied	**Pile Top Deflection Divided by Load Applied**	**Pile Top Deflection**
0	0.00000	0.00000
37	0.00136	0.05020
55	0.00189	0.10400
73	0.00258	0.18800
91	0.00279	0.25400
110	0.00284	0.31200
128	0.00302	0.38700
150	0.00308	0.46200
150	0.00323	0.48400

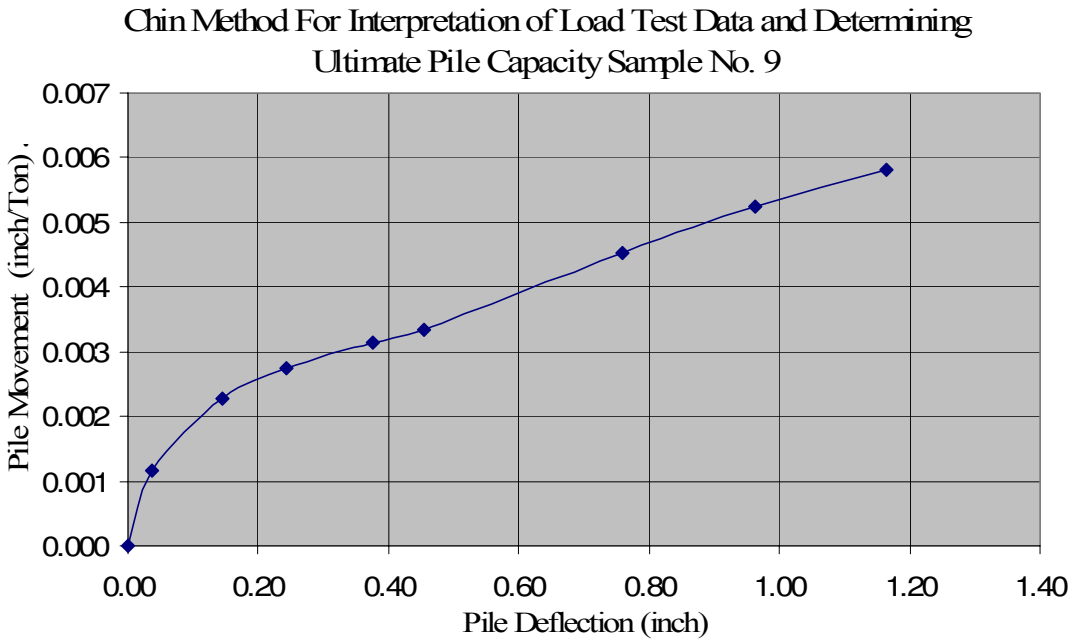

Figure 76-Chin's Method for Interpretation of Load Test Data Sample No. 9

Table 48-Chin's Load Test Data Sample No. 9

Compression Test - Sample No. 9		
Load / Unload Cycle		
Load Applied	**Pile Top Deflection Divided by Load Applied**	**Pile Top Deflection**
0	0.00000	0.00000
32	0.00116	0.03700
64	0.00227	0.14500
88	0.00276	0.24250
120	0.00313	0.37550
136	0.00335	0.45550
168	0.00452	0.76000
184	0.00524	0.96350
200	0.00582	1.16450

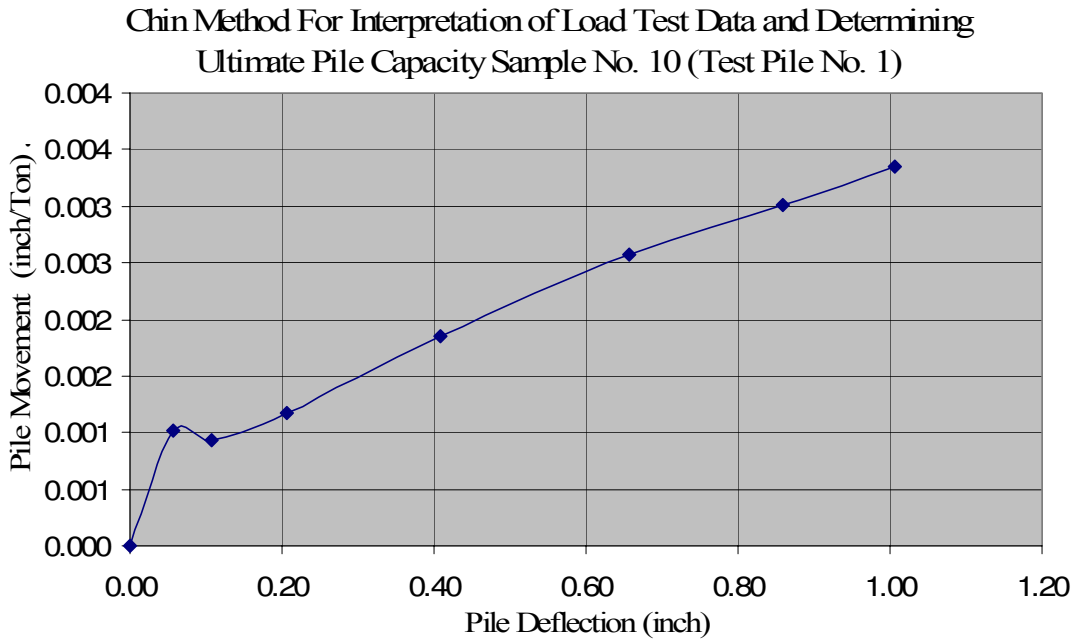

Figure 77-Chin's Method for Interpretation of Load Test Data Sample No. 10, Test Pile No. 1

Table 49-Chin's Load Test Data Sample No. 10, Test Pile No. 1

Compression Test - Sample No. 10 (Test Pile No. 1)		
Load / Unload Cycle		
Load Applied	**Pile Top Deflection Divided by Load Applied**	**Pile Top Deflection**
0	0.00000	0.00000
55	0.00102	0.05600
115	0.00094	0.10800
175	0.00118	0.20600
220	0.00185	0.40800
255	0.00258	0.65700
285	0.00301	0.85800
300	0.00335	1.00600

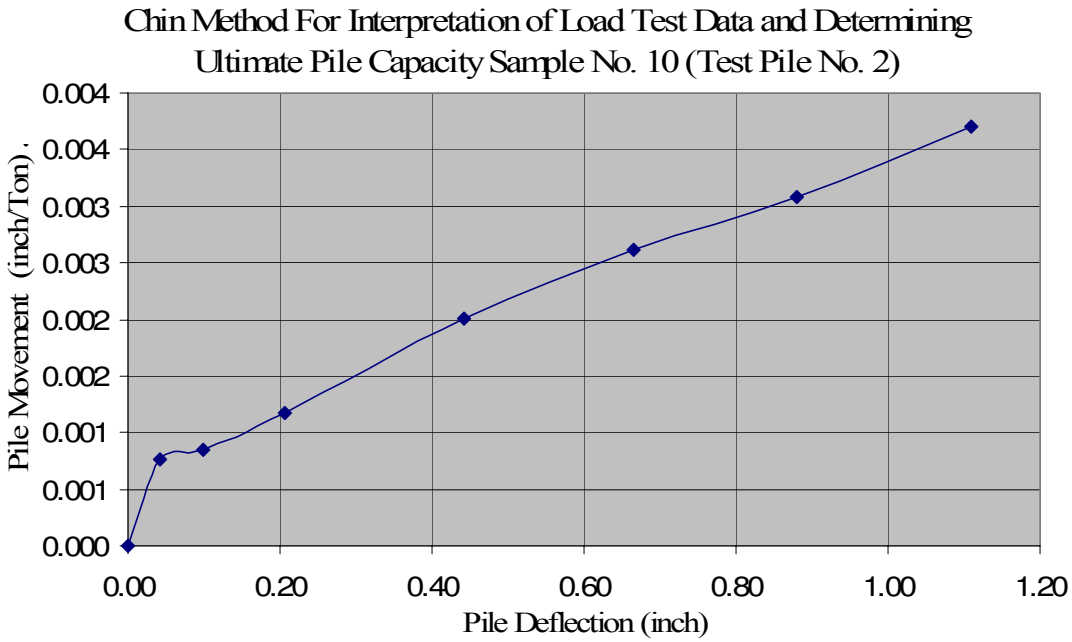

Figure 78-Chin's Method for Interpretation of Load Test Data Sample No. 10, Test Pile No. 2

Table 50-Chin's Load Test Data Sample No. 10, Test Pile No. 2

Compression Test - Sample No. 10 (Test Pile No. 2)		
Load / Unload Cycle		
Load Applied	**Pile Top Deflection Divided by Load Applied**	**Pile Top Deflection**
0	0.00000	0.00000
55	0.00076	0.04200
115	0.00085	0.09800
175	0.00118	0.20600
220	0.00201	0.44200
255	0.00261	0.66600
285	0.00308	0.87900
300	0.00370	1.11000

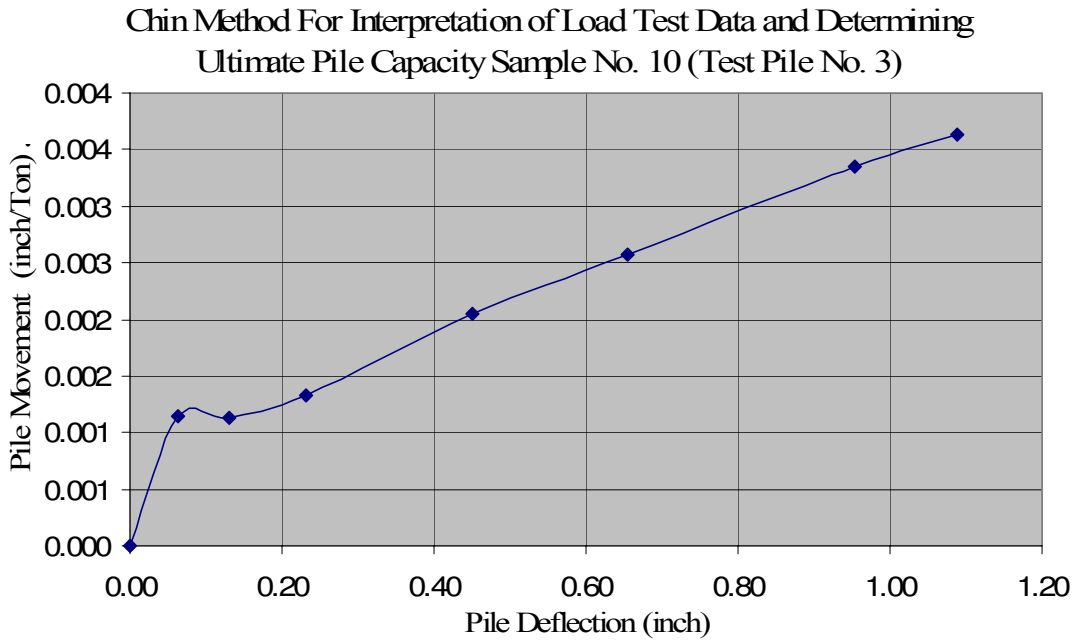

Figure 79-Chin's Method for Interpretation of Load Test Data Sample No. 10, Test Pile No. 3

Table 51-Chin's Load Test Data Sample No. 10, Test Pile No. 3

Compression Test - Sample No. 10 (Test Pile No. 3)		
Load / Unload Cycle		
Load Applied	**Pile Top Deflection Divided by Load Applied**	**Pile Top Deflection**
0	0.00000	0.00000
55	0.00115	0.06300
115	0.00113	0.13000
175	0.00133	0.23200
220	0.00205	0.45000
255	0.00257	0.65440
285	0.00335	0.95400
300	0.00363	1.08900

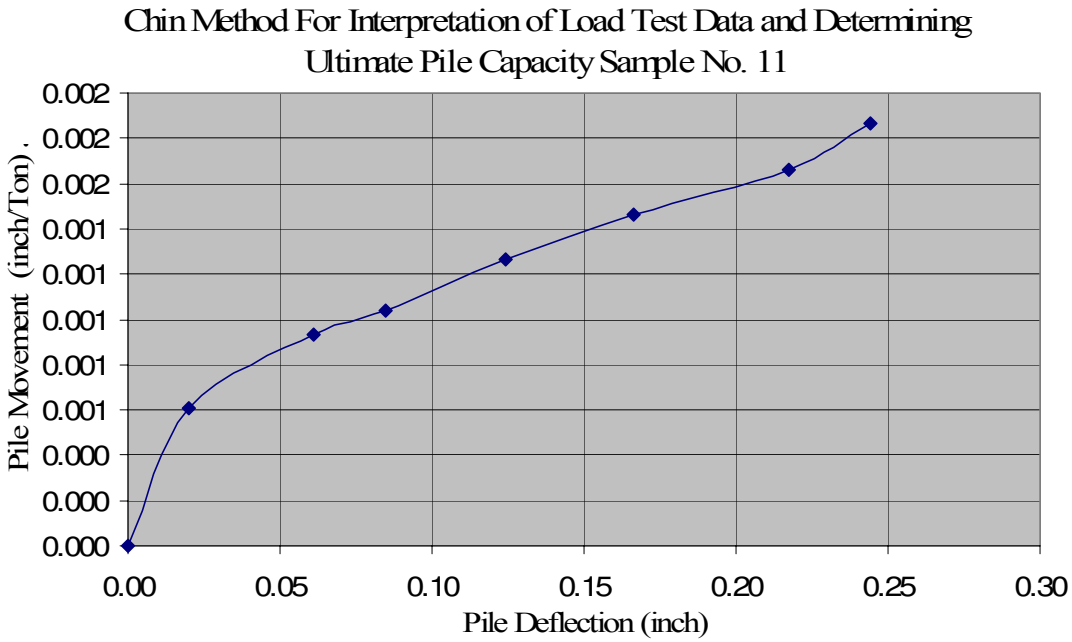

Figure 80-Chin's Method for Interpretation of Load Test Data Sample No. 11

Table 52-Chin's Load Test Data Sample No. 11

Compression Test - Sample No. 11		
Load / Unload Cycle		
Load Applied	**Pile Top Deflection Divided by Load Applied**	**Pile Top Deflection**
0	0.00000	0.00000
32.8	0.00061	0.02000
65.4	0.00093	0.06100
81.2	0.00104	0.08450
97.8	0.00127	0.12400
113.7	0.00146	0.16650
130.9	0.00166	0.21750
130.9	0.00186	0.24400

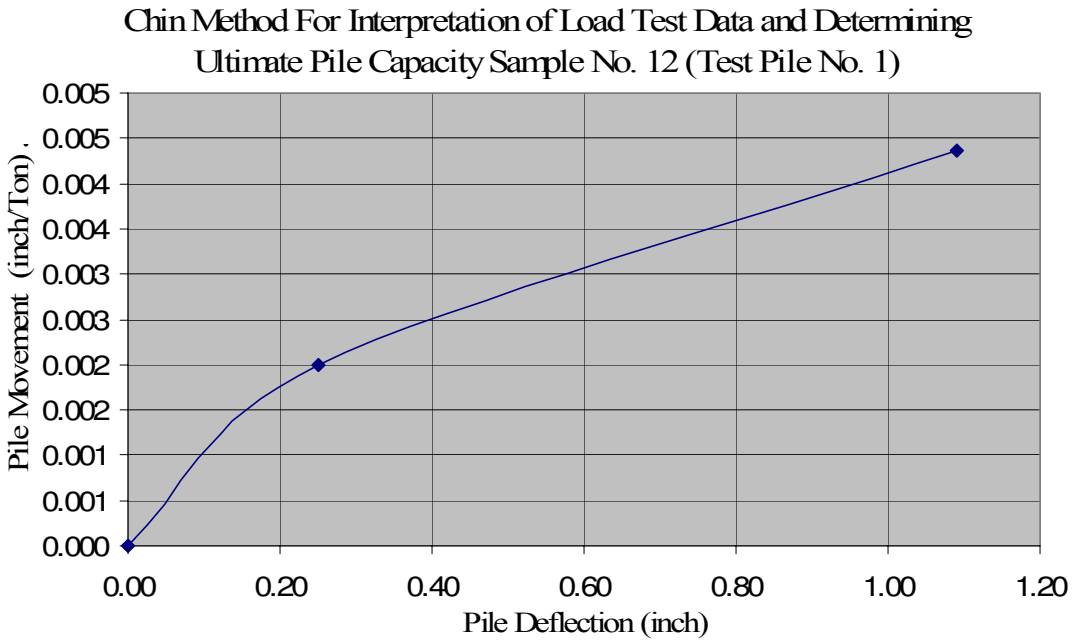

Figure 81-Chin's Method for Interpretation of Load Test Data Sample No. 12, Test Pile No. 1

Table 53-Chin's Load Test Data Sample No. 12, Test Pile No. 1

Compression Test - Sample No. 12 (Test Pile No. 1)		
Load / Unload Cycle		
Load Applied	**Pile Top Deflection Divided by Load Applied**	**Pile Top Deflection**
0	0.00000	0.00000
125	0.00200	0.25000
250	0.00436	1.09000

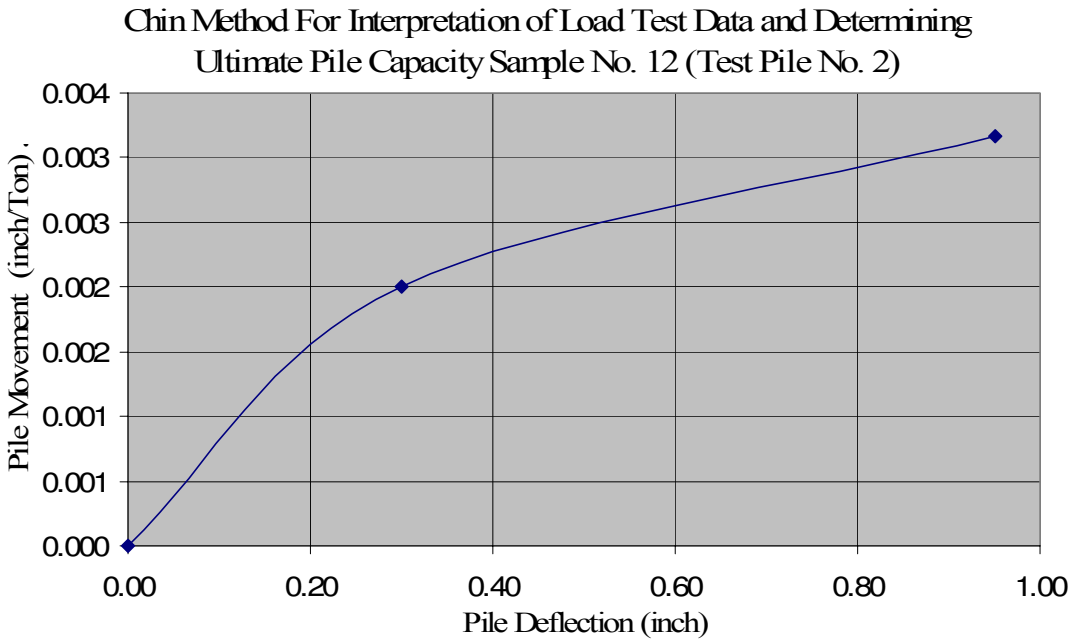

Figure 82-Chin's Method for Interpretation of Load Test Data Sample No. 12, Test Pile No. 2

Table 54-Chin's Load Test Data Sample No. 12, Test Pile No. 2

Compression Test - Sample No. 2 (Test Pile No. 12)		
Load / Unload Cycle		
Load Applied	**Pile Top Deflection Divided by Load Applied**	**Pile Top Deflection**
0	0.00000	0.00000
150	0.00200	0.30000
300	0.00317	0.95000

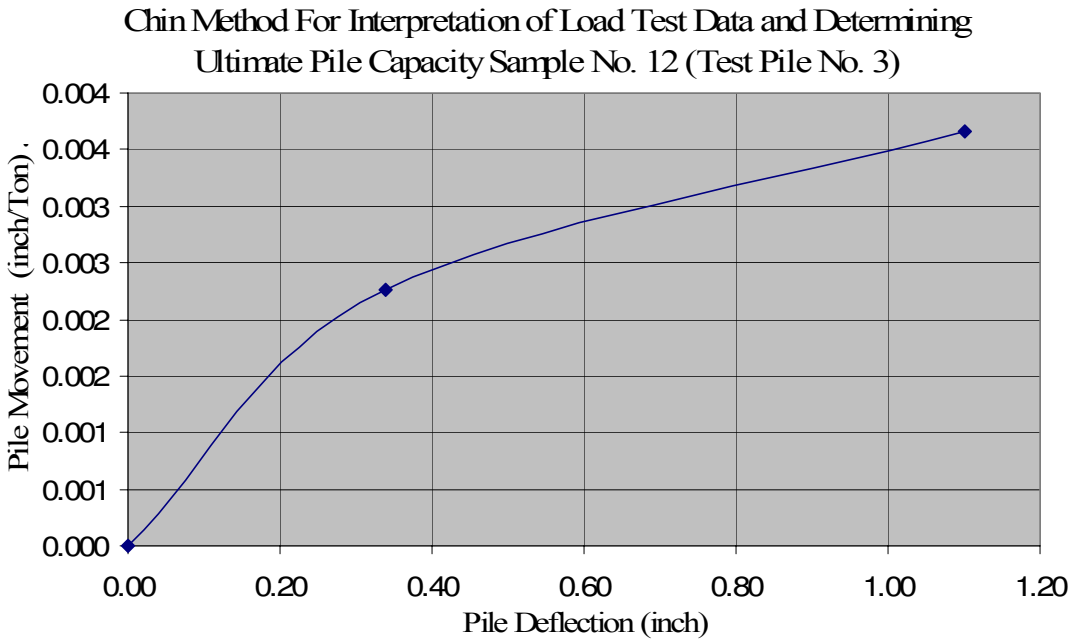

Figure 83-Chin's Method for Interpretation of Load Test Data Sample No. 12, Test Pile No. 3

Table 55-Chin's Load Test Data Sample No. 12, Test Pile No. 3

Compression Test - Sample No. 12 (Test Pile No. 3)		
Load / Unload Cycle		
Load Applied	**Pile Top Deflection Divided by Load Applied**	**Pile Top Deflection**
0	0.00000	0.00000
150	0.00226	0.33900
300	0.00367	1.10000

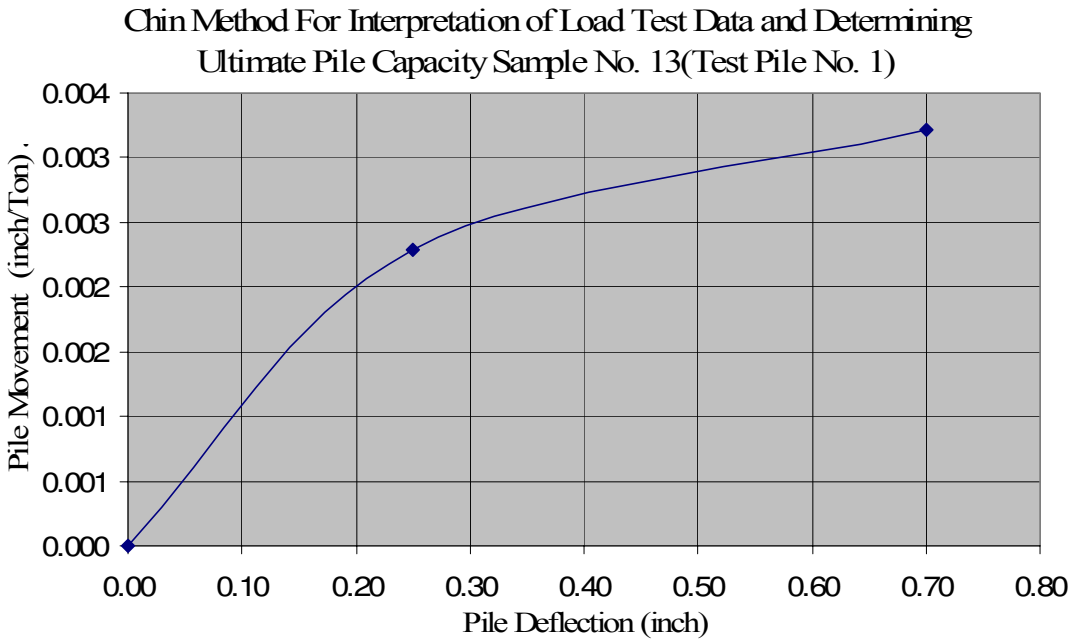

Figure 84-Chin's Method for Interpretation of Load Test Data Sample No. 13, Test Pile No. 1

Table 56-Chin's Load Test Data Sample No. 13, Test Pile No. 1

Compression Test - Sample No. 13 (Test Pile No. 1)		
Load / Unload Cycle		
Load Applied	**Pile Top Deflection Divided by Load Applied**	**Pile Top Deflection**
0	0.00000	0.00000
109	0.00229	0.25000
218	0.00321	0.70000

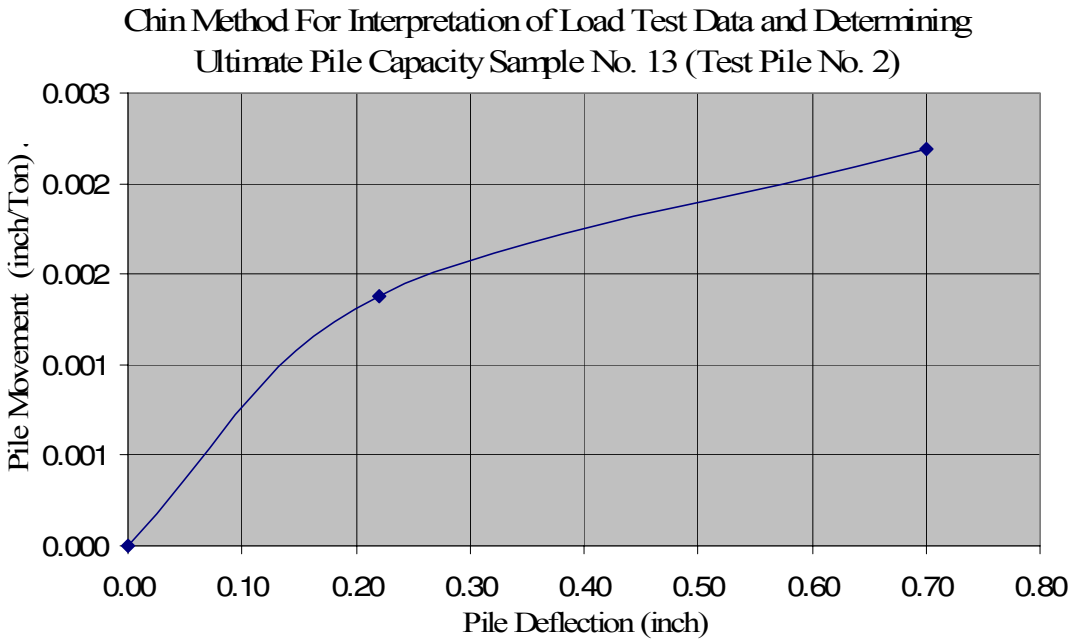

Figure 85-Chin's Method for Interpretation of Load Test Data Sample No. 13, Test Pile No. 2

Table 57-Chin's Load Test Data Sample No. 13, Test Pile No. 2

Compression Test - Sample No. 13 (Test Pile No. 2)		
Load / Unload Cycle		
Load Applied	**Pile Top Deflection Divided by Load Applied**	**Pile Top Deflection**
0	0.00000	0.00000
160	0.00138	0.22000
320	0.00219	0.70000

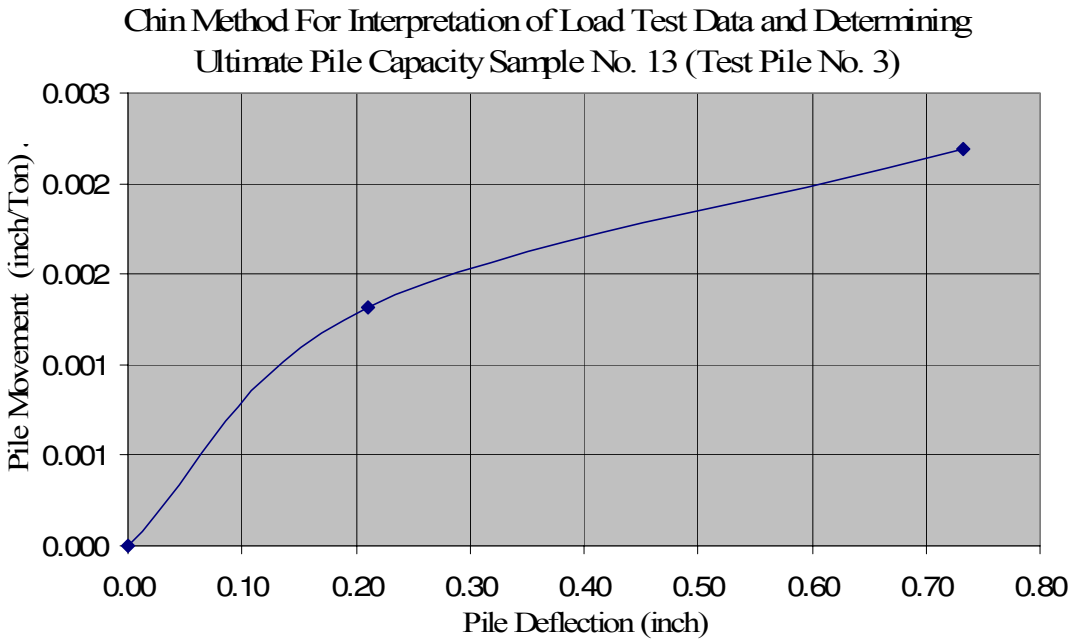

Figure 86-Chin's Method for Interpretation of Load Test Data Sample No. 13, Test Pile No. 3

Table 58-Chin's Load Test Data Sample No. 13, Test Pile No. 3

Compression Test - Sample No. 13 (Test Pile No. 3)		
Load / Unload Cycle		
Load Applied	**Pile Top Deflection Divided by Load Applied**	**Pile Top Deflection**
0	0.00000	0.00000
160	0.00131	0.21000
320	0.00219	0.73300

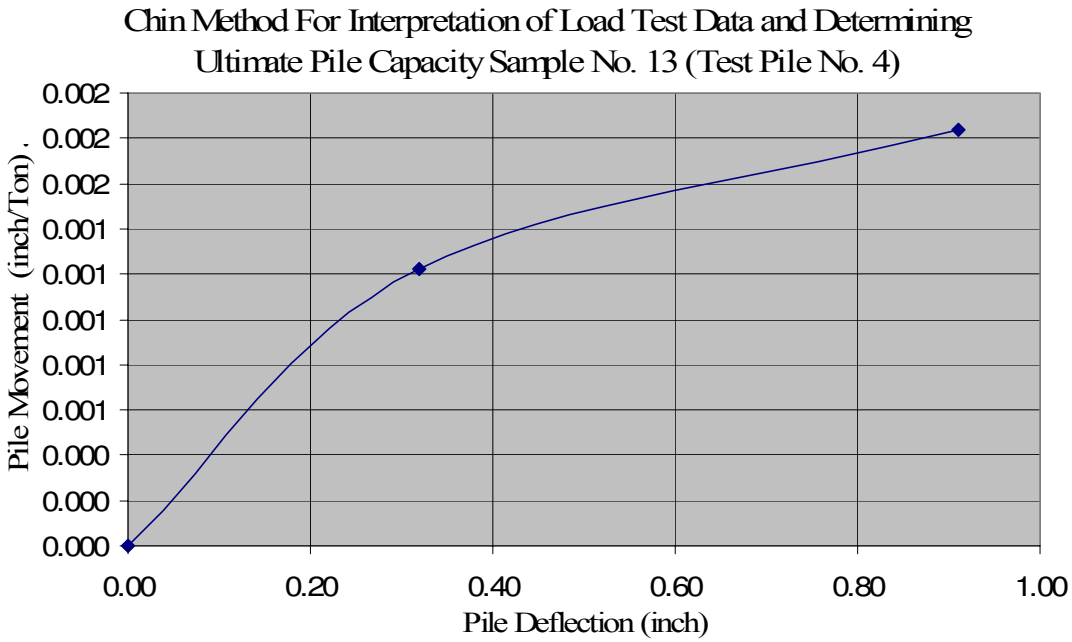

Figure 87-Chin's Method for Interpretation of Load Test Data Sample No. 13, Test Pile No. 4

Table 59-Chin's Load Test Data Sample No. 13, Test Pile No. 4

Compression Test - Sample No. 13 (Test Pile No. 4)		
Load / Unload Cycle		
Load Applied	**Pile Top Deflection Divided by Load Applied**	**Pile Top Deflection**
0	0.00000	0.00000
245	0.00122	0.32000
490	0.00184	0.91000

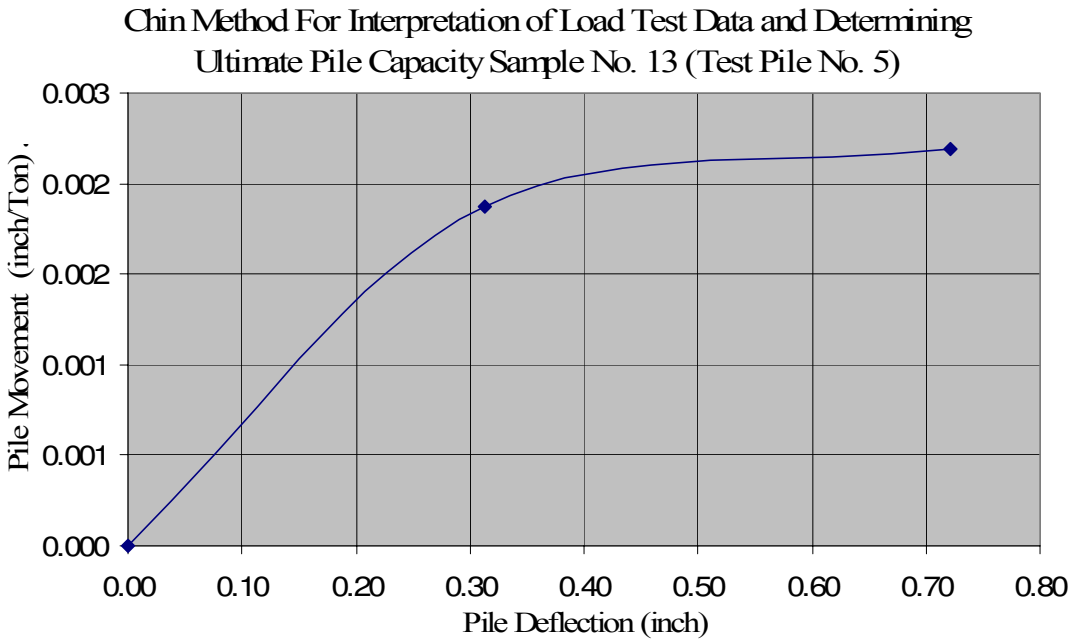

Figure 88-Chin's Method for Interpretation of Load Test Data Sample No. 13, Test Pile No. 5

Table 60-Chin's Load Test Data Sample No. 13, Test Pile No. 5

Compression Test - Sample No. 13 (Test Pile No. 5)		
Load / Unload Cycle		
Load Applied	**Pile Top Deflection Divided by Load Applied**	**Pile Top Deflection**
0	0.00000	0.00000
160	0.00188	0.31300
320	0.00219	0.72200

APPENDIX F
HISTOGRAPHS DEPICTING EMPIRICAL METHODS OF CALCULATING ULTIMATE CAPACITY vs. ALL PHYSICAL LOAD TEST INTERPRETATION METHODS, BASED ON THE AVERAGE OF ALL SAMPLES IN EACH CATEGORY

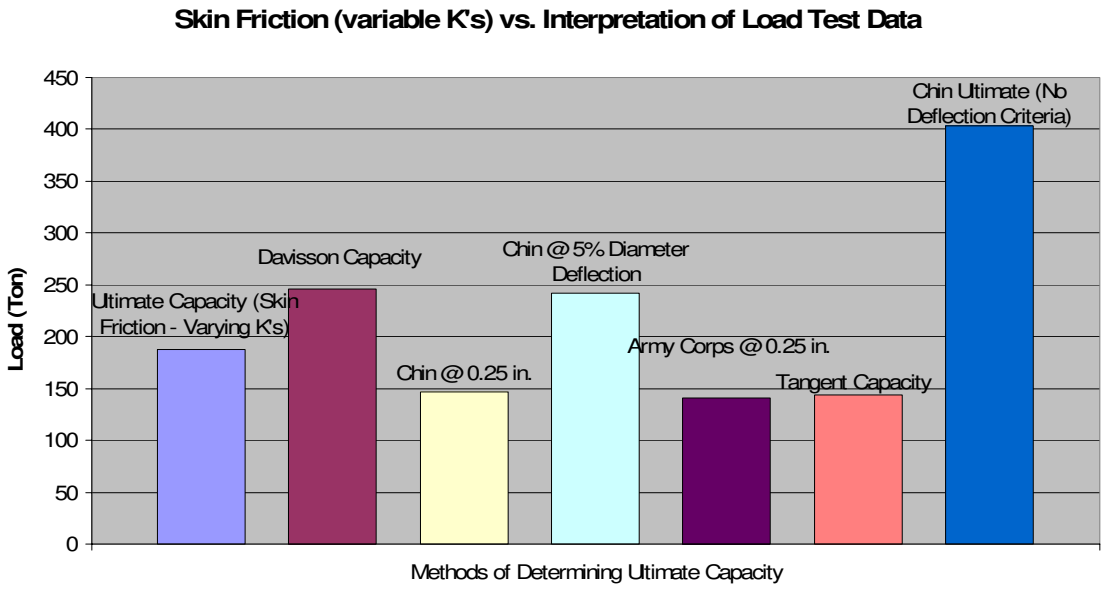

Figure 89-Ultimate Capacity (skin friction only – varying K's) vs. Physical Load Test Data Interpretation of Results

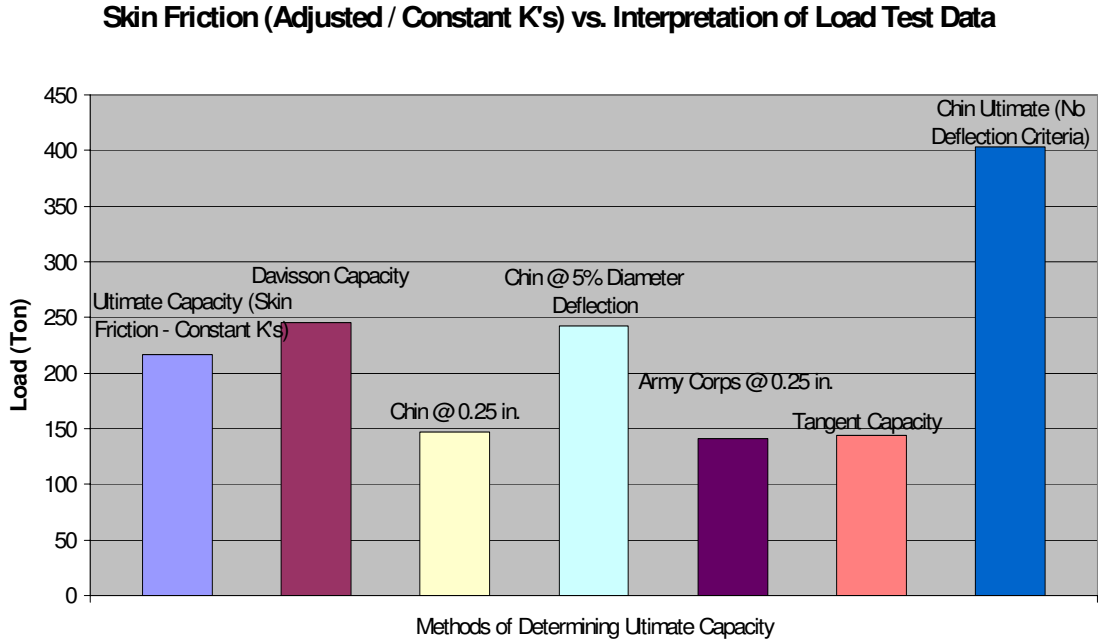

Figure 90-Ultimate Capacity (skin friction only – adjusted K's) vs. Physical Load Test Data Interpretation of Results

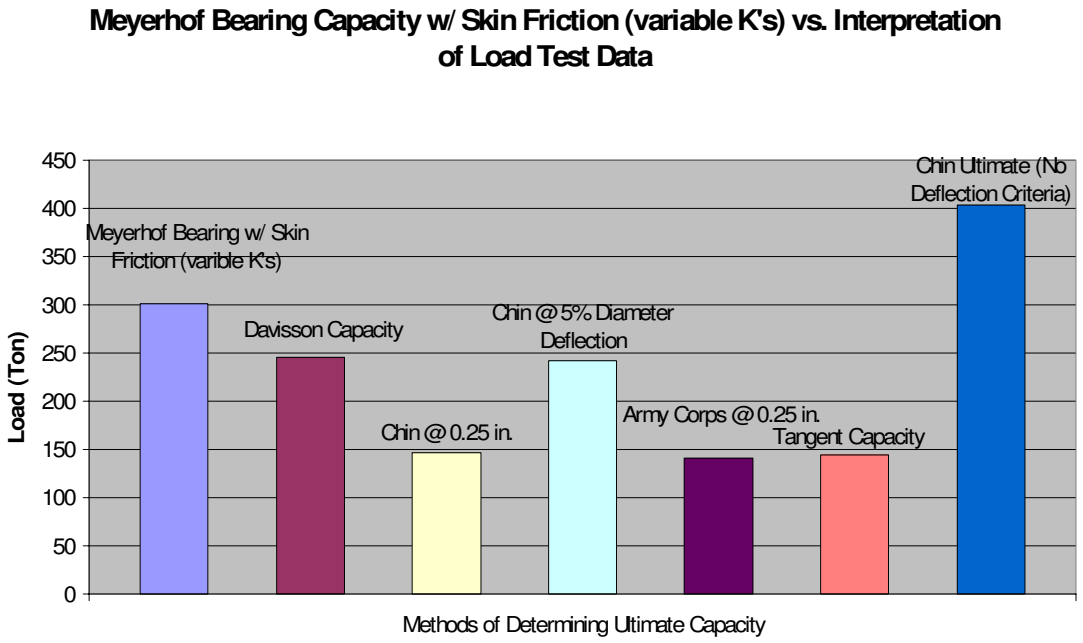

Figure 91-Ultimate Capacity (Meyerhof Bearing Capacity w/ skin friction – varying K's) vs. Physical Load Test Data Interpretation of Results

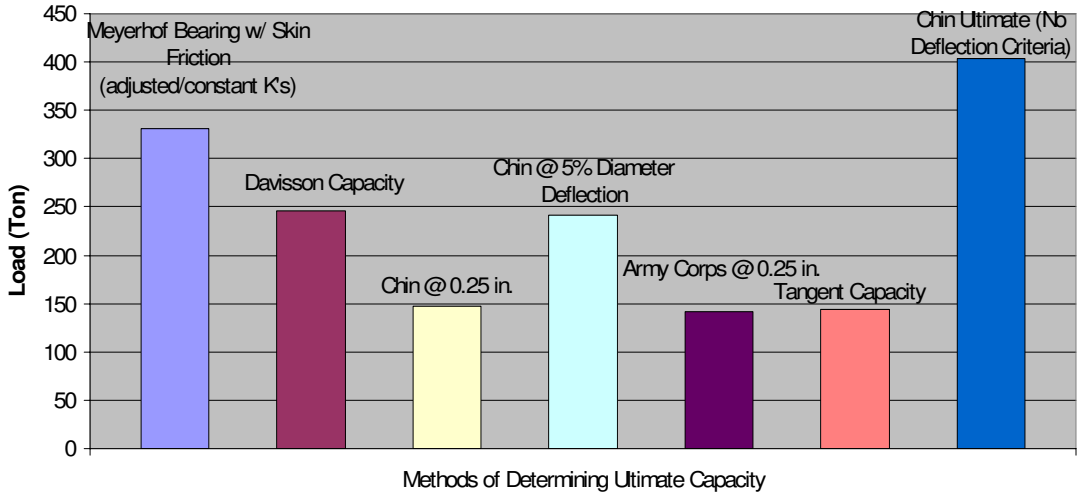

Figure 92-Ultimate Capacity (Meyerhof Bearing Capacity w/ skin friction adjusted K's) vs. Physical Load Test Data Interpretation of Results

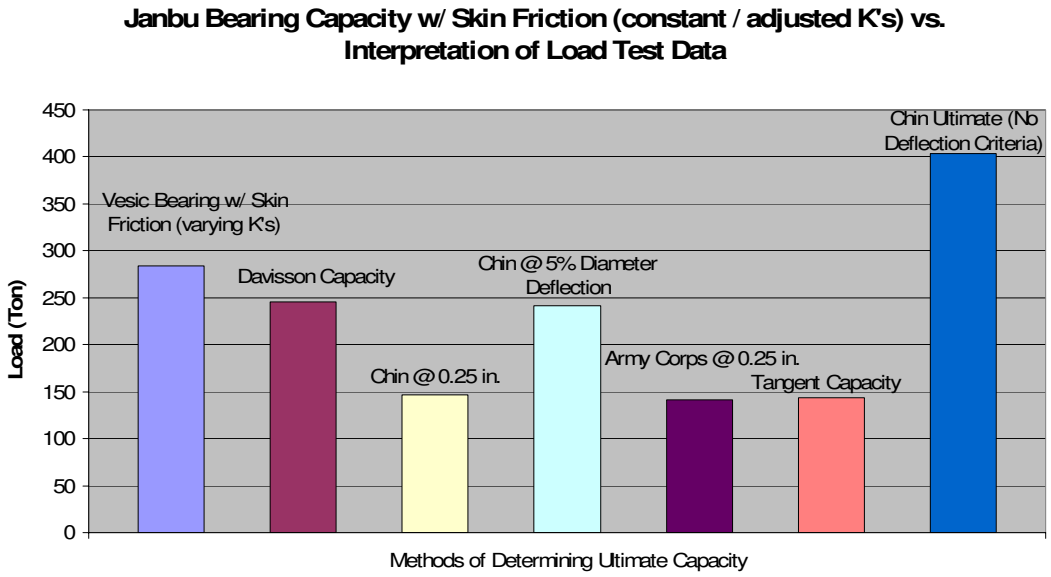

Figure 93-Ultimate Capacity (Vesic Bearing Capacity w/ skin friction – varying K's) vs. Physical Load Test Data Interpretation of Results

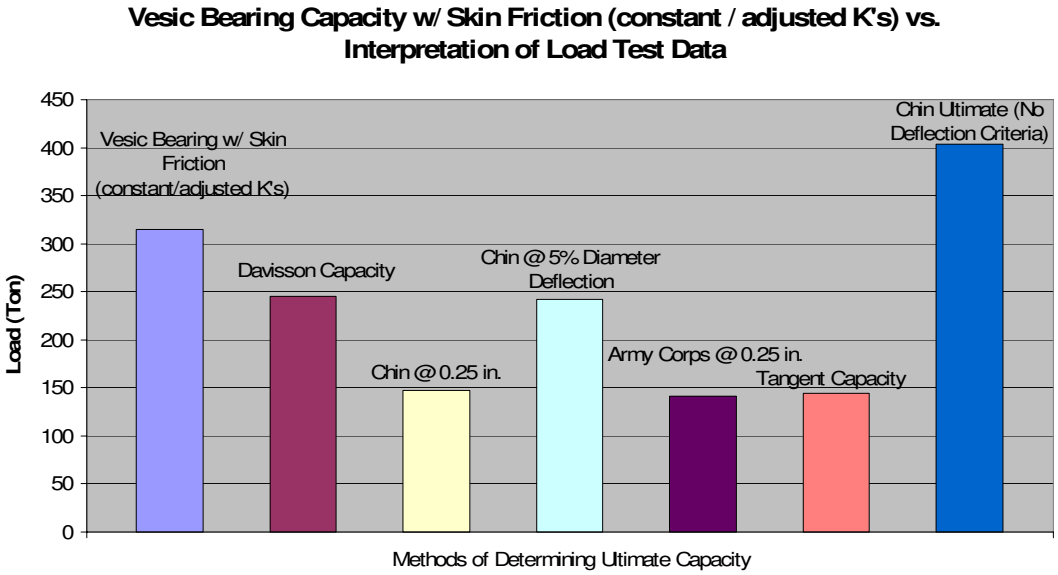

Figure 94-Ultimate Capacity (Vesic Bearing Capacity w/ skin friction adjusted K's) vs. Physical Load Test Data Interpretation of Results

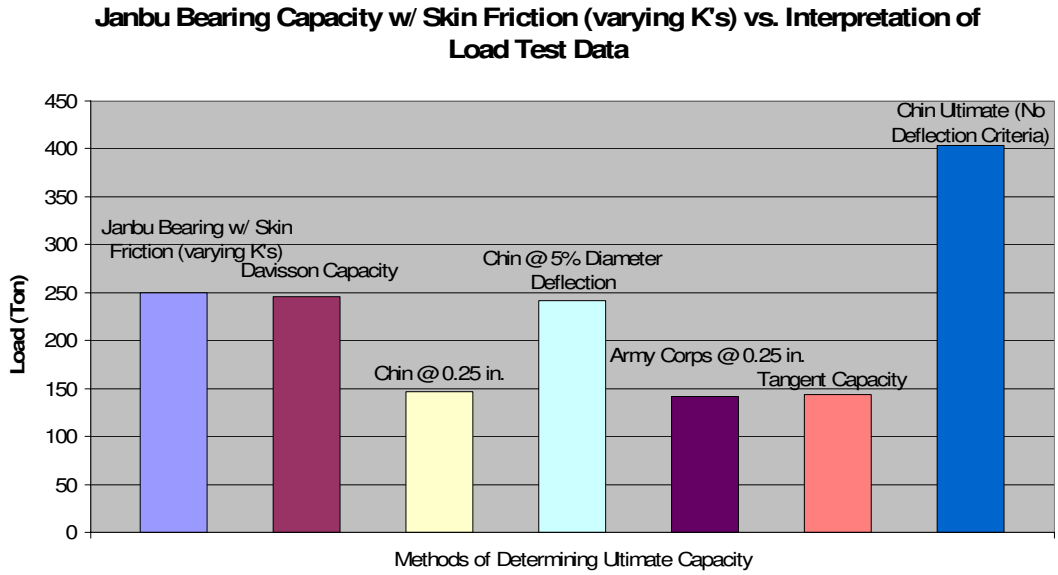

Figure 95-Ultimate Capacity (Janbu Bearing Capacity w/ skin friction – varying K's) vs. Physical Load Test Data Interpretation of Results

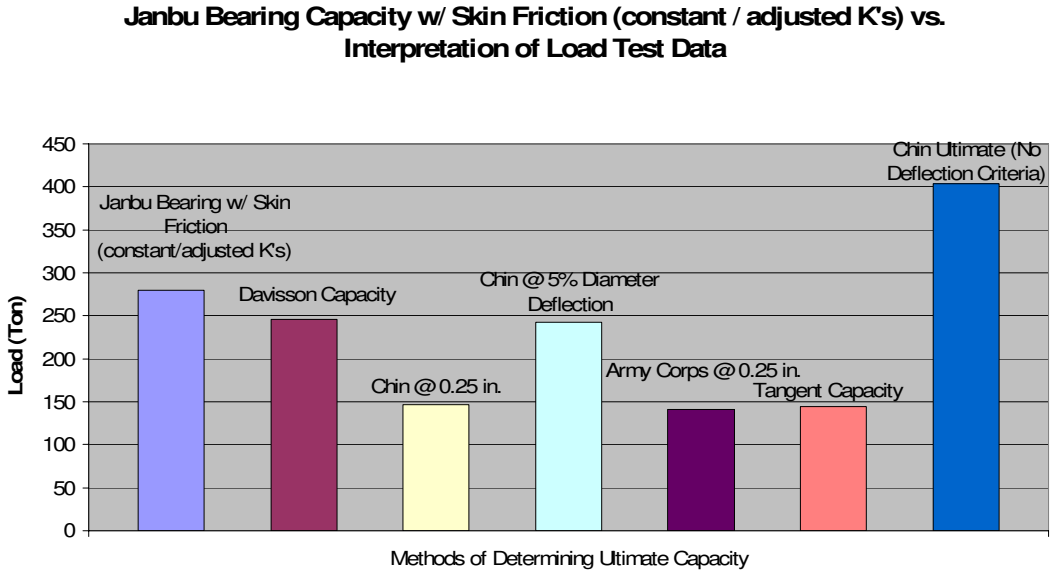

Figure 96-Ultimate Capacity (Janbu Bearing Capacity w/ skin friction adjusted K's) vs. Physical Load Test Data Interpretation of Results

APPENDIX G:
STATISTICAL OUTPUT (SPSS)

```
                GET
  FILE="H:\jeff's thesis data.sav".
DATASET NAME DataSet1 WINDOW=FRONT.
             NEW FILE.
DATASET NAME DataSet2 WINDOW=FRONT.
             CROSSTABS
   /TABLES=Method  BY LoadCapacity
        /FORMAT= AVALUE TABLES
    /STATISTIC=CHISQ CC ETA CORR
           /CELLS= COUNT
        /COUNT ROUND CELL
           /BARCHART .
```

Crosstabs

Notes		
Output Created		24-MAR-2008 18:42:22
Comments		
Input	**Active Dataset**	DataSet2
	Filter	<none>
	Weight	<none>
	Split File	<none>
	N of Rows in Working Data File	50
Missing Value Handling	**Definition of Missing**	User-defined missing values are treated as missing.
	Cases Used	Statistics for each table are based on all the cases with valid data in the specified range(s) for all variables in

		each table.
Syntax		CROSSTABS /TABLES=Method BY LoadCapacity /FORMAT= AVALUE TABLES /STATISTIC=CHISQ CC ETA CORR /CELLS= COUNT /COUNT ROUND CELL /BARCHART .
Resources	**Processor Time**	0:00:00.52
	Elapsed Time	0:00:00.66
	Dimensions Requested	2
	Cells Available	174876

[DataSet2]

Case Processing Summary						
	Cases					
	Valid		**Missing**		**Total**	
	N	**Percent**	**N**	**Percent**	**N**	**Percent**

Method * LoadCapacity	50	100.0%	0	.0%	50	100.0%

Chi-Square Tests			
	Value	**df**	**Asymp. Sig. (2-sided)**
Pearson Chi-Square	47.000(a)	40	.208
Likelihood Ratio	64.816	40	.008
Linear-by-Linear Association	7.061	1	.008
N of Valid Cases	50		
a 82 cells (100.0%) have expected count less than 5. The minimum expected count is .50.			

Directional Measures			
			Value
Nominal by Interval	**Eta**	**Method Dependent**	.970
		Load Capacity Dependent	.380

Symmetric Measures					
		Value	**Asymp. Std. Error(a)**	**Approx. T(b)**	**Approx. Sig.**
Nominal by Nominal	**Contingency Coefficient**	.696			.208
Interval by Interval	**Pearson's R**	.380	.117	2.843	.007(c)
Ordinal by Ordinal	**Spearman Correlation**	.408	.130	3.095	.003(c)
N of Valid Cases		50			
(a) Not assuming the null hypothesis.					
(b) Using the asymptotic standard error assuming the null hypothesis.					
(c) Based on normal approximation.					

APPENDIX H:
CHI-SQUARED STATISTICAL ANALYSIS FOR NULL HYPOTHESIS AND ALTERNATIVE HYPOTHESIS FOR PREDICTED VS. ACTUAL STATISTICAL OUTPUT

H_o: There is no difference between the mean of Davisson's interpretation of load test data and the mean average capacity of the pile define by the skin friction method in cohesionless soils.

H_1: There is a difference between the mean of Davisson's interpretation of load test data and the mean average capacity of the pile define by the skin friction method in a cohesionless soil profile.

H_o: There is no difference between the mean of Davisson's interpretation of load test data and the mean average capacity of the pile define by the skin friction method with adjusted lateral earth pressure coefficients in cohesionless soils.

H_2: There is a difference between the mean of Davisson's interpretation of load test data and the mean average capacity of the pile define by the skin friction method with adjusted lateral earth pressure coefficients in a cohesionless soils.

H_o: There is no difference between the mean of Davisson's interpretation of load test data and the mean average capacity of the pile define by the skin friction method and Meyerhof's point bearing capacity in cohesionless soils.

H_3: There is a difference between the mean of Davisson's interpretation of load test data and the mean average capacity of the pile define by the skin friction method and Meyerhof's point bearing capacity in cohesionless soils.

H_o: There is no difference between the mean of Davisson's interpretation of load test data and the mean average capacity of the pile define by the skin friction method with adjusted lateral earth pressure coefficients and Meyerhof's point bearing capacity in cohesionless soils.

H_4: There is no difference between the mean of Davisson's interpretation of load test data and the mean average capacity of the pile define by the skin friction method with adjusted lateral earth pressure coefficients and Meyerhof's point bearing capacity in cohesionless soils.

H_o: There is no difference between the mean of Davisson's interpretation of load test data and the mean average capacity of the pile define by the skin friction method and Vesic's point bearing capacity in cohesionless soils.

H_5: There is a difference between the mean of Davisson's interpretation of load test data and the mean average capacity of the pile define by the skin friction method and Vesic's point bearing capacity in cohesionless soils.

H_o: There is no difference between the mean of Davisson's interpretation of load test data and the mean average capacity of the pile define by the skin friction method with adjusted lateral earth pressure coefficients and Vesic's point bearing capacity in cohesionless soils.

H_6: There is a difference between the mean of Davisson's interpretation of load test data and the mean average capacity of the pile define by the skin friction method with adjusted lateral earth pressure coefficients and Vesic's point bearing capacity in cohesionless soils.

H_o: There is no difference between the mean of Davisson's interpretation of load test data and the mean average capacity of the pile define by the skin friction method and Janbu's point bearing capacity in cohesionless soils.

H_7: There is a difference between the mean of Davisson's interpretation of load test data and the mean average capacity of the pile define by the skin friction method and Janbu's point bearing capacity in cohesionless soils.

H_o: There is no difference between the mean of Davisson's interpretation of load test data and the mean average capacity of the pile define by the skin friction method with adjusted lateral earth pressure coefficients and Janbu's point bearing capacity in cohesionless soils.

H_8: There is a difference between the mean of Davisson's interpretation of load test data and the mean average capacity of the pile define by the skin friction method with adjusted lateral earth pressure coefficients and Janbu's point bearing capacity in cohesionless soils.

H_o: There is no difference between the mean of Chin-Kondner's interpretation of load test data at 0.25 inches of deflection and the mean average capacity of the pile define by the skin friction method in cohesionless soils.

H_9: There is a difference between the mean of Chin-Kondner's interpretation of load test data at 0.25 inches of deflection and the mean average capacity of the pile define by the skin friction method in a cohesionless soil profile.

H_o: There is no difference between the mean of Chin-Kondner's interpretation of load test data at 0.25 inches of deflection and the mean average capacity of the pile define by the skin friction method with adjusted lateral earth pressure coefficients in cohesionless soils.

H_{10}: There is a difference between the mean of Chin-Kondner's interpretation of load test data at 0.25 inches of deflection and the mean average capacity of the pile define by the skin friction method with adjusted lateral earth pressure coefficients in a cohesionless soils.

H_o: There is no difference between the mean of Chin-Kondner's interpretation of load test data at 0.25 inches of deflection and the mean average capacity of the pile define by the skin friction method and Meyerhof's point bearing capacity in cohesionless soils.

H_{11}: There is a difference between the mean of Chin-Kondner's interpretation of load test data at 0.25 inches of deflection and the mean average capacity of the pile define by the skin friction method and Meyerhof's point bearing capacity in cohesionless soils.

H_o: There is no difference between the mean of Chin-Kondner's interpretation of load test data at 0.25 inches of deflection and the mean average capacity of the pile define by the skin friction method with adjusted lateral earth pressure coefficients and Meyerhof's point bearing capacity in cohesionless soils.

H_{12}: There is no difference between the mean of Chin-Kondner's interpretation of load test data at 0.25 inches of deflection and the mean average capacity of the pile define by the skin friction method with adjusted lateral earth pressure coefficients and Meyerhof's point bearing capacity in cohesionless soils.

H_o: There is no difference between the mean of Chin-Kondner's interpretation of load test data at 0.25 inches of deflection and the mean average capacity of the pile define by the skin friction method and Vesic's point bearing capacity in cohesionless soils.

H_{13}: There is a difference between the mean of Chin-Kondner's interpretation of load test data at 0.25 inches of deflection and the mean average capacity of the pile define by the skin friction method and Vesic's point bearing capacity in cohesionless soils.

H_o: There is no difference between the mean of Chin-Kondner's interpretation of load test data at 0.25 inches of deflection and the mean average capacity of the pile define by the skin friction method with adjusted lateral earth pressure coefficients and Vesic's point bearing capacity in cohesionless soils.

H_{14}: There is a difference between the mean of Chin-Kondner's interpretation of load test data at 0.25 inches of deflection and the mean average capacity of the pile define by the skin friction method with adjusted lateral earth pressure coefficients and Vesic's point bearing capacity in cohesionless soils.

H_o: There is no difference between the mean of Chin-Kondner's interpretation of load test data at 0.25 inches of deflection and the mean average capacity of the pile define by the skin friction method and Janbu's point bearing capacity in cohesionless soils.

H_{15}: There is a difference between the mean of Chin-Kondner's interpretation of load test data at 0.25 inches of deflection and the mean average capacity of the pile define by the skin friction method and Janbu's point bearing capacity in cohesionless soils.

H_o: There is no difference between the mean of Chin-Kondner's interpretation of load test data at 0.25 inches of deflection and the mean average capacity of the pile define by the skin friction method with adjusted lateral earth pressure coefficients and Janbu's point bearing capacity in cohesionless soils.

H_{16}: There is a difference between the mean of Chin-Kondner's interpretation of load test data at 0.25 inches of deflection and the mean average capacity of the pile define by the skin friction method with adjusted lateral earth pressure coefficients and Janbu's point bearing capacity in cohesionless soils.

H_o: There is no difference between the mean of Chin-Kondner's interpretation of load test data at a deflection not to exceed 5% of the pile diameter and the mean average capacity of the pile define by the skin friction method in cohesionless soils.

H_{17}: There is a difference between the mean of Chin-Kondner's interpretation of load test data at a deflection not to exceed 5% of the pile diameter and the mean average capacity of the pile define by the skin friction method in a cohesionless soil profile.

H_o: There is no difference between the mean of Chin-Kondner's interpretation of load test data at a deflection not to exceed 5% of the pile diameter and the mean average capacity of the pile define by the skin friction method with adjusted lateral earth pressure coefficients in cohesionless soils.

H_{18}: There is a difference between the mean of Chin-Kondner's interpretation of load test data at a deflection not to exceed 5% of the pile diameter and the mean average capacity of the pile define by the skin friction method with adjusted lateral earth pressure coefficients in a cohesionless soils.

H_o: There is no difference between the mean of Chin-Kondner's interpretation of load test data at a deflection not to exceed 5% of the pile diameter and the mean average capacity of the pile define by the skin friction method and Meyerhof's point bearing capacity in cohesionless soils.

H_{19}: There is a difference between the mean of Chin-Kondner's interpretation of load test data at a deflection not to exceed 5% of the pile diameter and the mean average capacity of the pile define by the skin friction method and Meyerhof's point bearing capacity in cohesionless soils.

H_o: There is no difference between the mean of Chin-Kondner's interpretation of load test data at a deflection not to exceed 5% of the pile diameter and the mean average capacity of

the pile define by the skin friction method with adjusted lateral earth pressure coefficients and Meyerhof's point bearing capacity in cohesionless soils.

H_{20}: There is no difference between the mean of Chin-Kondner's interpretation of load test data at a deflection not to exceed 5% of the pile diameter and the mean average capacity of the pile define by the skin friction method with adjusted lateral earth pressure coefficients and Meyerhof's point bearing capacity in cohesionless soils.

H_o: There is no difference between the mean of Chin-Kondner's interpretation of load test data at a deflection not to exceed 5% of the pile diameter and the mean average capacity of the pile define by the skin friction method and Vesic's point bearing capacity in cohesionless soils.

H_{21}: There is a difference between the mean of Chin-Kondner's interpretation of load test data at a deflection not to exceed 5% of the pile diameter and the mean average capacity of the pile define by the skin friction method and Vesic's point bearing capacity in cohesionless soils.

H_o: There is no difference between the mean of Chin-Kondner's interpretation of load test data at a deflection not to exceed 5% of the pile diameter and the mean average capacity of the pile define by the skin friction method with adjusted lateral earth pressure coefficients and Vesic's point bearing capacity in cohesionless soils.

H_{22}: There is a difference between the mean of Chin-Kondner's interpretation of load test data at a deflection not to exceed 5% of the pile diameter and the mean average capacity of the pile define by the skin friction method with adjusted lateral earth pressure coefficients and Vesic's point bearing capacity in cohesionless soils.

H_o: There is no difference between the mean of Chin-Kondner's interpretation of load test data at a deflection not to exceed 5% of the pile diameter and the mean average capacity of the pile define by the skin friction method and Janbu's point bearing capacity in cohesionless soils.

H_{23}: There is a difference between the mean of Chin-Kondner's interpretation of load test data at a deflection not to exceed 5% of the pile diameter and the mean average capacity of the pile define by the skin friction method and Janbu's point bearing capacity in cohesionless soils.

H_o: There is no difference between the mean of Chin-Kondner's interpretation of load test data at a deflection not to exceed 5% of the pile diameter and the mean average capacity of the pile define by the skin friction method with adjusted lateral earth pressure coefficients and Janbu's point bearing capacity in cohesionless soils.

H_{24}: There is a difference between the mean of Chin-Kondner's interpretation of load test data at a deflection not to exceed 5% of the pile diameter and the mean average capacity of the pile define by the skin friction method with adjusted lateral earth pressure coefficients and Janbu's point bearing capacity in cohesionless soils.

H_o: There is no difference between the mean pile capacity based on the Army Corps of Engineers method defined by 0.25 inches of net deflection and the mean average capacity of the pile define by the skin friction method in cohesionless soils.

H_{25}: There is a difference between the mean pile capacity based on the Army Corps of Engineers method defined by 0.25 inches of net deflection and the mean average capacity of the pile define by the skin friction method in a cohesionless soil profile.

H_o: There is no difference between the mean pile capacity based on the Army Corps of Engineers method defined by 0.25 inches of net deflection and the mean average capacity of the pile define by the skin friction method with adjusted lateral earth pressure coefficients in cohesionless soils.

H_{26}: There is a difference between the mean pile capacity based on the Army Corps of Engineers method defined by 0.25 inches of net deflection and the mean average capacity of the pile define by the skin friction method with adjusted lateral earth pressure coefficients in a cohesionless soils.

H_o: There is no difference between the mean pile capacity based on the Army Corps of Engineers method defined by 0.25 inches of net deflection and the mean average capacity of the pile define by the skin friction method and Meyerhof's point bearing capacity in cohesionless soils.

H_{27}: There is a difference between the mean pile capacity based on the Army Corps of Engineers method defined by 0.25 inches of net deflection and the mean average capacity of the pile define by the skin friction method and Meyerhof's point bearing capacity in cohesionless soils.

H_o: There is no difference between the mean pile capacity based on the Army Corps of Engineers method defined by 0.25 inches of net deflection and the mean average capacity of the pile define by the skin friction method with adjusted lateral earth pressure coefficients and Meyerhof's point bearing capacity in cohesionless soils.

H_{28}: There is no difference between the mean pile capacity based on the Army Corps of Engineers method defined by 0.25 inches of net deflection and the mean average capacity of the

pile define by the skin friction method with adjusted lateral earth pressure coefficients and Meyerhof's point bearing capacity in cohesionless soils.

H_o: There is no difference between the mean pile capacity based on the Army Corps of Engineers method defined by 0.25 inches of net deflection and the mean average capacity of the pile define by the skin friction method and Vesic's point bearing capacity in cohesionless soils.

H_{29}: There is a difference between the mean pile capacity based on the Army Corps of Engineers method defined by 0.25 inches of net deflection and the mean average capacity of the pile define by the skin friction method and Vesic's point bearing capacity in cohesionless soils.

H_o: There is no difference between the mean pile capacity based on the Army Corps of Engineers method defined by 0.25 inches of net deflection and the mean average capacity of the pile define by the skin friction method with adjusted lateral earth pressure coefficients and Vesic's point bearing capacity in cohesionless soils.

H_{30}: There is a difference between the mean pile capacity based on the Army Corps of Engineers method defined by 0.25 inches of net deflection and the mean average capacity of the pile define by the skin friction method with adjusted lateral earth pressure coefficients and Vesic's point bearing capacity in cohesionless soils.

H_o: There is no difference between the mean pile capacity based on the Army Corps of Engineers method defined by 0.25 inches of net deflection and the mean average capacity of the pile define by the skin friction method and Janbu's point bearing capacity in cohesionless soils.

H_{31}: There is a difference between the mean pile capacity based on the Army Corps of Engineers method defined by 0.25 inches of net deflection and the mean average capacity of the pile define by the skin friction method and Janbu's point bearing capacity in cohesionless soils.

H_o: There is no difference between the mean pile capacity based on the Army Corps of Engineers method defined by 0.25 inches of net deflection and the mean average capacity of the pile define by the skin friction method with adjusted lateral earth pressure coefficients and Janbu's point bearing capacity in cohesionless soils.

H_{32}: There is a difference between the mean pile capacity based on the Army Corps of Engineers method defined by 0.25 inches of net deflection and the mean average capacity of the pile define by the skin friction method with adjusted lateral earth pressure coefficients and Janbu's point bearing capacity in cohesionless soils.

H_o: There is no difference between the mean pile capacity based on the Tangent Method of analyzing physical load test data and the mean average capacity of the pile define by the skin friction method in cohesionless soils.

H_{33}: There is a difference between the mean pile capacity based on the Tangent Method of analyzing physical load test data and the mean average capacity of the pile define by the skin friction method in cohesionless soil profile.

H_o: There is no difference between the mean pile capacity based on the Tangent Method of analyzing physical load test data and the mean average capacity of the pile define by the skin friction method with adjusted lateral earth pressure coefficients in cohesionless soils.

H_{34}: There is a difference between the mean pile capacity based on the Tangent Method of analyzing physical load test data and the mean average capacity of the pile define by the skin friction method with adjusted lateral earth pressure coefficients in a cohesionless soils.

H_o: There is no difference between the mean pile capacity based on the Tangent Method of analyzing physical load test data and the mean average capacity of the pile define by the skin friction method and Meyerhof's point bearing capacity in cohesionless soils.

H_{35}: There is a difference between the mean pile capacity based on the Tangent Method of analyzing physical load test data and the mean average capacity of the pile define by the skin friction method and Meyerhof's point bearing capacity in cohesionless soils.

H_o: There is no difference between the mean pile capacity based on the Tangent Method of analyzing physical load test data and the mean average capacity of the pile define by the skin friction method with adjusted lateral earth pressure coefficients and Meyerhof's point bearing capacity in cohesionless soils.

H_{36}: There is no difference between the mean pile capacity based on the Tangent Method of analyzing physical load test data and the mean average capacity of the pile define by the skin friction method with adjusted lateral earth pressure coefficients and Meyerhof's point bearing capacity in cohesionless soils.

H_o: There is no difference between the mean pile capacity based on the Tangent Method of analyzing physical load test data and the mean average capacity of the pile define by the skin friction method and Vesic's point bearing capacity in cohesionless soils.

H_{37}: There is a difference between the mean pile capacity based on the Tangent Method of analyzing physical load test data and the mean average capacity of the pile define by the skin friction method and Vesic's point bearing capacity in cohesionless soils.

H_o: There is no difference between the mean pile capacity based on the Tangent Method of analyzing physical load test data and the mean average capacity of the pile define by the skin

friction method with adjusted lateral earth pressure coefficients and Vesic's point bearing capacity in cohesionless soils.

H_{38}: There is a difference between the mean pile capacity based on the Tangent Method of analyzing physical load test data and the mean average capacity of the pile define by the skin friction method with adjusted lateral earth pressure coefficients and Vesic's point bearing capacity in cohesionless soils.

H_0: There is no difference between the mean pile capacity based on the Tangent Method of analyzing physical load test data and the mean average capacity of the pile define by the skin friction method and Janbu's point bearing capacity in cohesionless soils.

H_{39}: There is a difference between the mean pile capacity based on the Tangent Method of analyzing physical load test data and the mean average capacity of the pile define by the skin friction method and Janbu's point bearing capacity in cohesionless soils.

H_o: There is no difference between the mean pile capacity based on the Tangent Method of analyzing physical load test data and the mean average capacity of the pile define by the skin friction method with adjusted lateral earth pressure coefficients and Janbu's point bearing capacity in cohesionless soils.

H_{40}: There is a difference between the mean pile capacity based on the Tangent Method of analyzing physical load test data and the mean average capacity of the pile define by the skin friction method with adjusted lateral earth pressure coefficients and Janbu's point bearing capacity in cohesionless soils.

H_o: There is no difference between the mean pile capacity based on Chin-Kondner's method for determining ultimate pile capacity by physical interpretation of load test data and the mean average capacity of the pile define by the skin friction method in cohesionless soils.

H_{41}: There is a difference between the mean pile capacity based on Chin-Kondner's method for determining ultimate pile capacity by physical interpretation of load test data and the mean average capacity of the pile define by the skin friction method in a cohesionless soil profile.

H_o: There is no difference between the mean pile capacity based on Chin-Kondner's method for determining ultimate pile capacity by physical interpretation of load test data and the mean average capacity of the pile define by the skin friction method with adjusted lateral earth pressure coefficients in cohesionless soils.

H_{42}: There is a difference between the mean pile capacity based on Chin-Kondner's method for determining ultimate pile capacity by physical interpretation of load test data and the mean average capacity of the pile define by the skin friction method with adjusted lateral earth pressure coefficients in cohesionless soils.

H_o: There is no difference between the mean pile capacity based on Chin-Kondner's method for determining ultimate pile capacity by physical interpretation of load test data and the mean average capacity of the pile define by the skin friction method and Meyerhof's point bearing capacity in cohesionless soils.

H_{43}: There is a difference between the mean pile capacity based on Chin-Kondner's method for determining ultimate pile capacity by physical interpretation of load test data and the

mean average capacity of the pile define by the skin friction method and Meyerhof's point bearing capacity in cohesionless soils.

H_o: There is no difference between the mean pile capacity based on Chin-Kondner's method for determining ultimate pile capacity by physical interpretation of load test data and the mean average capacity of the pile define by the skin friction method with adjusted lateral earth pressure coefficients and Meyerhof's point bearing capacity in cohesionless soils.

H_{44}: There is no difference between the mean pile capacity based on Chin-Kondner's method for determining ultimate pile capacity by physical interpretation of load test data and the mean average capacity of the pile define by the skin friction method with adjusted lateral earth pressure coefficients and Meyerhof's point bearing capacity in cohesionless soils.

H_o: There is no difference between the mean pile capacity based on Chin-Kondner's method for determining ultimate pile capacity by physical interpretation of load test data and the mean average capacity of the pile define by the skin friction method and Vesic's point bearing capacity in cohesionless soils.

H_{45}: There is a difference between the mean pile capacity based on Chin-Kondner's method for determining ultimate pile capacity by physical interpretation of load test data and the mean average capacity of the pile define by the skin friction method and Vesic's point bearing capacity in cohesionless soils.

H_o: There is no difference between the mean pile capacity based on Chin-Kondner's method for determining ultimate pile capacity by physical interpretation of load test data and the mean average capacity of the pile define by the skin friction method with adjusted lateral earth pressure coefficients and Vesic's point bearing capacity in cohesionless soils.

H_{46}: There is a difference between the mean pile capacity based on Chin-Kondner's method for determining ultimate pile capacity by physical interpretation of load test data and the mean average capacity of the pile define by the skin friction method with adjusted lateral earth pressure coefficients and Vesic's point bearing capacity in cohesionless soils.

H_0: There is no difference between the mean pile capacity based on Chin-Kondner's method for determining ultimate pile capacity by physical interpretation of load test data and the mean average capacity of the pile define by the skin friction method and Janbu's point bearing capacity in cohesionless soils.

H_{47}: There is a difference between the mean pile capacity based on Chin-Kondner's method for determining ultimate pile capacity by physical interpretation of load test data and the mean average capacity of the pile define by the skin friction method and Janbu's point bearing capacity in cohesionless soils.

H_o: There is no difference between the mean pile capacity based on Chin-Kondner's method for determining ultimate pile capacity by physical interpretation of load test data and the mean average capacity of the pile define by the skin friction method with adjusted lateral earth pressure coefficients and Janbu's point bearing capacity in cohesionless soils.

H_{48}: There is a difference between the mean pile capacity based on Chin-Kondner's method for determining ultimate pile capacity by physical interpretation of load test data and the mean average capacity of the pile define by the skin friction method with adjusted lateral earth pressure coefficients and Janbu's point bearing capacity in cohesionless soils.

REFERENCES

ASTM D1143, 1981, (1994) "Standard Test Method for Individual Piles Under Axial Compressive Load," ASTM International,. West Conshohocken, PA, **www.astm.org**

ASTM D2487, (2006) "Standard Practice for Classification of Soils for Engineering Purposes (Unified Soil Classification System)," ASTM International,. West Conshohocken, PA, **www.astm.org**

Bowles, J.E. (1996). *Foundation Analysis and Design (5th ed.).* New York: McGraw-Hill. Charles, W.W. Ng (2004). "A Short Course in Soil-Structure Engineering of Deep Foundations Excavations and Tunnels"; Thomas Telford, 27.

Butler, H.D., & Hoy, H.E., 1977, *Users Manual for The Texas Quick-Load Method for Foundation Testing.* Federal Highway Administration, Office of Development, Report No. FHWA-Tp-77-0. Washington, D.C.

Chen, J-R & Kulhawy, FH (2002). "Axial Uplift Behavior of Pressure-Injected Footings in Cohesionless Soil", *Deep Foundations, 2002 (GSP 116)*, Ed. MW O'Neill & FC Townsend, ASCE, Reston, 1275-1289.

Chin, F.K. and Vail, A.J. (1973). "Behavior of piles in alluvium." *Proceedings from the 6th International Conference on Soil Mechanics and Foundation Engineering, 21*. 47-52

Chin, F.K. (1970). "Estimation of the ultimate load of piles not carried to failure": *Proc. 2nd Southeast Asian Conference on Soil Engineering,* 81-90.

Coyle, H.M. and Castello, R.R. (1981). "New design correlations for piles in sand," *Journal of the Geotechnical Engineering Division*, American Society of Civil Engineers, *107*(7), 965-986.

Craig, R.F. (1999). Soil Mechanics (6th ed.). London: Spon Press.

Creswell, J. W. (1994). *Research design: Qualitative & quantitative approaches.* Thousand Oaks, CA: Sage.

Crowther, C.L. (1988). *Load Testing of Deep Foundations: the planning, Design, and Conduct of Pile Load Tests*: John Wiley & Sons, Inc.

Das, B.M. (2007). *Principles of Geotechnical Engineering (5th ed.).* Specific Grove, California: Brooks/Cole.

Das, B.M. (2007). *Principles of Foundation Engineering (6th ed.).* Toronto: Nelson.

Duzceer and Saglamer, (2002). "Evaluation of Pile Load Test Results.": 9th International Conference on Piling and Deep Foundations, Deep Foundation Institute.

Esrig, MI, Leznicki, JK & Gaibrois, RG (1994). "Managing Installation of Augered-Cast-In-Place Piles", *Record 1447*, Trans. Research Board, Washington, 27-29.

Evertson, C. M., & Green, J. L. (1986). Observation as inquiry and method. In M. C. Wittrock (Ed.), *Handbook of Research on Teaching (3rd ed., pp. 162-213).* New York: Macmillan.

Fleming, W (1994). "Current Understanding & Control of Continuous Flight Auger Piling", *Proc..,* Intl. Conf. Design & Const. Deep Foundations (1), Orlando, 260-278.

Fleming, W.G.K., Weltman, A.J. and Randolph, M.F. (1985). *Piling Engineering*. New York: John Wiley & Sons. 301-340.

Garson, G.D. (2006). *Quantitative Research in Public Administration.* February 5, 2008, **http://www2.chass.ncsu.edu/garson/pA765/chisq.htm**

Gay, L. R. (2001). *Educational research: Competencies for analysis and applications (6th ed.).* Columbus, OH: Merrill.

Han, Y. (1999). *Axial Load Test and Analysis for Open-Ended Steel Tubular Piles Driven into Weathered Rock.* University of Ottawa: Master Thesis.

Hirany, A & Kulhawy, FH (1988). "Conduct & Interpretation of Load Tests on Drilled Shafts", *Rpt EL-5915*, Electric Power Res. Inst., Palo Alto.

International Building Code (2003). International Code Council County Club Hills IL. Chapter 18.

Janbu, N. (1976). "Static bearing capacity of friction piles," *Proceedings, 6th European Conference on Soil Mechanics and Foundation Engineering*, Vol. 1.2, 479-482.

Jacobs, Larry M. & Associates, Inc., *Static Load Testing Services*, March 11, 2008 **http://lmj-a.com/geotechnical_engineering.htm**.

Kirk, R. E. (1982). *Experimental design: Procedures for the behavioral sciences (2nd ed.).* Belmont, CA: Brooks/Cole.

Kulhawy, F.H. and Chen, Jie-Ru (2005). "Axial Compression Behavior of Augered Cast- In-Place (ACIP) Piles in Cohesionless Soils", Advances in Deep Foundations, American ASCE, 2-12.

Leonards, G.A. (1982). “Investigation of Failures.” Journal of Geotechnical Engineering. *American Society of Civil Engineers*, *117*(1) 172-188.

McVay, M, Armaghani, B & Casper, R (1994). “Design & Construction of Augercast Piles in Florida”, *Record 1447*, Trans. Research Board, Washington, 10-18.

Meyerhof, G.G. (1976). “Bearing capacity and settlement of pile foundations,” *Journal of the Geotechnical Engineering Division,* 102 (3), 197-228.

Naval Facilities Engineering Command (1986). *“Foundations and Earth Structures”,* Design Manual 7.02, (chap. 5) Neate, J. J. (1988). "Augered cast-in-place piles.": 13th Annual Meeting, Deep Foundations Institute, Atlanta, Ga., 167-175.

Neely, W.J. (1991). Bearing capacity of auger-cast piles in sand. *Journal of Geotechnical Engineering,117*(2), 133-335.

Neely, WJ (1991). “Bearing capacity of auger cast-in-place piles in Sand”, *Journal of Geotechnical Engineering,* ASCE, 117(2), 331-345.

NIST/SEMATECH e-Handbook of Statistical Methods, February 5, 2008. **http://www.itl.nist.gov/div898/handbook/eda/section3/eda35f.htm**

O’Neill, MW, et al. (2002). “Axial Performance of ACIP Piles in Texas Coastal Soils”, *Deep Foundations. 2002 (GSP 116)*, Ed. MW O'Neill & FC Townsend, ASCE, Reston, 1290-1314.

Patton, M. Q. (2002). *Qualitative research & Evaluation Methods*. California: Sage.

Roscoe, G.H., Dic, Mice, (1984). “The Behavior of Flight Auger Bored Piles in Sand” *Proceedings of the International Conference on Advances in Piling and Ground Treatment for Foundations,* 241-242.

Snedecor, G. W. & Cochran, W. G. (1989), *Statistical Methods, (4th ed,)*, Iowa State: University Press.

Tabachnick, B. G., & Fidell, L. S. (1989). *Using multivariate statistics (2nd ed.).* New York: Harper & Row.

Tolosko, T.A. (1999). “*Extrapolation of pile capacity from non-failed load test.”* University of Massachusetts Lowell: Master Thesis.

Touma, F.T. and Reese, L.C. (1974). “Behavior of bored piles in sand.” *Journal of the Geotechnical Engineering,. 100*, 749-761.

Turner, J.P. and Kulhawy, F.H., (1994) "Physical modeling of drilled shaft side resistance in sand," *Geotechnical Testing Journal*, GTJODJ, *17*(3), 282-290.

US Army Corps of Engineers (1991) *"Design of Pile Foundations"*; Engineering Manual (EM 110-2-2906), (chap. 5).

US Army Corps of Engineers (1992) *"Design of Pile Foundations"*; Engineering Manual (EM 1110-1-1905), (chap. 5).

US Army Corps of Engineers (1993) *"Design of Pile Foundations"*; Engineering Manual (EM 110-2-2906), (chap. 2).

U.S. Department of the Interior Bureau of Reclamation. (1998). "Earth Manual," 3rd ed. Part 1. Washington, DC: Government Printing Office.

Van Den Elzen, L.W.A. (1983). "Concrete screw piles, a vibration-less, non-displacement piling method." *Conference on Recent Developments in the Design and Construction of Piles," 100*, 749-761.

Van Impe, W (1988). "Consideration on Auger Pile Design", *Proc.,* International Geotechnical Seminar Deep Foundations on Bored & Augered Piles, Ghent, 193-218.

Vesic, A.S. (1963). "Design of pile foundations.": *National Co-operative Highway Research Program and Synthesis of Highway Practice,* 2, 1-68.

Vesic, A.S. (1964). "Model testing of deep foundations and scaling laws." *Proceedings, North American Conference on Deep Foundations*, *2*. 525-533.

Zelada, GA & Stephenson, RW (2000). "Design Methods for Auger CIP Piles in Compression", *New Technology & Design Developments in Deep Foundations (GSP 100)*, Ed. ND Dennis, R Castelli & MW O'Neill, ASCE, Reston, 418-432.